


3-30-2017

# Optimization and Performance Study of Select Heating Ventilation and Air Conditioning Technologies for Commercial Buildings

Rajeev Kamal

University of South Florida, rajeev@mail.usf.edu

Follow this and additional works at: <http://scholarcommons.usf.edu/etd>

 Part of the [Engineering Commons](#), and the [Oil, Gas, and Energy Commons](#)

## Scholar Commons Citation

Kamal, Rajeev, "Optimization and Performance Study of Select Heating Ventilation and Air Conditioning Technologies for Commercial Buildings" (2017). *Graduate Theses and Dissertations*.  
<http://scholarcommons.usf.edu/etd/6656>

This Dissertation is brought to you for free and open access by the Graduate School at Scholar Commons. It has been accepted for inclusion in Graduate Theses and Dissertations by an authorized administrator of Scholar Commons. For more information, please contact [scholarcommons@usf.edu](mailto:scholarcommons@usf.edu).

Optimization and Performance Study of Select Heating Ventilation and Air Conditioning Technologies for  
Commercial Buildings

by

Rajeev Kamal

A dissertation submitted in partial fulfillment  
of the requirements for the degree of  
Doctor of Philosophy  
Department of Chemical and Biomedical Engineering  
College of Engineering  
University of South Florida

Major Professor: D. Yogi Goswami, Ph.D.  
Elias Stefanakos, Ph.D.  
Babu Joseph, Ph.D.  
Tapas Das, Ph.D.  
Herbert A. Ingley, Ph.D.

Date of Approval:  
March 2, 2017

Keywords: Gas Engine-driven Heat Pump, Thermal Storage, HVAC, Demand Side Management

Copyright © 2017, Rajeev Kamal

## **Dedication**

To my family and friends for their endless support and motivation.

## Acknowledgments

I express my sincere gratitude to Dr. D. Yogi Goswami, my advisor, for his support, constructive guidance and advice throughout my research and this dissertation. His knowledge and reputation in the academic and research community allowed me to obtain necessary funding and opportunity to conduct this research.

I would also like to extend my gratitude to my doctoral committee, Dr. Elias Stefanakos for his mentorship and encouragement, Dr. Babu Joseph and Dr. Tapas Das for helping me bring this work to a practical industry acceptance and especially for Dr. Herbert A. Ingley for his training and inputs from his experience in HVAC field. Special thanks to the staff at Clean Energy Research Center (CERC) Barbara Graham, Dr. Chand Jotshi, Charles Garretson, and David Goslin who helped me from time to time in conducting this research and during my tenure at the University of South Florida.

I am thankful to my friends and colleagues at the CERC lab who have been helpful throughout my research through their personal support and professional contributions, Chatura Wickramaratne, Arun Kumar Narasimhan, Francesca Moloney, Abhinav Bhardwaj, and Saumya Sharma.

## Table of Contents

List of Tables	iv
List of Figures	vi
Abstract	x
Chapter 1 Introduction	1
1.1 Energy Consumption in Buildings	2
1.1.1 HVAC in Buildings	2
1.2 Challenges for Power Utilities	3
1.3 Theoretical Background	5
1.3.1 Heating Ventilation and Air Conditioning in Commercial Buildings	5
1.3.2 Heat Pumps	5
1.3.3 Working Principle of Heat Pumps	6
1.4 Heat Pump Technology	7
1.4.1 Vapor Compression Heat Pump	7
1.4.2 Absorption Systems	8
1.4.3 Heat Pump Heat Sources	10
1.4.4 Classification	10
1.5 Gas Engine-driven Heat Pump	10
1.5.1 Description of GEHPs	11
1.6 Thermal Energy Storage for Cooling/Heating	12
1.6.1 Benefits to Consumer	14
1.6.2 Benefits to Utilities	15
Chapter 2 Research Objectives	17
Chapter 3 Performance Study of GEHPs	19
3.1 Field Setup and Measurement Devices	19
3.1.1 Instrumentation	20
3.1.2 Installation of Data Acquisition System	23
3.1.3 LabView Program	24
3.2 Data Collection	25
3.3 Data Processing and Synchronization	26
3.4 Analysis	27
3.5 Uncertainty in COP Calculation	30
3.6 Field Operation and Performance Results	31
3.7 Measured Performance	34
3.8 Comparison with Laboratory and Other Field Experiments	35
3.9 Energy Efficiency of GEHP Operations	36

3.10 Economic Analysis	40
3.11 Performance of GEHP vs. EHP	41
3.11.1 DeBary Building Model	41
3.11.2 Economic Analysis	43
3.12 Performance Prediction at Okaloosa, FL and Plant City, FL	44
3.13 Summary and Discussion	45
Chapter 4 Integration of Cooling Thermal Energy Storage in Commercial Buildings	47
4.1 Benefits of Adopting Thermal Energy Storage	47
4.1.1 Benefits to Power Generators	47
4.1.2 Thermal Energy Storage for Air-conditioning	48
4.2 Research Methodology - Thermal Energy Storage for Peak Reduction	49
4.2.1 Location and Case	49
4.3 Building Energy Modeling	50
4.3.1 Building Information Model for Reference Building	51
4.3.2 Model Operation Requirements	54
4.3.3 Cost Minimization	55
4.3.4 Control Requirements	56
4.4 Modified Plant Loop Description	56
4.4.1 Control Strategy	59
4.4.2 System Sizing for Demand Side Management	60
4.5 Performance with New Configuration	61
4.6 Optimization of the System Size for Storage	62
4.6.1 Ice Storage Model Optimization	63
4.6.2 System Optimization for Chilled Water Mixed and Stratified Tank Storage	64
4.7 Results After System Optimization	65
4.8 Economic Comparison and Discussion: Optimal TES System for Commercial Buildings	68
Chapter 5 Impact of Adopting Thermal Energy Storage in Buildings	71
5.1 Tampa Utility Generation and Demand Analysis	71
5.1.1 Benefits of Peak Demand Shifting from Commercial Buildings	72
5.2 TES Adoption Impact on Regional Demand Profile	74
5.3 Benefits of Storage to Power Grid and Renewable Energy Systems	78
5.3.1 Energy Storage Applications	80
5.3.2 Thermal Energy Storage Value for Grid	80
5.3.3 Renewable Generation from Solar	80
Chapter 6 Conclusion	83
6.1 Summary	83
6.2 Conclusions and Recommendations	84
List of References	87
Appendix A Abbreviations	94
Appendix B Copyright Permissions	95

Appendix C Supporting Information for Chapter 3	96
C.1 Data Collection of Operating Parameters	97
C.2 Procedure of Processing Collected Data from GEHP Data Logger	100
C.3 Power Query Code for Data Compilation	119
Appendix D Optimization Results - JEPlus	120
About the Author	End Page

## List of Tables

Table 1. Specifications of GEHP systems at the field	20
Table 2. Measurements sensors accuracy	22
Table 3. June performance of GEHP units	34
Table 4. July performance of GEHP units	34
Table 5. August performance of GEHP units	34
Table 6. September performance of GEHP units	35
Table 7. Engine specification	37
Table 8. Performance variation of GEHP3 for engine RPM range of 1000 to 1950	38
Table 9. Maximum load operation performance	39
Table 10. Case for maximum possible average COP <sub>unit</sub>	40
Table 11. Building characteristics for EnergyPlus model	52
Table 12. GSDT consumer electricity rates for Tampa, FL	56
Table 13. Tactical control functions	60
Table 14. Annual simulation results of optimized configuration	65
Table 15. Commercial building share based on activity	74
Table C.1. Specification of sensors installed at DeBary, FL	96
Table C.2. Validation of correct source files	101
Table C.3. Measured performance data for 4 GEHP units	104
Table C.4. Running costs calculated for the DeBary four GEHP units	105
Table C.5. Model results EER-9.2 EHP system	106



Table C.6. Model results EER-11.8 EHP system	108
Table C.7. Model results EER-12.8 EHP system	110
Table C.8. Model results EER-15.0 EHP system	112
Table C.9. Model results for Okaloosa, FL	114
Table C.10. Model results for Plant City, FL	116
Table C.11. Cost comparison of actual GEHP vs. EHP of different performance ratings for DeBary, FL	118

## List of Figures

Figure 1. World petroleum and liquid fuel consumption by end-use sector 2010 [3]	1
Figure 2. Building energy consumption outlook-US Energy Information Administration	2
Figure 3. Buildings primary energy end-use in the US (2010)	3
Figure 4. 'The Duck Curve' - California ISO's prediction of the demand-supply gaps till 2020 [6]	4
Figure 5. Operation of heat pump and heat engine between two temperature levels	6
Figure 6. Schematic of a vapor compression heat pump [15]	8
Figure 7. Schematic of an absorption heat pump	9
Figure 8. Working principle of a GEHP	12
Figure 9. Useful work lost from the fuel source to cooling end use [23]	12
Figure 10. Office building of Florida Public Utilities, Debary, FL	19
Figure 11. GEHP and AHU configuration at the site	20
Figure 12. Remote data logging system	21
Figure 13. 8-ton units housing condenser and gas-engine	21
Figure 14. Field instrumentation for remote data collection	21
Figure 15. Location of the sensors in the GEHP unit	22
Figure 16. Krohne 1000 coriolis meter with MFC 300 converter	23
Figure 17. IMAC system pulser attached to the natural gas flow meter	23
Figure 18. Dwyer temperature and humidity sensor	23
Figure 19. cDAQ-9138 data acquisition system	23
Figure 20. Natural gas consumption meter	23

Figure 21. Wattmeters for the outdoor units	23
Figure 22. Wattmeters for the AHU's	24
Figure 23. Data logging system	24
Figure 24. Refrigerant flow meters wired and connected to the DAQ system	24
Figure 25. DAQ logging installation inside the warehouse	24
Figure 26. Post-installation setup	25
Figure 27. Schema of USF database	27
Figure 28. Source and host database communication setup for USF server	27
Figure 29. Monthly natural gas consumption by the four gas heat pumps	29
Figure 30. Electricity use by the GEHP1 indoor and outdoor units for the month of August-2014	30
Figure 31. Field performance during summer	32
Figure 32. Cooling delivered and energy use for a typical summer day	32
Figure 33. The performance of the GEHP on a typical summer day	33
Figure 34. Effect of ambient temperature on the COP achieved at 1950 RPM	33
Figure 35. Monthly average unit COP of the four GEHP units	35
Figure 36. Measured performance compared with other studies	36
Figure 37. Efficiencies inside a gas heat pump	38
Figure 38. Brake thermal efficiencies of spark ignition and compression ignition engines	38
Figure 39. Engine efficiency at full load on 1 <sup>st</sup> July-2014	39
Figure 40. Model developed for study building	42
Figure 41. Seven thermal zones air-conditioned by four GEHP units	43
Figure 42. Cost comparison of actual vs. modeled systems	44
Figure 43. Operating costs (\$) of similar systems and loads as DeBary for Okaloosa and Plant City	45
Figure 44. Classification of storage systems [73]	48

Figure 45. Study components for TES use for building	50
Figure 46. DOE reference large office building	52
Figure 47. Occupancy definition for the building	53
Figure 48. Annual cooling electricity	53
Figure 49. Typical daily cooling electricity demand in a building during summer and winter	54
Figure 50. Chilled water cooling loop	54
Figure 51. Two-season peak pricing window for Tampa	55
Figure 52. Ice storage loop configuration	57
Figure 53. Chilled water storage loop configuration	58
Figure 54. Control strategy algorithm	61
Figure 55. Charging and discharging heat transfer	62
Figure 56. Optimization result: annual cost vs. annual cooling electricity	64
Figure 57. Optimization result: average part load ratio vs. annual electricity	64
Figure 58. Chiller power after optimizing the three models	66
Figure 59. Pumping power after optimizing the storage models	66
Figure 60. Chiller part load ratios after optimizing the storage models	67
Figure 61. Week operation in winter (8-15 <sup>th</sup> January)	67
Figure 62. Week operation peak summer (30 <sup>th</sup> July – 6 <sup>th</sup> August)	68
Figure 63. Reduction in annual cost of electricity after optimizing	69
Figure 64. Annual electricity use from three models for selected locations	70
Figure 65. Annual cost of electricity use from three models for selected locations	70
Figure 66. Generation capacity utilization in summer-2013, Tampa	71
Figure 67. Utility load profile for January-2013	72
Figure 68. Utility load profile for August-2013	73

Figure 69. Electricity consumption by end-use in all buildings in South Atlantic Region, 2012, US-EIA	73
Figure 70. Aggregate building electricity demand on 13 <sup>th</sup> August-2013, Tampa, FL	75
Figure 71. Building full peak shifting scenario	76
Figure 72. Partial control- 50% peak shifting scenario	77
Figure 73. Load levelling scenario	77
Figure 74. All scenarios of peak load shifting in buildings	78
Figure 75. Variability in solar generation in four locations	81
Figure 76. Variability in wind generation in four locations	81
Figure C.1. Parameters recorded by GEHP data logger	97
Figure C.2. LabVIEW code front-end at the logging system	98
Figure C.3. LabVIEW back-end program logic	99
Figure C.4. Procedure for processing GEHP data files	100
Figure C.5. PowerQuery used for merging the individual data file to daily data files	103
Figure D.1. System optimization results for ice storage model	120
Figure D.2. System optimization results for chilled water mixed tank storage model	122
Figure D.3. System optimization results for chilled water stratified tank storage model	124

## Abstract

Buildings contribute a significant part to the electricity demand profile and peak demand for the electrical utilities. The addition of renewable energy generation adds additional variability and uncertainty to the power system. Demand side management in the buildings can help improve the demand profile for the utilities by shifting some of the demand from peak to off-peak times.

Heating, ventilation and air-conditioning contribute around 45% to the overall demand of a building. This research studies two strategies for reducing the peak as well as shifting some demand from peak to off-peak periods in commercial buildings:

1. Use of gas heat pumps in place of electric heat pumps, and
2. Shifting demand for air conditioning from peak to off-peak by thermal energy storage in chilled water and ice.

The first part of this study evaluates the field performance of gas engine-driven heat pumps (GEHP) tested in a commercial building in Florida. Four GEHP units of 8 Tons of Refrigeration (TR) capacity each providing air-conditioning to seven thermal zones in a commercial building, were instrumented for measuring their performance. The operation of these GEHPs was recorded for ten months, analyzed and compared with prior results reported in the literature. The instantaneous  $COP_{unit}$  of these systems varied from 0.1 to 1.4 during typical summer week operation. The COP was low because the gas engines for the heat pumps were being used for loads that were much lower than design capacity which resulted in much lower efficiencies than expected.

The performance of equivalent electric heat pump was simulated from a building energy model developed to mimic the measured building loads. An economic comparison of GEHPs and conventional

electrical heat pumps was done based on the measured and simulated results. The average performance of the GEHP units was estimated to lie between those of EER-9.2 and EER-11.8 systems. The performance of GEHP systems suffers due to lower efficiency at part load operation. The study highlighted the need for optimum system sizing for GEHP/HVAC systems to meet the building load to obtain better performance in buildings.

The second part of this study focusses on using chilled water or ice as thermal energy storage for shifting the air conditioning load from peak to off-peak in a commercial building. Thermal energy storage can play a very important role in providing demand-side management for diversifying the utility demand from buildings. Model of a large commercial office building is developed with thermal storage for cooling for peak power shifting. Three variations of the model were developed and analyzed for their performance with 1) ice storage, 2) chilled water storage with mixed storage tank and 3) chilled water storage with stratified tank, using EnergyPlus 8.5 software developed by the US Department of Energy. Operation strategy with tactical control to incorporate peak power schedule was developed using energy management system (EMS). The modeled HVAC system was optimized for minimum cost with the optimal storage capacity and chiller size using JEPlus.

Based on the simulation, an optimal storage capacity of 40-45 GJ was estimated for the large office building model along with 40% smaller chiller capacity resulting in higher chiller part-load performance. Additionally, the auxiliary system like pump and condenser were also optimized to smaller capacities and thus resulting in less power demand during operation. The overall annual saving potential was found in the range of 7-10% for cooling electricity use resulting in 10-17% reduction in costs to the consumer. A possible annual peak shifting of 25-78% was found from the simulation results after comparing with the reference models. Adopting TES in commercial buildings and achieving 25% peak shifting could result in a reduction in peak summer demand of 1398 MW in Tampa.

## Chapter 1 Introduction

Energy is a critical driver for the economic development of the society. There has been a continuous rise in the demand for energy over the last few decades. From 1993 to 2011, the total electricity production increased by 76% whereas the world's population increased by 27% [1]. Despite such increase in electricity production, about 1.3 billion people are still without access to electricity [2].

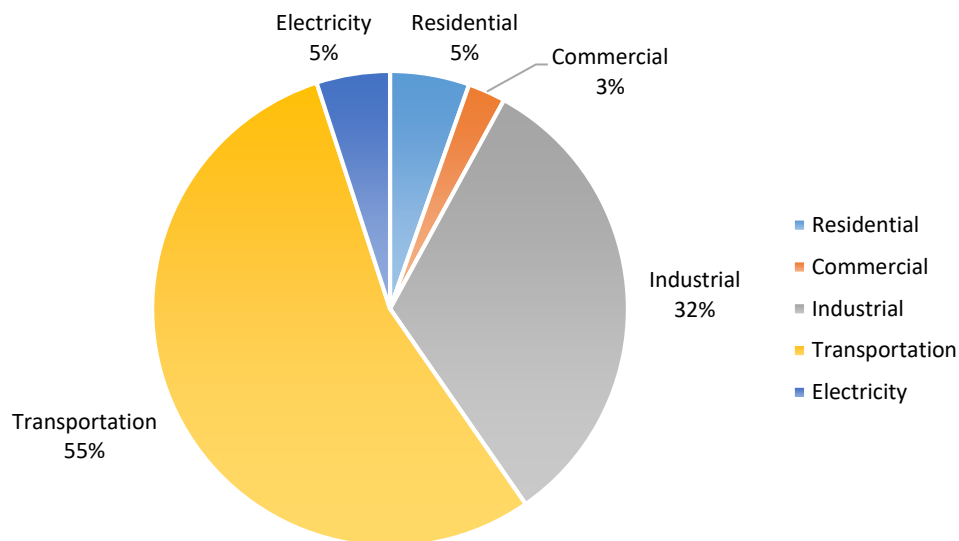


Figure 1. World petroleum and liquid fuel consumption by end-use sector 2010 [3]

Most of the countries rely mostly on fossil fuels for generation of power to serve their industrial, commercial, and residential energy requirements. In 2010, the world petroleum and liquid fuel consumption were 52.3 TWh of which the transportation sector was 55% followed by the industrial sector at 32% and remaining 13% for electricity, residential and commercial sectors (Figure 1). Use of fossil fuels is a significant reason behind increasing global warming. CO<sub>2</sub> emissions have increased by 44% globally, which makes it imperative to use various renewable energy resources and improve the efficiency of current technologies [1].



## 1.1 Energy Consumption in Buildings

In 2010, building energy needs accounted for 23.7 TWh of the world delivered energy demand. It is projected to grow at a rate of 1.6 % per year to 38.4 TWh by 2040. The growth of energy consumption is projected to be maximum in residential sectors in developing nations (Figure 2) [4].

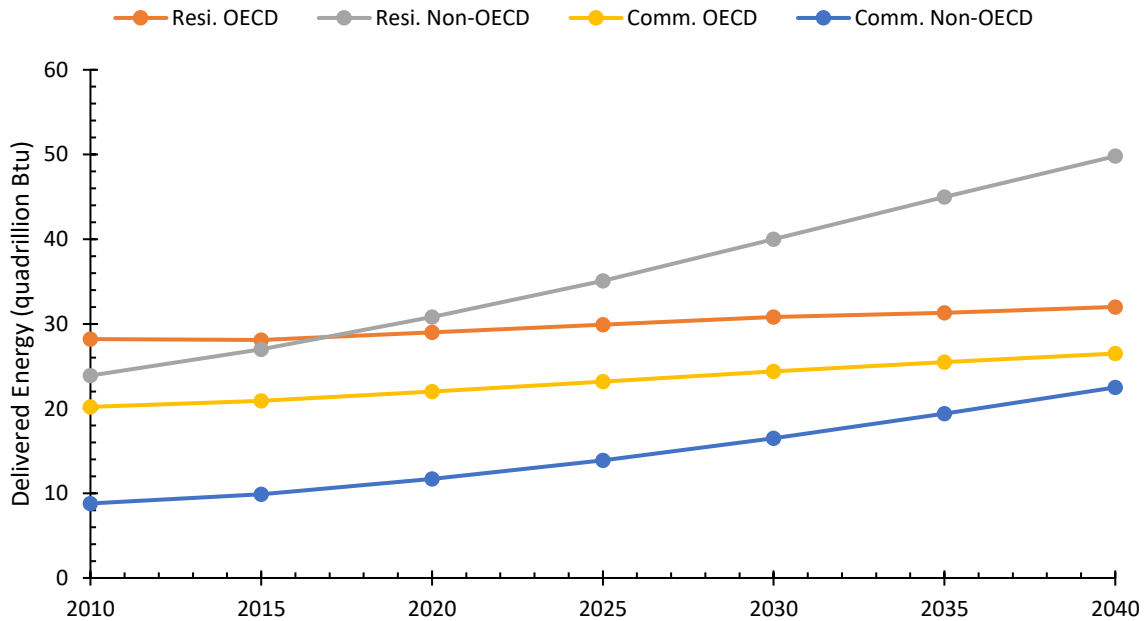


Figure 2. Building energy consumption outlook-US Energy Information Administration

Buildings typically are classified as single or multi-family residential and commercial buildings, of which commercial buildings comprise offices, stores, restaurants, warehouses, government buildings and other buildings used for commercial purposes. In the US, the buildings sector accounted for about 41% of the primary energy consumption in 2010, which included space heating, cooling, and lighting as the dominant end-uses [5].

### 1.1.1 HVAC in Buildings

Heating Ventilation and Air-Conditioning (HVAC) and refrigeration in the US accounted for 47.9% of the total primary energy consumption in buildings in 2010. This energy demand was predicted to fall to 43.7% by 2015 due to improvements in efficiency and upgrade of the existing HVAC technology [5]. Building energy demand varies according to the type of activities, occupancy and weather conditions.

Heat pump (HP) is considered to be a mature technology among the commercial HVAC technologies, and it is found that the residential HVAC market is moving more towards heat pumps instead of furnaces [5]. The estimated industrial energy demand for heat consumption in Europe for 2009 was 12.3 TWh, whereas, in the residential sector it was 18.7 TWh for heating and 4.3 TWh for cooling. In addition, the estimated energy usage in the service sector was 6.1 TWh for heating and 1.7 TWh for cooling. In the US, buildings alone had primary energy end-usage of 11.8 TWh out of which the HVAC&R totaled 5.6 TWh in 2010 (Figure 3). In the US, the aggregated energy expenditure in buildings is projected to rise from \$108.6 Billion (1980) to \$225 Billion by 2035 (USD 2010) [5].

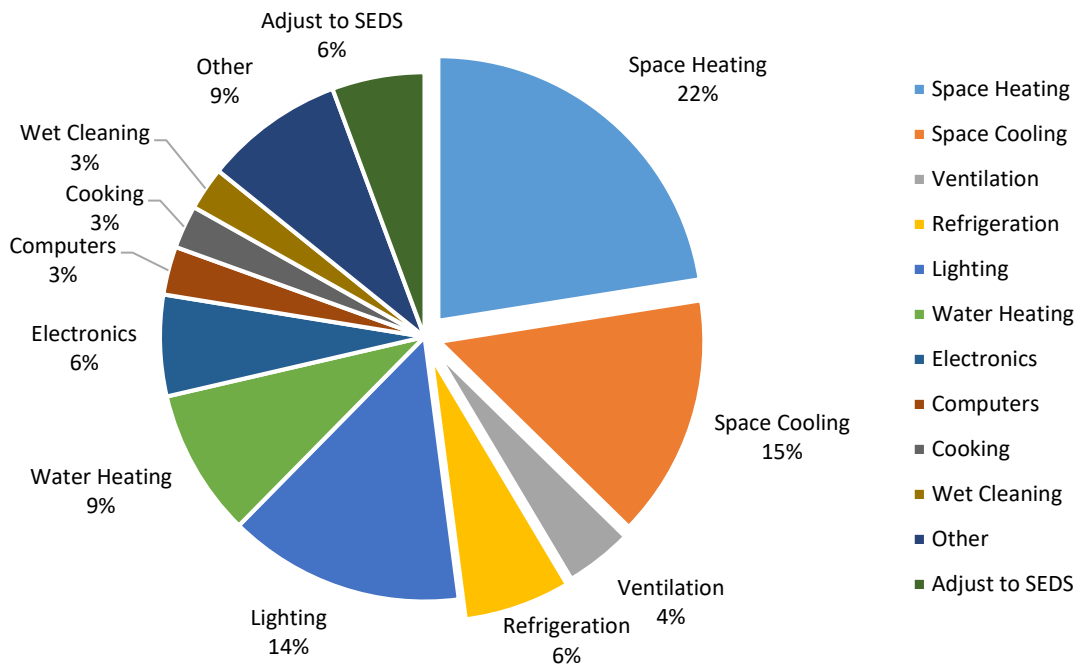


Figure 3. Buildings primary energy end-use in the US (2010)

## 1.2 Challenges for Power Utilities

All possible sources of power are usually exploited to meet the requirements during peak power demands. The cost of electricity for conventional plants is higher during peak hours due to lower efficiencies and higher fuel costs. It can be challenging to match the ever-changing demand of cities and regions while relying on just baseload conventional fossil-based power plants. With the diurnal and nocturnal variations of the energy demand, it becomes difficult for base load power plants to ramp up

and down within a short duration. Use of peaking power plants during such intervals is the only feasible option for the power utilities, and this option is linked to lower efficiencies and high fuel costs [6].

Power utilities must incorporate peak power costs in their tariff to recover the investments and to run their business profitably. For the purpose of billing the consumers based on their usage, many utilities have adopted 'time of day' (TOD) billing that includes different tariffs during different time slots. Being able to meet peak demand, remains a challenge for the power utilities, though TOD billing provides economic viability to the utilities [7]. During peak power demands, the base-load power plants are not able to ramp-up or down to match the immediate changes in power demand. The gaps between peak and off-peak power will keep increasing unless the demand-side energy profile is managed. Figure 4 represents the widely known as 'The Duck Curve' of California Independent System Operator (ISO). This clearly shows that the base load generators experience a sharp dip in demand during the day, and the utilities have to address the increased ramp needed to match the energy demand during evenings [6]. Such ramp rates are a technical challenge for the present baseload power generation plants.

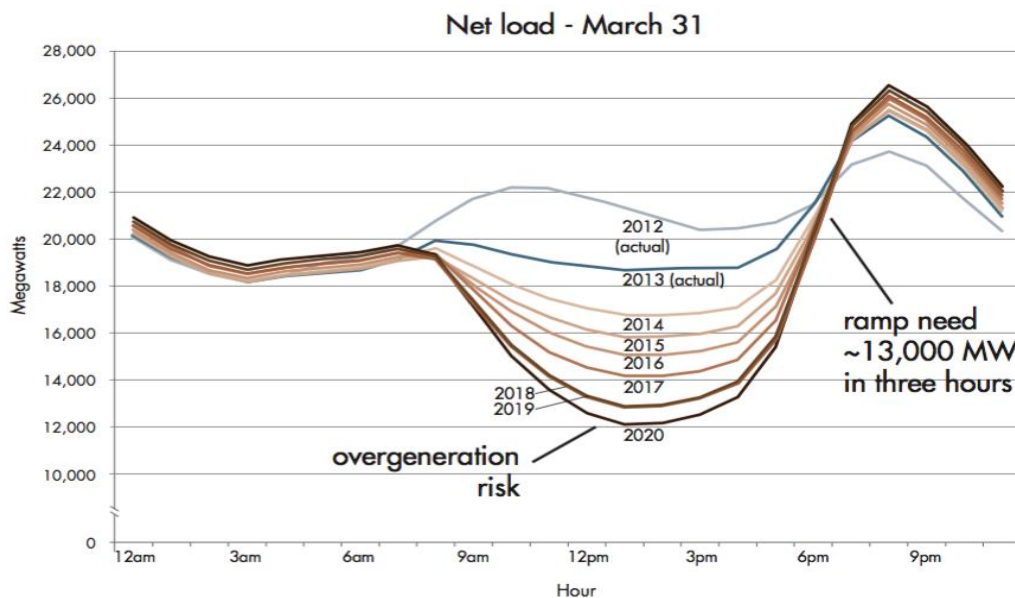


Figure 4. 'The Duck Curve' - California ISO's prediction of the demand-supply gaps till 2020 [6]

Utilities across the world focus on adopting different measures to address such present and future challenges. The gap can be addressed either by adopting (i) supply-side approach or (ii) load-modifier

approach. In the supply-side approach, the generation capacity is increased continuously until the demand-supply gap is bridged or implementing large energy storage for power plants[8]. On the other hand, the load-modifier approach involves changing the demand patterns, increasing efficiencies, and implementing distributed storage.

Since a majority of this demand is attributed to HVAC in buildings, the demand-side-management strategies for HVAC become inevitable to address such a critical issue for future buildings. This study focusses on solutions for demand shaping using two methods: i) alternative HVAC technologies such as Gas heat pumps and ii) adoption of Thermal Energy Storage for air-conditioning. Gas heat pumps use natural gas or biogas to generate the necessary compression work. Alternatively, thermal energy storage can shift electricity demand for cooling and heating thus reducing the peaks and troughs of the energy demand [9].

### **1.3 Theoretical Background**

#### **1.3.1 Heating Ventilation and Air Conditioning in Commercial Buildings**

The need for reliable and economical cooling/heating technologies is ever increasing globally. We realize how humanity will continue to seek higher levels of comfort at their place of work, residence, and commute despite the growing concerns of global environmental impact and related issues. However, the need for more efficient ways to achieve cooling/heating has been a research focus throughout the HVAC&R industry. Industry research focuses mainly on (1) improvement in equipment performance and efficiency, (2) alternative energy sources to power the system and (3) hybrid/combined applications to maximize the useful output by integrating with other technologies.

#### **1.3.2 Heat Pumps**

In 1852, the British physicist William Thomson (Lord Kelvin) described the working principle of “pumping” heat with a thermodynamic cycle for the first time [1852]. In 1856-57, Peter Ritter von Rittinger introduced first “heat pump” of 14 kW in Ebensee/Austria for salt production [1855].

Most widely used heat pumps (HP) work on either vapor compression or vapor absorption cycle. The history of vapor compression cycle goes back to 1834 with the first commercialized system made in 1850. Heat pumps are used for both heating and cooling across the globe all year round. Commercial production of HP's in the United States began in the 1930's, and they became very popular by 1970's as their costs came down significantly. By 1984 about 30% of all the new buildings, both residential and commercial were using HP's [10]. The industrial sector also started to use these technologies for drying agricultural products, and dehumidification [11]–[13]. In Europe, about 4,50,000 electrical heat pumps were installed in the year 2008 [14].

### 1.3.3 Working Principle of Heat Pumps

A Heat Pump is based on a thermodynamic cycle that transports heat from lower temperature source to higher temperature sink. A heat pump works as a reverse heat engine by utilizing work 'W' to extract heat 'Q1' from a lower temperature heat source at 'T1' and deliver 'Q2' to a higher temperature sink at 'T2' and thereby creating a cooling effect as shown in Figure 5.

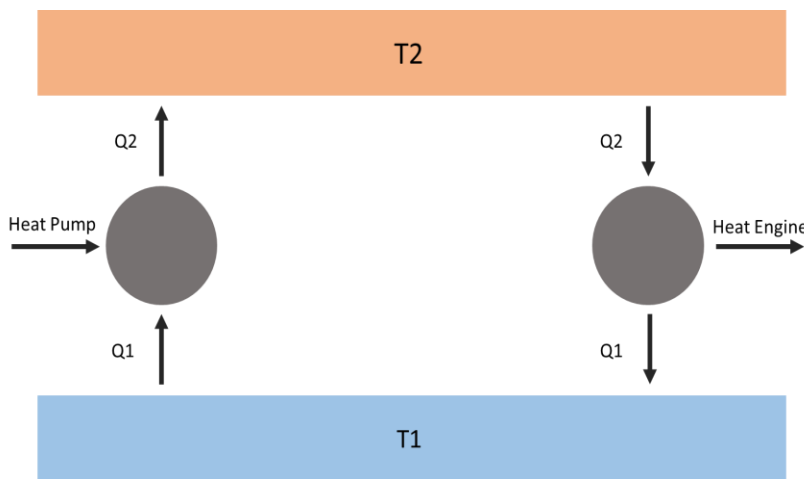


Figure 5. Operation of heat pump and heat engine between two temperature levels

The Coefficient of Performance (COP) is the performance indicator of a heat pump and is calculated as:

$$COP_H = Q_2 / W$$

Primary Energy Ratio (PER) is used as a performance indicator in the case of engines and thermally driven heat pumps. For electrically driven heat pumps this PER can be defined as the product of the COP and the power generation efficiency of the engine that provides the work.

An ideal Carnot cycle operating between the temperatures  $T_1$  and  $T_2$  has the maximum COP, which is given as:

$$COP_C = \frac{T_2}{T_2 - T_1}$$

Real heat pumps cannot work ideally as a reversible cycle due to the presence of losses and limitations of real working fluids. Hence, the  $COP_C$  is used as a reference for the maximum possible limit of performance for real systems. The ratio of the real COP and  $COP_C$  is defined a Carnot efficiency  $\eta_c$ , which varies between 0.3 to 0.5 for small electric heat pumps and 0.5 to 0.7 for large highly efficient electric heat pumps [15].

#### 1.4 Heat Pump Technology

Most commonly used commercial heat pump technologies are (i) the vapor compression heat pumps that use mechanical energy to drive a vapor compression cycle and (ii) the absorption heat pumps that use thermal energy to drive a thermodynamic cycle to create the desired effect. Theoretically, many other thermodynamic cycle and processes can be used for heat pumps, i.e., Sterling cycle, Vuilleumier cycles, single-phase cycles (air or  $CO_2$  gas), adsorption systems, solid-vapor sorption systems, hybrid systems, electromagnetic and acoustic processes. Heat pumps are making way into many sectors due to their advantages of efficiencies and dual conditioning (heating/cooling). Heat pumps are being researched even for mobile applications like vehicles [16]. Many of these technologies have not matured as commercially viable options, with some of them being in their early stage of development [17].

##### 1.4.1 Vapor Compression Heat Pump

A vapor compression cycle uses volatile liquids that have a lower evaporating temperature to generate cooling exploiting the properties of these fluids at different temperatures and pressures. A

compressor pressurizes the refrigerant which heats it to a higher temperature than the selected sink temperature enabling rejection of heat. The cooled refrigerant is then allowed to expand through an expansion nozzle which cools it further to a temperature much lower than the environment (normally outdoors) which becomes the heat source for the heat pump (Figure 6). Vapor compression systems are the most commonly and widely used technology for air conditioning and have been very successful in buildings and other applications. Much research has been already gone in the advancement of modeling and simulation of these systems which has evolved over time with either steady state models or dynamic models [18].

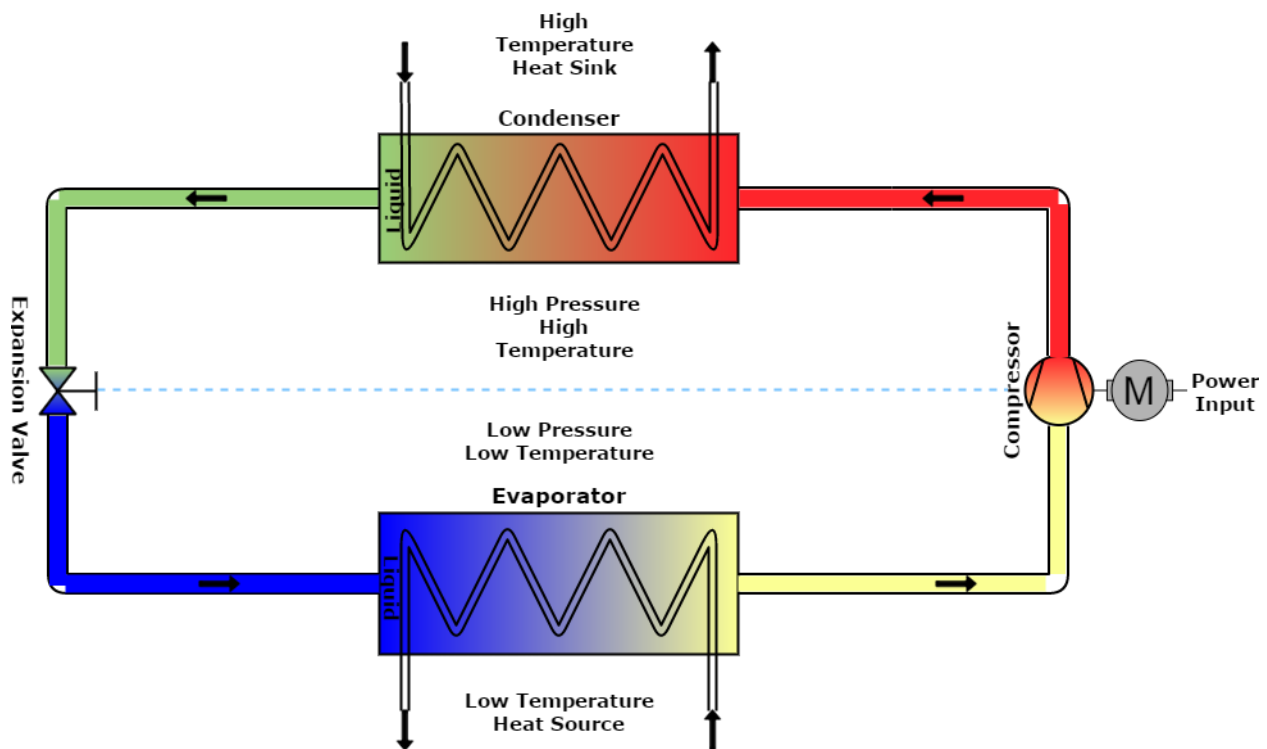


Figure 6. Schematic of a vapor compression heat pump [15]

#### 1.4.2 Absorption Systems

In absorption systems, the working fluid is compressed by using thermal energy in a solution circuit consisting of the absorber, a solution pump, a generator and an expansion valve. Absorption condenses the low-pressure vapor from the evaporator by the absorbent which gets heated by the heat of condensation of the vapor. The solution is pumped to the generator, where the fluid is evaporated

using heat from an external source at a higher temperature. The vaporized working fluid is then condensed in a condenser, whereas the absorbent returns to the absorber after getting cooled further via an expansion valve. The working fluid absorbs additional heat from the heat source in the evaporator. Heat rejected from condenser and absorber can be utilized for auxiliary purposes by modifying the cycle further (Figure 7).

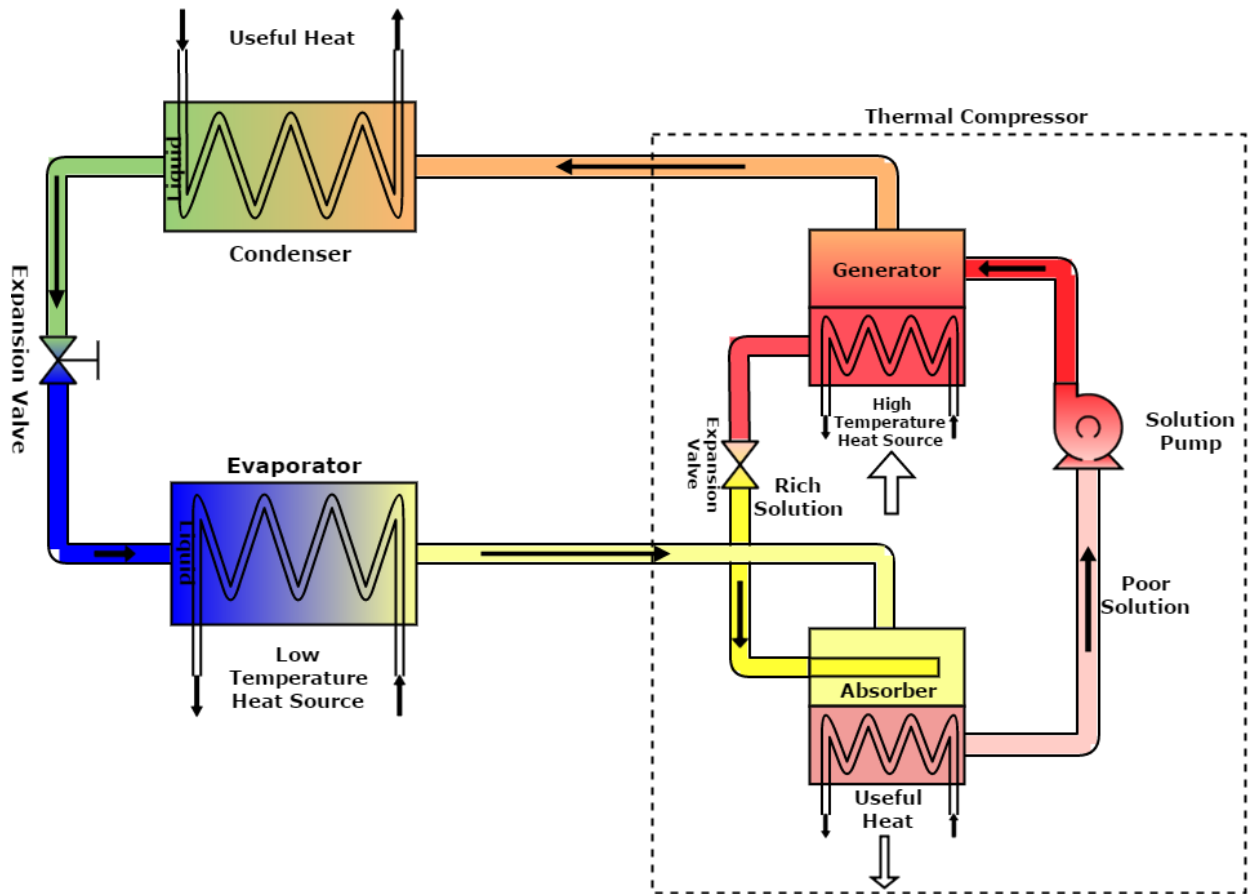


Figure 7. Schematic of an absorption heat pump

In absorption heat pumps, a relatively small amount of electricity is needed to run the pump as compared to an electrically driven vapor compression heat pump. Absorption based cooling and combined absorption cycle based cooling and heating systems have been in use for large cooling systems for commercial and industrial applications historically. Recent developments have enabled the use of heat sources like solar energy and waste heat for absorption based air-conditioning applications [8].



### 1.4.3 Heat Pump Heat Sources

The advantage of a heat pump over conventional heating is that it utilizes the environmental heat or waste heat from another process instead of generating lower grade heat from combustion of high-grade energy source. The most preferred available sources are ambient air, soil and groundwater. These sources of energy indirectly store the energy from the sun and are referred as renewable energy.

COP or performance is related to the temperature difference between the source and sink. Hence, a high temperature of the heat source and a lower sink temperature are preferred to maximize the output.

### 1.4.4 Classification

Types of heat pumps in residential and commercial buildings are:

- Space heating with or without water heating
- Heating and cooling heat pump, providing both space heating and cooling for buildings
- Heat pump water heater

Commonly used heat pumps can be classified based on the type of work input as:

1. Mechanically driven HP
  - a. Package unit
  - b. Split systems
2. Thermally driven HP
  - a. Geothermal Heat Pumps
  - b. Absorption Heat Pumps

There are many other types of HPs depending on the energy source i.e. electric HP (EHP), ground source HP, solar assisted HP, chemical HP, hybrid power systems and gas heat pumps [21].

## 1.5 Gas Engine-driven Heat Pump

Gas engine-driven heat pumps (GEHP) use an internal combustion gas engine to provide mechanical work to the compressor of a heat pump. The first GEHP that was introduced in 1985. Since

then the use of GEHP has spread across the globe for both, space and water heating/cooling purposes [22].

A GEHP brings the benefit of generating the desired mechanical power to run the system by burning gas at the site of use. On-site conversion avoids a two-stage conversion, one at the power station and the other with an electrical motor. This energy conversion can give a higher energy efficiency especially for heating [23].

A GEHP consists of a vapor-compression HP with a compressor that is driven by a gas fired spark-ignition (SI) engine. GEHP's also have an advantage of being able to perform better at part-loads by controlling the fuel supply to the engine and thus providing an ease of control and heat recovery for higher work output [24]–[26]. Additionally, the cooling loads coincide significantly with the utility peak demand, and thus the use of GEHP's can offset the peak energy demand with the use of fuel on site.

#### **1.5.1 Description of GEHPs**

As the name suggests, a GEHP is a gas engine driven vapor-compression HP. The spark ignition engine mechanically powers the compressor instead of an electric motor as in the case of a conventional Electrical Heat Pump (EHP). A GEHP, therefore, is characterized by two main parts (1) an HP with a compressor, evaporator, condenser, and expansion valve and (2) a gas-fired Spark Ignition(SI) engine [26]. In a GEHP, the gas engine produces the necessary mechanical power to drive the compressor using natural gas or any other fuel. The rest of the cycle operates like a conventional vapor compression heat pump involving a reversing valve for the cooling and heating modes (Figure 8).

SI engine part of the GEHP normally has an efficiency in the range of 30-40%. With the use of heat recovery, about 80% of the waste heat from the engine be recovered and utilized, thereby increasing the overall efficiency [22], [27]. The waste heat is recovered from the exhaust gas and the engine cylinder jacket [28], [29]. With higher overall efficiency, the overall negative environmental impact can be reduced. With the use of fuels like natural gas, propane or LPG the overall cost of energy may also be cheaper [26],

[30]. Additionally, the transmission of electricity from remote power plants to the point of use also involves transmission and distribution losses [31]. Based on the above discussion the GEHPs may be more efficient and thus consume less fuel for the same amount of cooling/heating in comparison to EHPs, thus contributing to sustainability by minimizing losses and improving energy availability elsewhere [32].

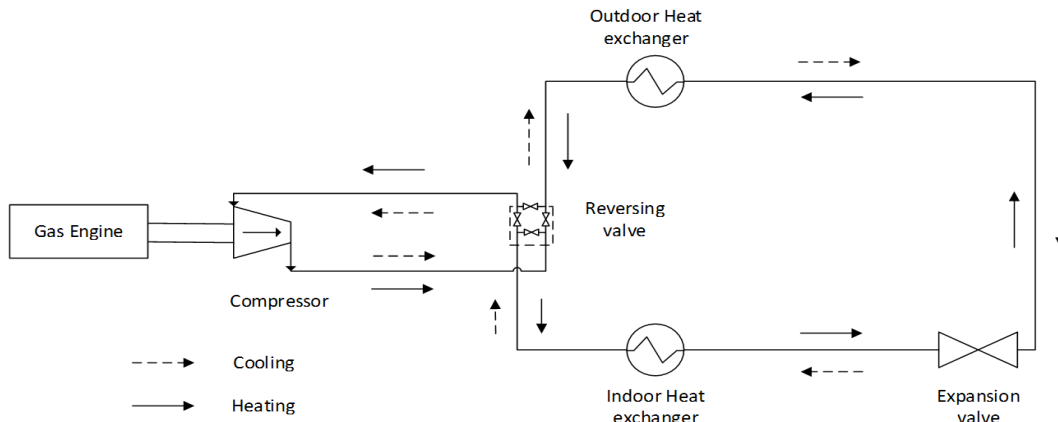


Figure 8. Working principle of a GEHP

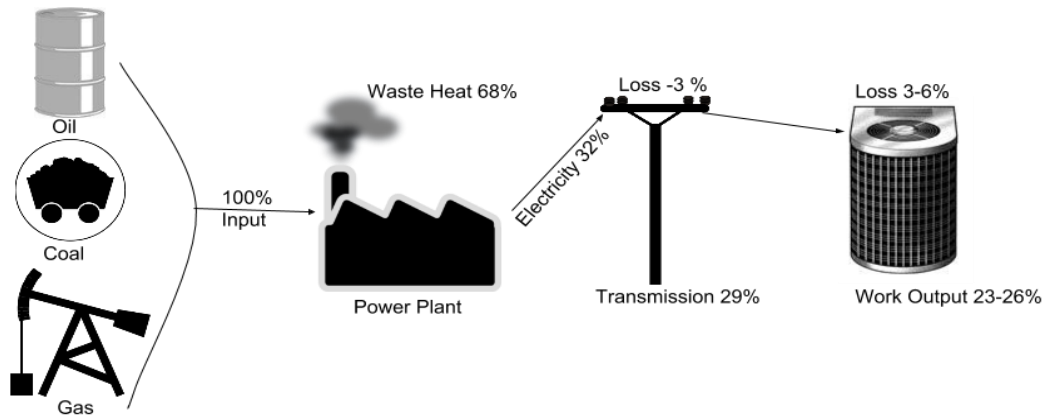


Figure 9. Useful work lost from the fuel source to cooling end use [23]

In the US, the overall efficiency of electricity supply from generation to end use was 33.42% for the year 2013. In other words, to produce 1 unit of electrical energy 2.99 units of the primary energy source were used (Figure 9) [33].

### 1.6 Thermal Energy Storage for Cooling/Heating

With the ever-increasing demand for power and inclusion of non-schedulable sources of energy, the challenges of providing reliable power to the people also increase. To integrate renewable energy

sources into the power grid and to be able to support the demand, thermal energy storage is an excellent option. However, the success and scale of use for different energy storage technologies are yet to be tested globally. Research in this direction is going on from a buildings perspective or larger utility scale storage systems.

Thermal Energy Storage (TES) and other storage technologies can help level the peaks and troughs of power demand by storing energy during off-peak hours and supplying energy during the peak hours. TES can help in improved demand management with reduced uncertainties in the available generation capacities.

TES can benefit the grid by providing quick response storage as needed. Additionally, TES in buildings can also help the load side to overcome disturbances due to power failures. It is, therefore, important to quantify such benefits in terms of avoided costs and system improvements resulting from the avoidance of expensive peaking power plants.

Various energy conservation approaches are implemented globally to shave the peaks of power demand curves and reduce the overall energy use. Such approaches include changing the energy consumption patterns by motivating behavioral changes and upgrading with efficient technologies. Another perspective on the improvement in this scenario is to manage the demand profile in a way that is economical and efficient.

Building Thermal energy storage has been researched over the past few decades. Most studied storage media for air conditioning have been ice and chilled water. Laybourn et al. in 1985 highlighted such benefits of TES for a commercial building through an experimental demonstration [34].

TES is one of the most feasible solutions to achieving sustainable energy utilization by buildings. The applicability of TES for heating and cooling applications have been studied by many researchers [35]–[40]. Hasnain et al. compared the pros and cons of most common TES technologies for cooling (i.e. chilled water and ice storage) in 1998 [41]. Sebzali et al. compared the performance of chilled water thermal

storage and conventional air-conditioning systems and reported a potential reduction of peak power in the range of 36.7 - 87.5% and annual energy consumption of about 4.5 - 6.9% [42].

The implementation of TES for buildings requires control strategies that can be active or passive [43]. TES in buildings would involve understanding the optimum level or charge and discharge of the storage and its interaction with the building thermal loads. Various simulation-based studies have been done to understand the technical feasibility and operational strategies of using different types of active TES for buildings. Zhang et al. demonstrated the optimum storage sizing for an integrated four chilled-water plants and single storage system for a payback period of 12.5 years in Austin, TX [44]. Henze et al. proposed optimal operation strategies to maximize the performance of ice storage systems adopted for commercial buildings in their simulation-based study [45]. Some researchers worked on the reduction of energy costs and peak electrical demand with the use of TES [46]–[50]. Many of these studies focused on developing and demonstrating control strategies for the operation of a storage system with buildings HVAC systems [46], [51], [52].

Once such optimization strategy is developed, TES can be used to meet a part of the peak power demand [53]. Utilities that face capacity constraints and purchase peak power from third-party power generators would benefit by minimizing peak demands and utilizing the off-peak base load power capacities.

### **1.6.1 Benefits to Consumer**

Although benefits of TES are meaningful and relevant, they have not translated into significant implementation. The benefits must consider performance without sacrificing the comfort of the occupants in the building. TES helps in reducing the consumer's peak cooling demand which also reduces the needed chiller capacity required to meet peak loads.

Additionally, USGBC's (U.S. Green Building Council) LEED (Leadership in Energy and Environmental Design) certification program for buildings provide motivation and encouragement to building owners and

planners to improve building energy performance [54]. TES for buildings is considered as a green technology in LEED system as it provides the option of using low-cost off-peak electricity at night as compared to high-cost peak electricity during days [55]. In addition, the generation units operate at higher efficiencies during off-peak hours as compared to peak hours [56].

Use of thermal energy storage in existing and new buildings helps to gain additional LEED points by surpassing ASHRAE standards, which is based on the cost of energy savings. TES is also beneficial economically where time-of-day tariffs exist. There are different categories under LEED building rating system where TES is accounted for improvements for 'Energy and Atmosphere credit (EA Credit)' as [54]:

- EA Credit for Optimize energy performance: Can provide an opportunity to earn points up to 18 by surpassing ASHRAE standard by 50%. The potential efficiency measure target at load reduction, HVAC- related strategies for energy savings.
- EA Credit for Demand Response Point: The building owner can earn up to 2 points by Participating in any existing demand response program and reducing the peak demand by at least 10% determined under EA Minimum Energy Performance Prerequisite.

### 1.6.2 Benefits to Utilities

Utilities face significant challenges to maintain reliable, on-demand, quality power requiring rapid ramp up and down generation in response to the demand. Significant penetration of energy storage is envisaged as the key to successful adoption of renewable generation from solar and wind electric generators that are intermittent in nature. Power plants use this stored energy to provide schedulable electric power. However, building TES can provide the same benefit to the electric utility by decreasing the peak power demands, when resources such as the wind and solar are not available. The response time for such storage systems can be small as compared to the time taken by fossil fuel based power plants to ramp up and down. This can benefit utilities by reducing additional capacity requirements to meet future peak demands. Avoided cost of peaking power plants by utilities and optimization can be an added value.

As building thermal energy systems typically are managed by the owner, their actual value can be derived from the reduction in heating and cooling capacity requirements and a reduction in running costs [57].

Few considerations highlighting the benefits are:

- Higher ramp challenges faced by the power plant can be limited to operable limits, thereby reducing the operation and maintenance challenges. Improvement by increasing the demand for off-peak generation from the base load power plants.
- Shifting the operation of the power plant to ambient conditions when the generation efficiency is higher, i.e. higher efficiencies during the night vs. hot summer day. The cost of generation is lower for a base load plant during night time due to underutilized capacities with lower PLF operation.
- Reduction of the peak demand from HVAC systems as they run at higher COPs for longer durations. The reduction in HVAC capacity reduces the burden on the utilities to provide the power and, hence, the growth rate of peak power demand is flattened or even reduced.

## Chapter 2 Research Objectives

- Objective 1: Measure the field performance of a GEHP and analyze it in comparison with EHP for commercial buildings.

Gas heat pumps are expected to be more economical in providing cooling and heating for offices located in Florida and other hot and humid regions. Study the operating efficiency during part-load operations compared to electric heat pumps.

- Objective 2: Design a TES model with chilled water and ice storage for air conditioning in commercial buildings.

Develop a cost minimization strategy for energy use by commercial buildings.

- Objective 3: Quantify the benefits of adoption of TES for HVAC applications for consumers and power utilities.

Find and quantify how the adoption of TES for HVAC in commercial buildings has higher technical viability, economic benefits, improved power profile, increased renewable energy generation capacity and reduced baseload power plant capacity requirement.

GEHPs have been in use since 1985, and since then, there has not been much research published highlighting their field performance. A recent laboratory study has demonstrated that GEHP is favorable for energy conservation and are economical than conventional electric heat pumps in the field [58]. Lack of rigorous research on this topic limits the scientific validity of the GEHP performance and needs to be tested. Additionally, a study in a laboratory usually differs significantly from the actual field operation performance. The research under Objective 1 presents detailed field performance testing of GEHP vs. EHP for a commercial building along with the analysis and proposed improvements. A comparative economic



analysis is also presented for GHEP and EHP systems for providing cooling and heating for an office located in Florida for a yearlong operation. The operational efficiencies of field GEHP systems are also compared with published studies by other researchers for part-load operations and compared to equivalent models of EHP systems under similar conditions. This research is aimed to validate the findings of the previous research and contribute to the scientific community to understand and improve the design and sizing of GHEPs for higher efficiency.

Studies have shown the viability of using large scale storage by utilities aimed to meet the dynamic electric demand [57]. However, the benefits of using TES for HVAC in buildings are not quantified to show benefits for both utilities and consumers. The current research objectives are focussed on: (a) developing a TES model for HVAC with a cost minimization strategy of the energy used by commercial buildings, and (b) quantifying the benefits of using TES in HVAC applications for both consumers and power utilities. These benefits are quantified by avoided costs by the utility, advantages of adoption of renewable power, and improvements in grid quality by using storage to overcome the intermittency of renewable power generation. The results will help in making decisions related to long-term power planning, efficient adoption of renewable technologies and support of policies for TES as a demand side option for utilities. The results will also highlight the potential economic benefit of using TES in buildings by consumers by reducing operating costs.

## Chapter 3 Performance Study of GEHPs<sup>1</sup>

### 3.1 Field Setup and Measurement Devices

Four sets of variable refrigerant volume (VRV) GEHP outdoor units and fan coil units are installed and being used at a commercial office at Debary, Florida (Figure 10). Each GEHP unit has a capacity of 8 TR (Ton of Refrigeration) and together supply to seven thermal zones in the building with an area of about 10000 ft<sup>2</sup> (Figure 11). Unlike other studies of GEHP in the past that were done in laboratory setups where the operating temperatures are set constant to evaluate the maximum performance of the systems, the present study was designed to monitor field operation and analyze the performance of these units under actual outdoor conditions. The specifications of the GEHP units installed at the study site are given in Table 1.



Figure 10. Office building of Florida Public Utilities, Debary, FL

<sup>1</sup> This chapter was previously published in [76]. Permission is included in Appendix B

Table 1. Specifications of GEHP systems at the field

S No.	Item	Description
1	GEHP- Natural gas powered outdoor units	8 TR multi-zone
2	Engine capacity	7.9 kW
3	Air Handling Units	7 units
4	Rated cooling capacity of each GEHP unit	96,000 BTU/h
5	Rated heating capacity of each GEHP unit	103,000 BTU/h
6	Compressors	2- one fixed and one variable flow
7	Refrigerant	R410a

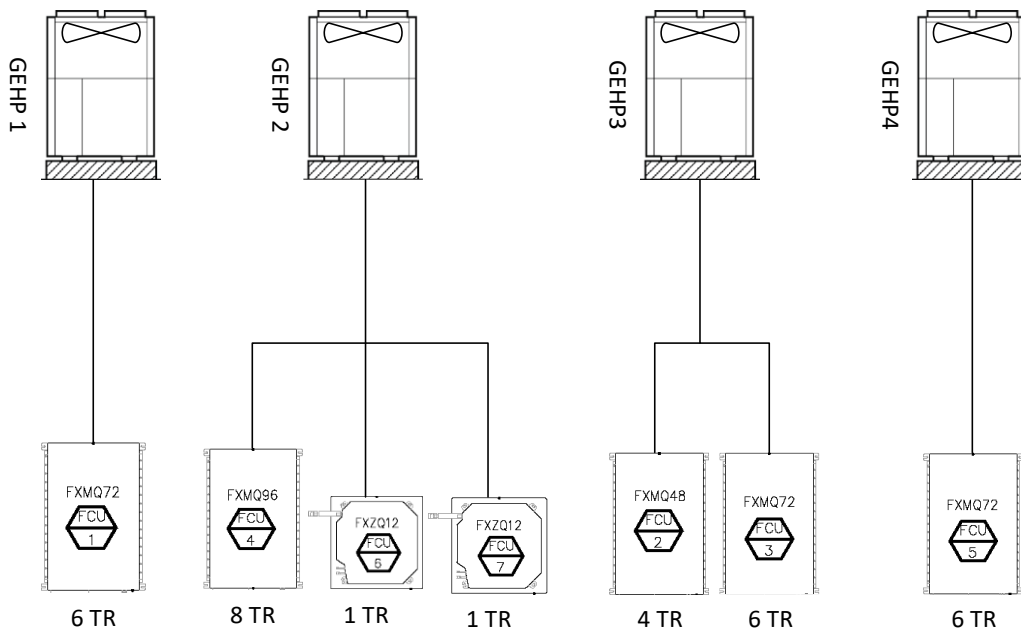


Figure 11. GEHP and AHU configuration at the site

### 3.1.1 Instrumentation

The indoor and outdoor units were already equipped with sensors to measure temperature, pressure, engine rpm, an electronic expansion valve (EEV) position and other operating parameters as shown in Figure C.1. The operational data was recorded on a local computer in a proprietary file format provided by the manufacturer. Additional sensors were installed to measure the temperature/humidity of the zones, refrigerant flow rates, natural gas consumption, and electricity use. A data acquisition system (NI-cDAQ9138) with an onboard computer to run a local data server for recording operation data was also installed (Figures 12, 13). Sensors were installed and connected to the data logger as shown in Figure 14.

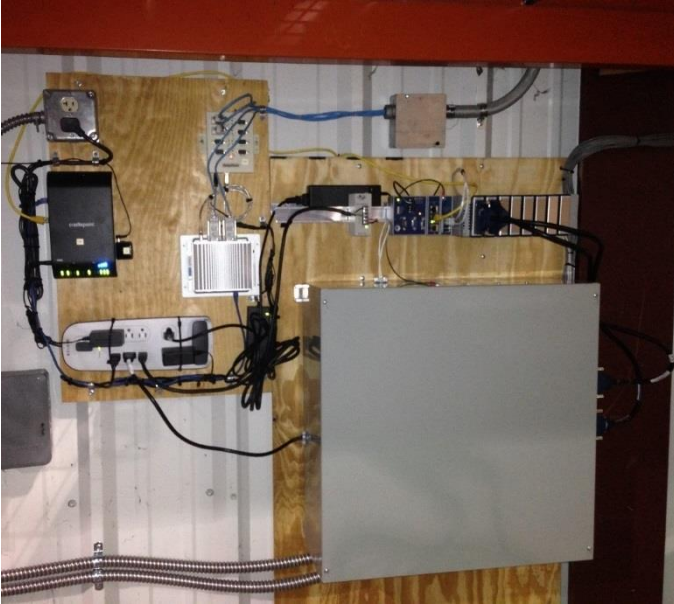


Figure 12. Remote data logging system



Figure 13. 8-ton units housing condenser and gas-engine

A second server was setup at the University of South Florida to store the data remotely from the on-site server. The instantaneous performance data was stored locally and then transferred every day to the USF server in batches to provide enough redundancy in times of network failures.

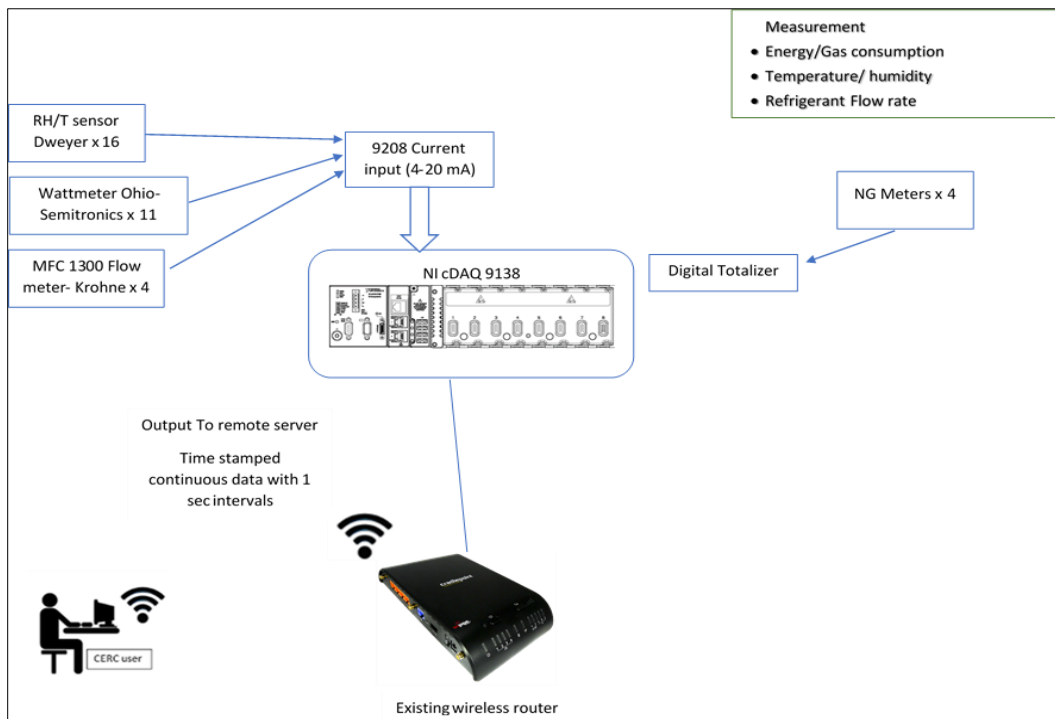


Figure 14. Field instrumentation for remote data collection

Table 2 presents the specifications of the additional sensors installed to measure the ambient conditions, refrigerant flow, temperature, humidity, pressure, gas consumption and the indoor comfort along with their rated accuracy. Figure 15 shows the location of the sensors in each GEHP unit that provide the operating parameters recorded by the data logger.

Table 2. Measurements sensors accuracy

S. No.	Measurement	Sensor Type	I/O	Range	Accuracy
1	Power consumption	Watt meter	4-20 mA	0 - 5000 W	±0.5% of full scale
2	Refrigerant flow (Figure 16)	Coriolis meter	4-20 mA	0 - 6500 kg/h	±0.15% liquid and ±0.5% for gas (-40°C to 130°C)
3	Temperature (Figure 18)	Temperature sensor	4-20 mA	(-)10°C - 120°C	± 0.1°C at 0°C and ± 0.3 at 100 °C
4	Humidity	Humidity sensor	4-20 mA	0 - 100 %	± 2% (10-90% RH) at 25°C
5	Gas consumption (Figure 17)	Volumetric flow meter	Digital counter	0 - 7.8 m <sup>3</sup> /h	± 2% (-28.8°C to 48.8°C)
6	Pressure	Pressure	NA	0 - 4.5 MPa	± 2% of full scale

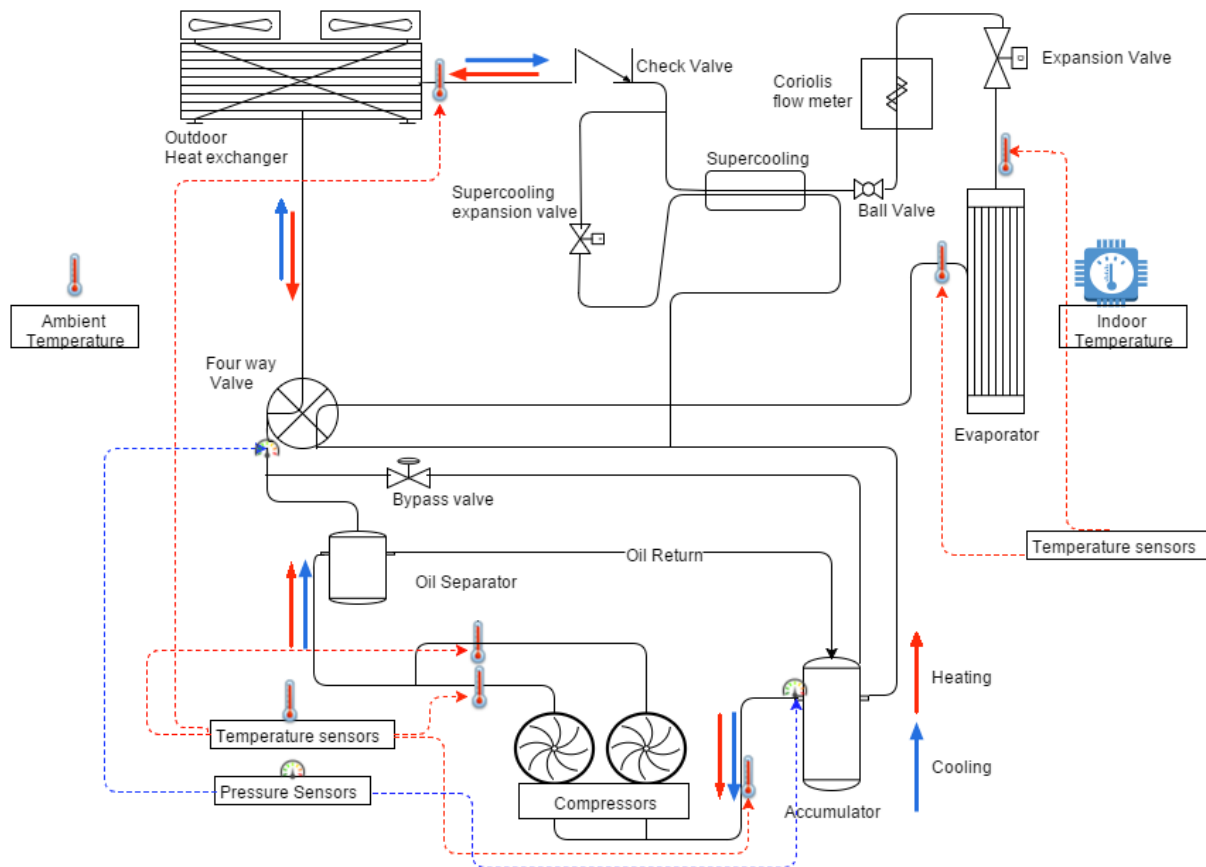


Figure 15. Location of the sensors in the GEHP unit



Figure 16. Krohne 1000 coriolis meter with MFC 300 converter



Figure 17. IMAC system pulser attached to the natural gas flow meter



Figure 18. Dwyer temperature and humidity sensor



Figure 19. cDAQ-9138 data acquisition system

### 3.1.2 Installation of Data Acquisition System

Installation of the sensors and the data acquisition (DAQ) system (Figure 19) was started in the first week of May 2014. Figures 20 and 21 show the installed gas meter and Wattmeters on the site.



Figure 20. Natural gas consumption meter



Figure 21. Wattmeters for the outdoor units

The DAQ system displays and records timestamped operating parameters every second from the connected sensors. The data collected is then transferred to a remote server (located at USF, Tampa)

twice daily and is deleted from the on-site database to clear the limited onboard memory. This approach provided us the flexibility of storing operating parameters in a structured database, improving the availability, and usability of the collected data.

Figures 22 and 23 show the installed data logger and the Wattmeter inside a safe enclosure. Krohne 1300 refrigerant flowmeters were connected to the data logger and were externally powered (Figure 24). Figure 25 shows the completed instrumentation of the GEHP outdoor units wired and connected to record the energy input and flow rate.

### 3.1.3 LabView Program



Figure 22. Wattmeters for the AHU's



Figure 23. Data logging system



Figure 24. Refrigerant flow meters wired and connected to the DAQ system



Figure 25. DAQ logging installation inside the warehouse

A LabVIEW program was developed to record data remotely with the following features:

- Recording the instantaneous and timestamped values from each sensor every second;
- Connecting to the remote PostgreSQL server and writing the data;
- Writing scaled and unscaled values of the sensors incorporating unit conversion.

The development of the program to capture the data took about a month of testing and debugging with the final representative tool as shown in Appendix Figures C.2 and C.3. This program was configured to record all the additional sensors installed for this study. The LabVIEW program was capable of running locally on the data logging system and recording data from the new sensors on a PostgreSQL database. The native GEHP data logger was used for recording all the pre-existing sensors within the GEHP and AHU units.



Figure 26. Post-installation setup

### 3.2 Data Collection

The data collection at the FPU site started on May 9, 2014, which was tested and commissioned on May 30, 2014 (Figure 26). The GEHP data logger captured the operating parameters in 108 fields from the outdoor unit and 20 parameters from the air-handling units that were time-stamped every second. The structure of instantaneous data record is available from the '\*.AnD' files generated as shown in Appendix C.2.



A select number of operational parameters were used to estimate the energy consumption and cooling delivered from the collected data of each GEHP unit. The sequence of operations involved in the periodic data collection and migration is as follows:

- Connection triggered to field data logger by the server,
- Flag data 'to be copied' on the host computer,
- Move data to USF server,
- Flag data as 'copied,'
- Check data for correctness and completeness after copy process,
- Flag data on CERC data logger as copied,
- Delete the data copied in the last transaction from field database,
- Disconnect from the remote data logger.

### 3.3 Data Processing and Synchronization

The native GEHP data logging tool was highly unstable and vulnerable to power failures resulting in loss of data without alerts to the operator. This data was collected in a proprietary '\*.AND' file format that was not readable unless converted to separate CSV files using a manufacturer provided program (each file had 3600 rows of data from the outdoor and indoor units). The indoor unit data file did not have a timestamp and hence merging the data to the outdoor unit file for correct interpretation was deemed necessary. Procedures were developed for conversion as explained in Appendix C.2.

The PostgreSQL database structure of both the datasets is shown in Figure 27, where 'sensor\_data\_backup' is the table for all the data collected through CERC data logging procedures and GEHP1 through 4 are the tables with the data gathered by the native GEHP data logger. The CERC database included all the processed data from all sources with correct timestamps for analysis. Figure 28 details the communication infrastructure deployed to perform this task continuously.

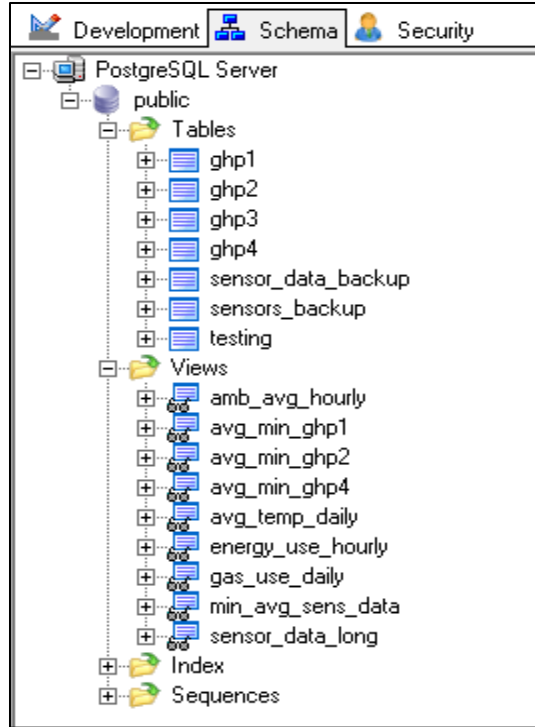


Figure 27. Schema of USF database

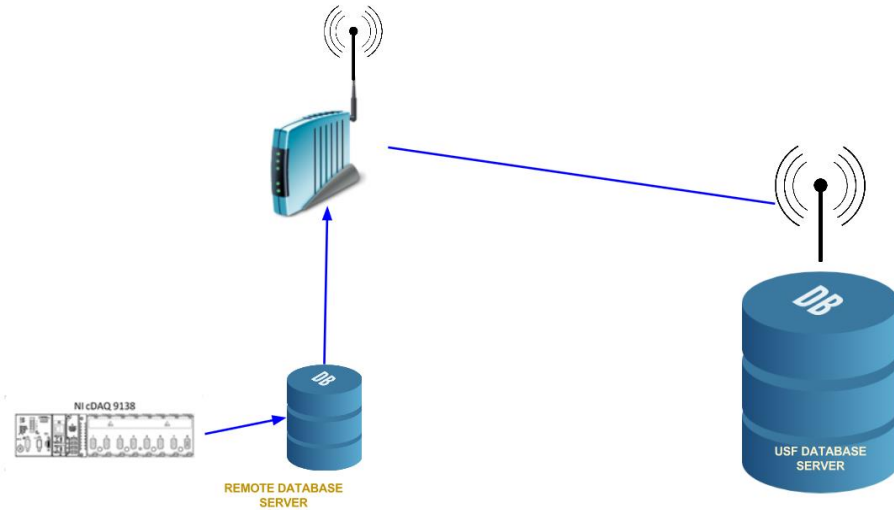


Figure 28. Source and host database communication setup for USF server

### 3.4 Analysis

Refrigerant-side capacity measurement technique was used to estimate the cooling delivered by each GEHP unit. During Operation, as the refrigerant passes through the evaporator, the specific enthalpy change in the process was calculated using the temperature and pressure measured at the inlet and outlet of the coil.

The evaporator-side heat delivery rate is found from the relation:

$$Q_{evap} = \dot{m}(h_o - h_i)$$

where  $\dot{m}$  is the refrigerant mass flow rate  
 $h_o = h_{vap}(T_o, P_o)$  vapor enthalpy at the evaporator exit, and  
 $h_i = h(T_i, P_i)$  enthalpy of two phase mixture at the evaporator inlet

The thermodynamic properties of refrigerant R410a were acquired from REFPROP© for all calculations [59][60]. The electric energy consumed by each GEHP unit is the sum of all the electricity during selected period is found by integrating the power over the period as:

$$\text{Electric energy used by each GEHP} = \int W_e dt$$

The energy from the natural gas consumed is given by

$$\text{Total energy from NG used} = \int W_{ng} dt$$

The cooling/heating delivered is calculated as:

$$q_{cool/heat} = \dot{m}(h_o - h_i)$$

$$COP = \frac{\text{Cooling}}{\text{Energy Input}}$$

where  $W_e$ =energy from electricity  
 $W_{ng}$ =energy from natural gas

The natural gas consumed by each GEHP unit was used as the prediction baseline for annual performance. Figure 29 shows the monthly natural gas consumption for the four GEHP units at DeBary, FL during the study period. It was observed that the natural gas consumption of the GEHP1 was lowest among all the units. However, this does not imply that this unit performed most efficiently. The COP for each GEHP unit was used as the performance indicator in this study during field operation.

Typically, the performance of heat pumps is measured by calculating the coefficient of performance (COP) for cooling or heating application, which is the ratio of the delivered cooling to the primary energy used.

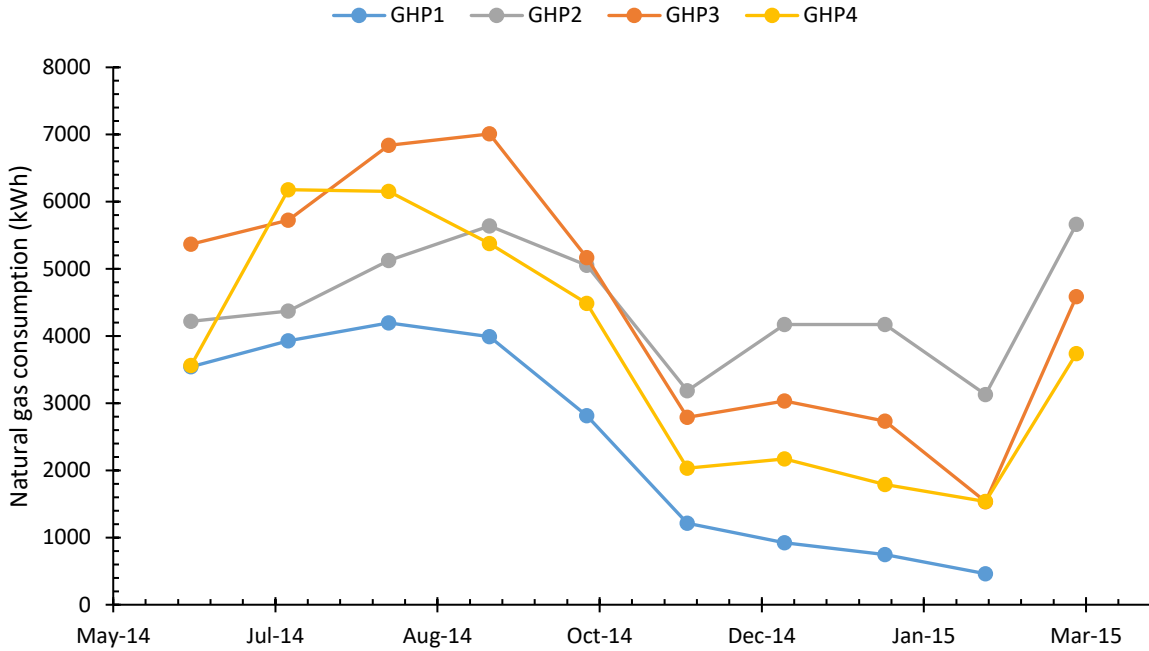


Figure 29. Monthly natural gas consumption by the four gas heat pumps

In the case of a GEHP system, the energy input is from natural gas as compared to electricity in conventional heat pumps widely used in the sector. Therefore, a direct comparison of such systems is difficult, unless it is based on the primary energy input. Hence, for comparative analysis,  $COP_{unit}$  is considered which excludes the electricity use.

$$COP_{unit} = \frac{\text{Cooling delivered}}{\text{Primary energy input from fuel}}$$

The indoor AHU's and the condenser fans use electricity for both electric heat pumps and gas heat pumps. The technological difference between the two systems is the type of energy used to drive the compressor, which is gas in case of the GEHP units, whereas electricity for the electric heat pumps. Therefore, for a meaningful comparison of the performance.  $COP_{unit}$  is calculated as the ratio of the cooling/heating delivered to the primary energy that is natural gas in the current study.

Figure 30 shows the electricity consumption of the GEHP4 and the corresponding air handling units (AHU) during the month of August 2014. As the compressor is driven by a natural gas based gas-engine, the electricity used by the outdoor units was significantly lower than the corresponding AHU. In a

complete system, the electricity consumed by a condenser fan is considerably lower than electricity used by AHU.

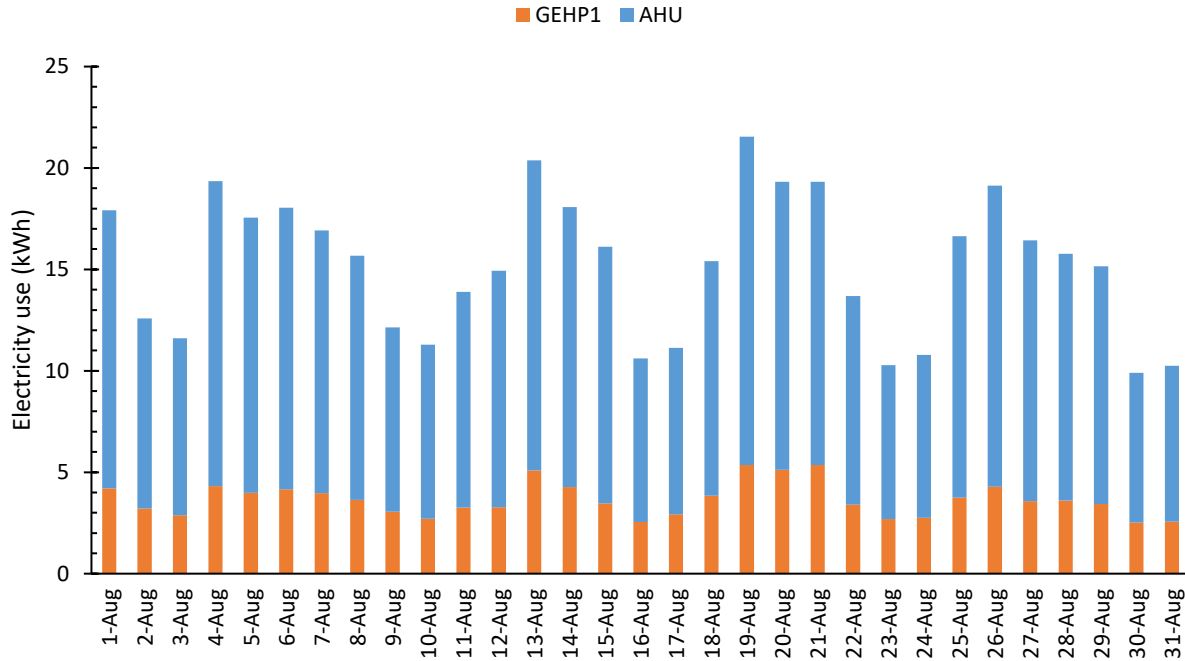


Figure 30. Electricity use by the GEHP1 indoor and outdoor units for the month of August-2014

In a vapor-compression heat pump systems, the electrical consumption of fans and other auxiliary components of a condensing unit and AHU's for a heat pump are identical whether the heat pump is a traditional electric or based on the natural gas engine. Hence, the electricity used by the outdoor unit fan is excluded from the calculation of  $COP_{unit}$  for meaningful comparison which is usually less than 3% of the natural gas use.

### 3.5 Uncertainty in COP Calculation

Table 2 presents the sensors and their measurement accuracy used in this study. The uncertainty in calculated  $COP_{unit}$  is determined based on the following equation [61].

$$W_{COP} = \left[ \left( \frac{dCOP}{dx_1} * w_1 \right)^2 + \left( \frac{dCOP}{dx_2} * w_2 \right)^2 + \left( \frac{dCOP}{dx_3} * w_3 \right)^2 + \left( \frac{dCOP}{dx_4} * w_4 \right)^2 + \left( \frac{dCOP}{dx_5} * w_5 \right)^2 \right]^{1/2}$$

where x=measured variable (temperature, refrigerant flow rate, gas consumption, enthalpy, and pressure)

$W$ =uncertainty associated with each measurement

Assuming a confidence interval of the measurement devices to be within 95% and using the above relation, the maximum uncertainty in  $COP_{unit}$  was calculated as  $\pm 18.02\%$ . The higher uncertainty is contributed by the reported refrigerant temperatures by the onboard data logging system. The temperature was reported as whole numbers instead of fractions that resulted in higher uncertainty in COP calculations.

### 3.6 Field Operation and Performance Results

The performance of the GEHP units was determined by calculating the cooling produced using the refrigerant side capacity method as explained in section 3.4. The heat content of the natural gas (primary energy source) was taken as 1,016 Btu/ft<sup>3</sup> for calculations [62]. Natural gas SI engine coupled with a compressor producing the mechanical work required in a GEHP system. Each unit of primary energy used in the SI engine produce some units of cooling in the building zones, which varied based on the local weather and load conditions. During the summer season, the average  $COP_{unit}$  of the GEHP over a weeks' time was found as shown in Figure 31.

The instantaneous  $COP_{unit}$  of the GEHP's varied during this period from 0.1 to 1.4 during the GEHP's daily operation. Observed  $COP_{unit}$  low values are primarily during the system idle mode once the setpoint temperature is reached and higher values are found when the full load operation is triggered as shown in Figure 31. It was also observed that during hot and humid days, the GEHP running time significantly increased resulting in higher  $COP_{unit}$ .

The operating parameters of one GEHP unit for a typical day are presented in Figure 32, while the performance indicator ( $COP_{unit}$ ) is shown in Figure 33. The GEHP operation was found to be unsteady, and hence, resulted in fluctuations in the recorded data points. The natural gas consumption and cooling produced was intermittent as the GEHP units cycle 'on' and 'off' frequently while controlling the indoor temperature.

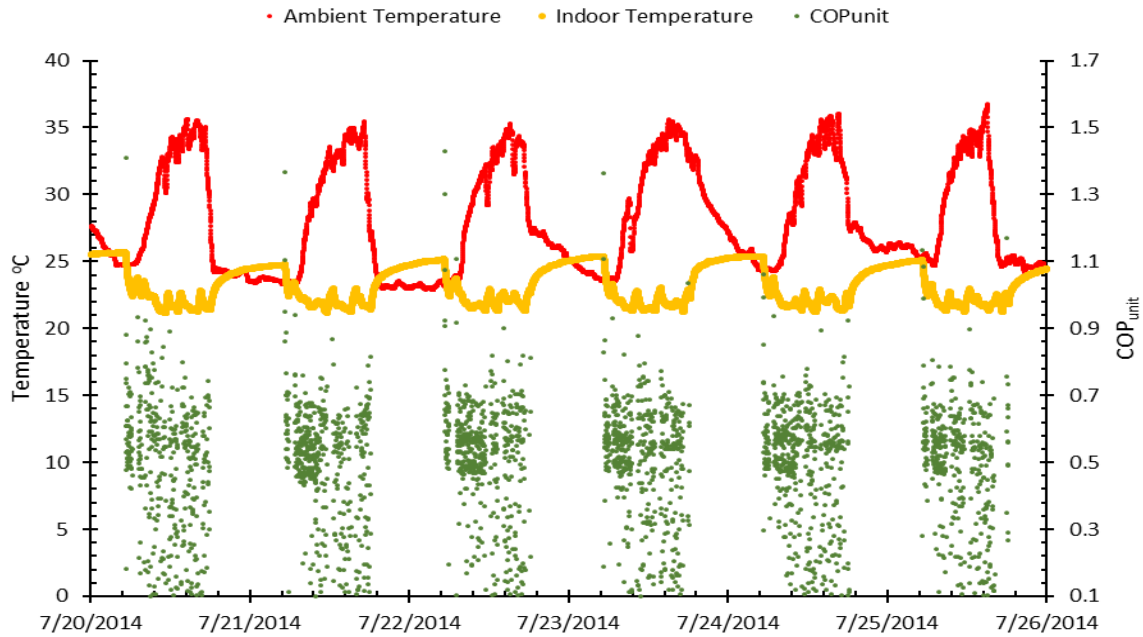


Figure 31. Field performance during summer

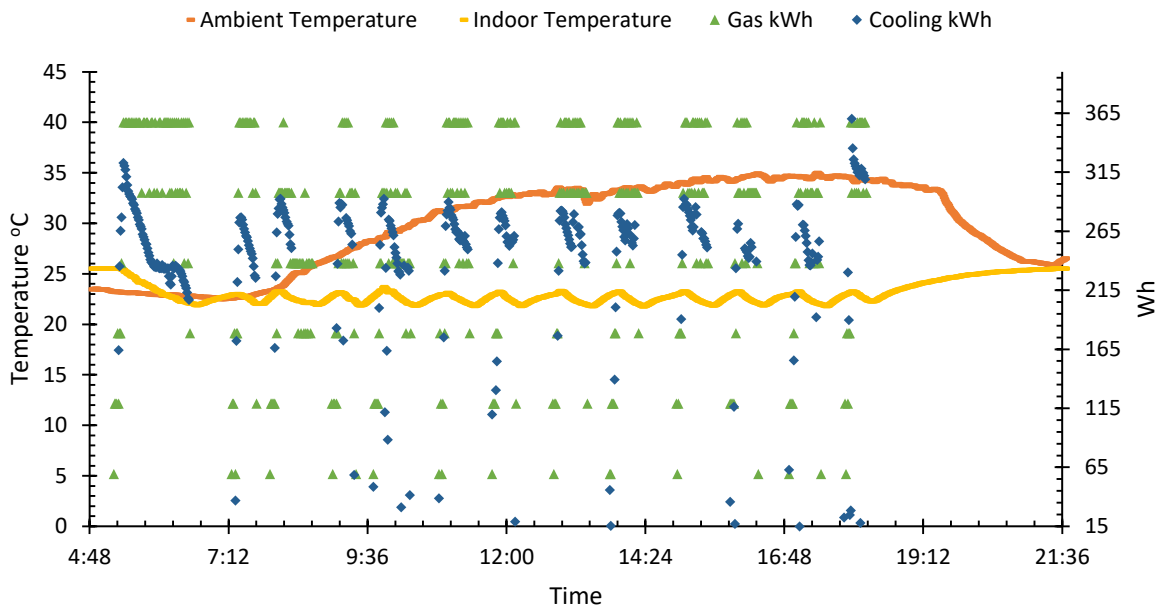


Figure 32. Cooling delivered and energy use for a typical summer day

The operation schedule at the study location was set between 5 a.m. - 7 p.m. for all GEHP units. During morning hours, the GEHP units ran continuously and for longer durations due to the accumulated thermal load overnight. However, during later hours of operation, the GEHP units provide cooling for shorter cycles. The total cooling delivered during such operations ranged between 165 to 365 Wh.

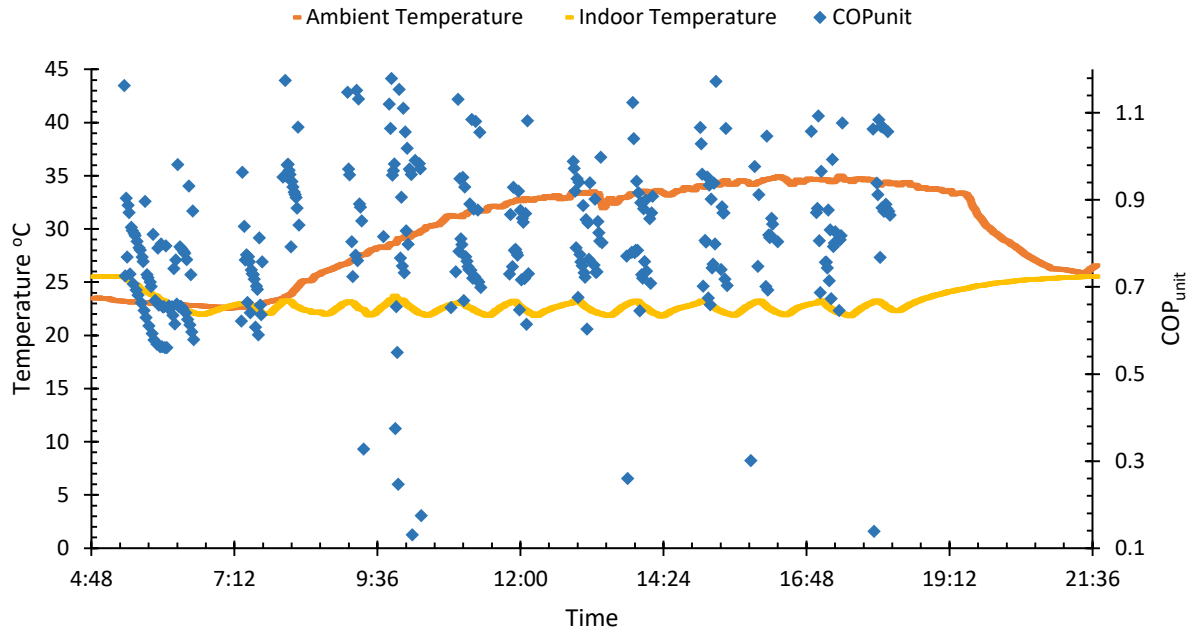


Figure 33. The performance of the GEHP on a typical summer day

The GEHP units operated continuously during the initial hours of a typical day, with the highest gas engine RPM of 1950. The calculated  $COP_{unit}$  during such operation was found to be steady, and its variation with ambient temperature is shown in Figure 34. As expected, it was observed that as the ambient temperature increases the corresponding  $COP_{unit}$  declines.

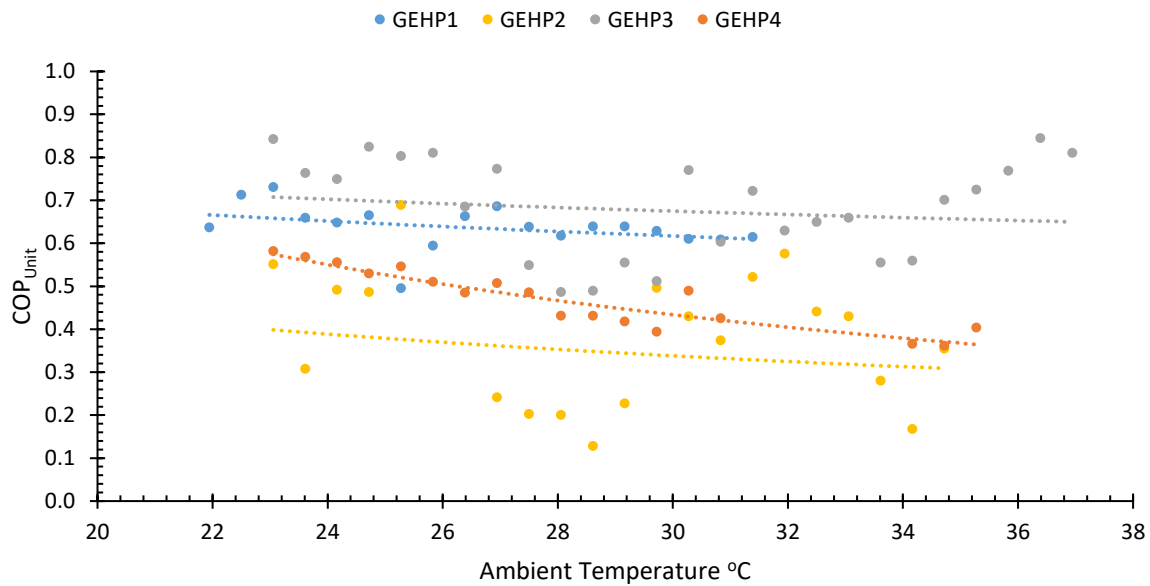


Figure 34. Effect of ambient temperature on the COP achieved at 1950 RPM



Figure 34 presents the variation of COP<sub>unit</sub> with the temperature at maximum rpm found during the study. However, the performance of all the GEHP units does not reflect a similar trend. This variation was due to the difference in configuration of each GEHP unit and corresponding thermal zones during operation (Figure 11).

### 3.7 Measured Performance

Monthly performance of the four GEHP units during the summer months is summarized in Table 3 to 6 below. The data collected for GEHP2 during June-14 of was not complete and, therefore, the COP could not be determined. The system COP presented in Table 3 is the ratio of cooling produced divided by the combined electrical and natural gas energy used by the outdoor unit. The complete measured data summary is provided in Appendix Table C.3.

Table 3. June performance of GEHP units

Jun-14	Natural Gas use (kWh)	Electricity Use (kWh)	Total Energy Input (kWh)	Cooling (kWh)	Average COP <sub>unit</sub>	Average System COP
GEHP1	3661	101	3763	2478	0.68	0.66
GEHP2	4245	#N/A	4245	#N/A	#N/A	#N/A
GEHP3	5414	145	5560	4586	0.85	0.82
GEHP4	3780	92	3872	1705	0.45	0.44

#N/A-Data not available

Table 4. July performance of GEHP units

Jul-14	Natural Gas use (kWh)	Electricity Use (kWh)	Total Energy Input (kWh)	Cooling (kWh)	Average COP <sub>unit</sub>	Average System COP
GEHP1	3928	104	3969	2541	0.65	0.63
GEHP2	4372	117	4418	1687	0.39	0.38
GEHP3	5726	149	5782	4525	0.79	0.77
GEHP4	6179	130	6210	2567	0.42	0.41

Table 5. August performance of GEHP units

Aug-14	Natural Gas use (kWh)	Electricity Use (kWh)	Total Energy Input (kWh)	Cooling (kWh)	Average COP <sub>unit</sub>	Average System COP
GEHP1	4196	108	4236	2727	0.65	0.63
GEHP2	5123	137	5178	1511	0.29	0.29
GEHP3	6840	176	6905	5044	0.74	0.72
GEHP4	6155	133	6189	2167	0.35	0.34

Table 6. September performance of GEHP units

Sep-14	Natural Gas use (kWh)	Electricity Use (kWh)	Total Energy Input (kWh)	Cooling (kWh)	Average COP <sub>unit</sub>	Average System COP
GEHP1	3993	95	4023	2543	0.64	0.62
GEHP2	5639	127	5675	1613	0.29	0.28
GEHP3	7008	151	7047	5042	0.72	0.70
GEHP4	5378	109	5400	1931	0.36	0.35

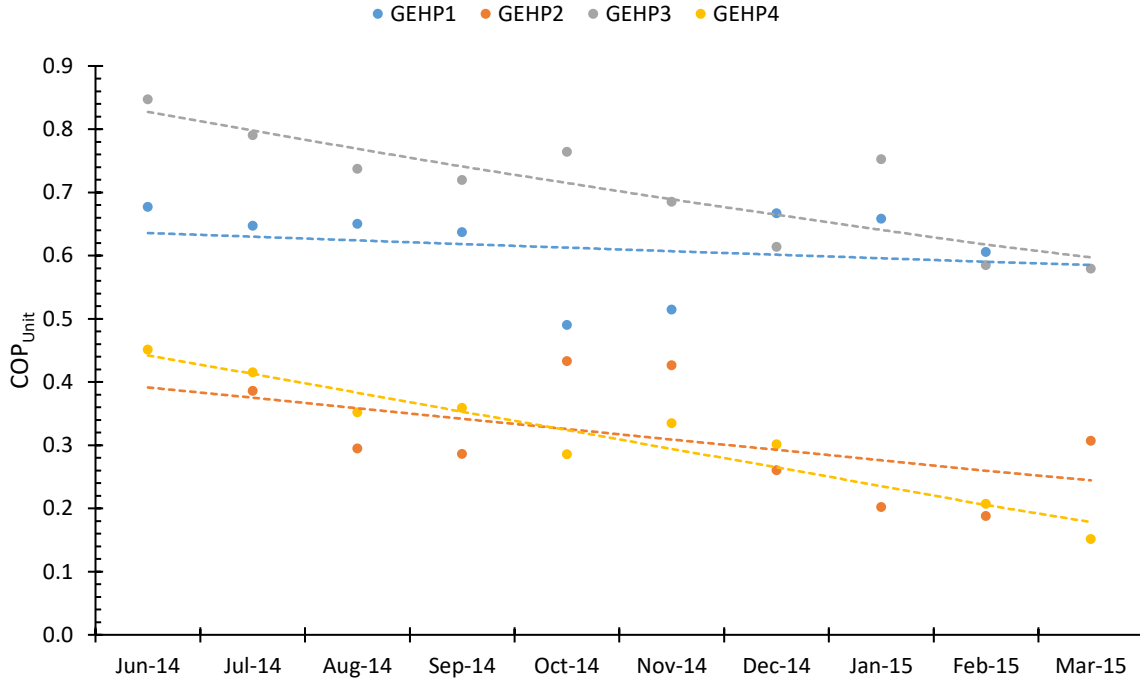


Figure 35. Monthly average unit COP of the four GEHP units

During the summer operation, GEHP3 had achieved the highest COP<sub>unit</sub> among the four units, and GEHP2 was at the lowest COP<sub>unit</sub>, as shown in Figure 35. The monthly performance data is summarized for all four units in Appendix C (Table C.3). The observed variations were due to many system variables that are different for each unit and hence they influence the performance differently.

### 3.8 Comparison with Laboratory and Other Field Experiments

Zaltash et al. [63] 2007 reported COP of GEHP units tested in a laboratory under a controlled environment. Sohn et al. [58] in 2008 reported field operation and performance of six GEHP units. Performance reported in these studies was used for comparison for the current study. Figure 36 shows

the comparative performance (cooling COP) of GEHP unit obtained in laboratory experiments by Zaltash et al., the field testing results by Sohn et al. and the COP<sub>unit</sub> found in the current research.

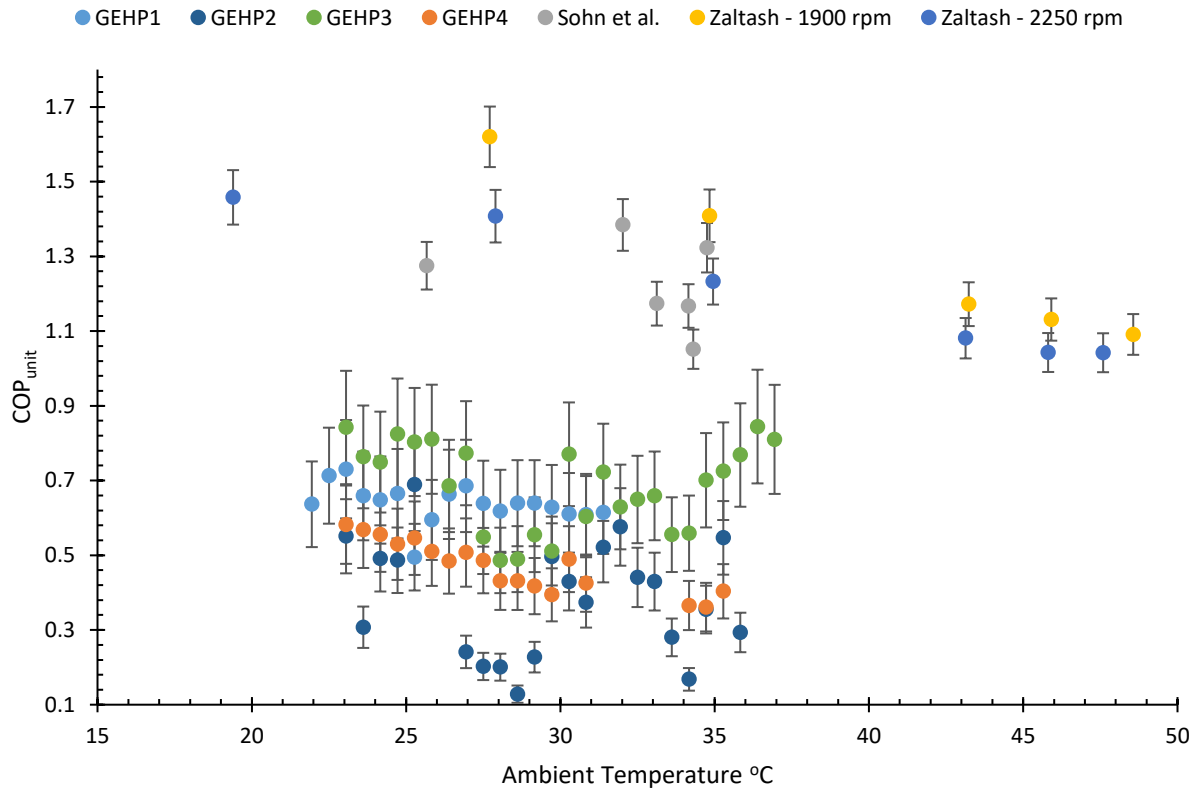


Figure 36. Measured performance compared with other studies

The decline in the COP<sub>unit</sub> in the present study with an increase in ambient temperature agrees with the reported research. However, the COPs reported by Zaltash et al. and Sohn et al. are almost double the COP<sub>unit</sub> obtained from the GEHP units studied in the current work. It should be noted that the conditions in all these three studies are different and hence an exact comparison is not possible.

### 3.9 Energy Efficiency of GEHP Operations

To understand the observed low performance during field operation, the individual performance of various components of the system was determined using the maximum load operation data for analysis. The fuel input, compressor output and cooling delivered were calculated which were then used to estimate the delivered performance. The overall efficiency of the engine and compressor unit is a

combination of the engine thermodynamic efficiency, transmission efficiency and compressor efficiency as depicted in Figure 37.

The following typical efficiencies were assumed to determine the engine efficiency:

- Transmission efficiency- 95%,
- Compressor mechanical efficiency-92% [64].

The performance of GEHP3 unit was studied for August 1<sup>st</sup> operation by separating the time of operation at maximum RPM and minimum RPM to determine the performance at different loading conditions of the engine. The transmission and compressor efficiencies were assumed as mentioned above to determine the output of the engine.

Table 7. Engine specification

S No.	Description	Details
1	Engine type	4-cylinder OHV- spark ignition
2	Displacement	0.952 liter
3	Rated output	7.9 kW
4	Cooling - RPM	1000-1950
5	Heating - RPM	1000-1900

Table 8 shows the average performance of the GEHP3 gas engine and its COP<sub>unit</sub> during steady operation at the highest and lowest engine RPMs. During the steady operation at 1950 RPM, the maximum load on the engine was maintained around 48% of the rated output. The minimum output at this speed was 28% of the rated design output of the engine. At 1000 RPM, the maximum load on the engine was around 28% while the minimum was 6%. During steady operation, the engine was loaded between 14 - 36% of the design rated output, thus leaving most of the available capacity underutilized, as shown in Table 8. As the load on the machine reduces, the corresponding COP<sub>unit</sub> also reduces. However, the reduction in COP<sub>unit</sub> was nonlinear as a result of high losses at part load operation.

A GEHP unit includes an SI engine to power the compressor, which operates similar to gasoline engines. It is known that the SI engines work at lower efficiencies at lower loads as depicted in Figure 38

(Goering et al.[65]; adapted with permission). As shown in this Figure 38, the efficiency of SI engine can vary from as high as 25% at full capacity to as low as 10% at 20% load [65].

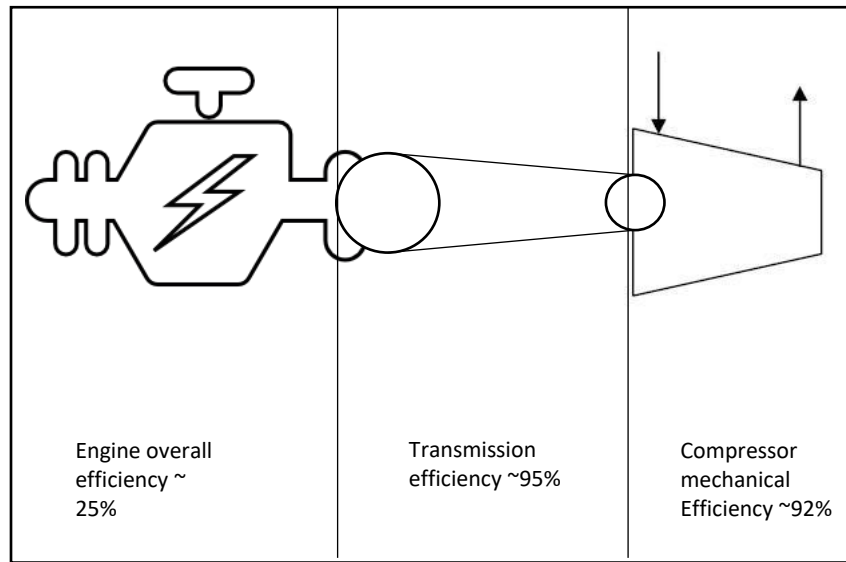


Figure 37. Efficiencies inside a gas heat pump

Table 8. Performance variation of GEHP3 for engine RPM range of 1000 to 1950

Engine RPM	Cooling (Wh)	Natural gas - (Wh)	Avg. Compressor output - (W)	COP <sub>unit</sub>	Average load on engine
1000	1440.7	8277.7	998.5	0.17	14.46%
1950	36250.1	46927.0	2505.3	0.77	36.28%

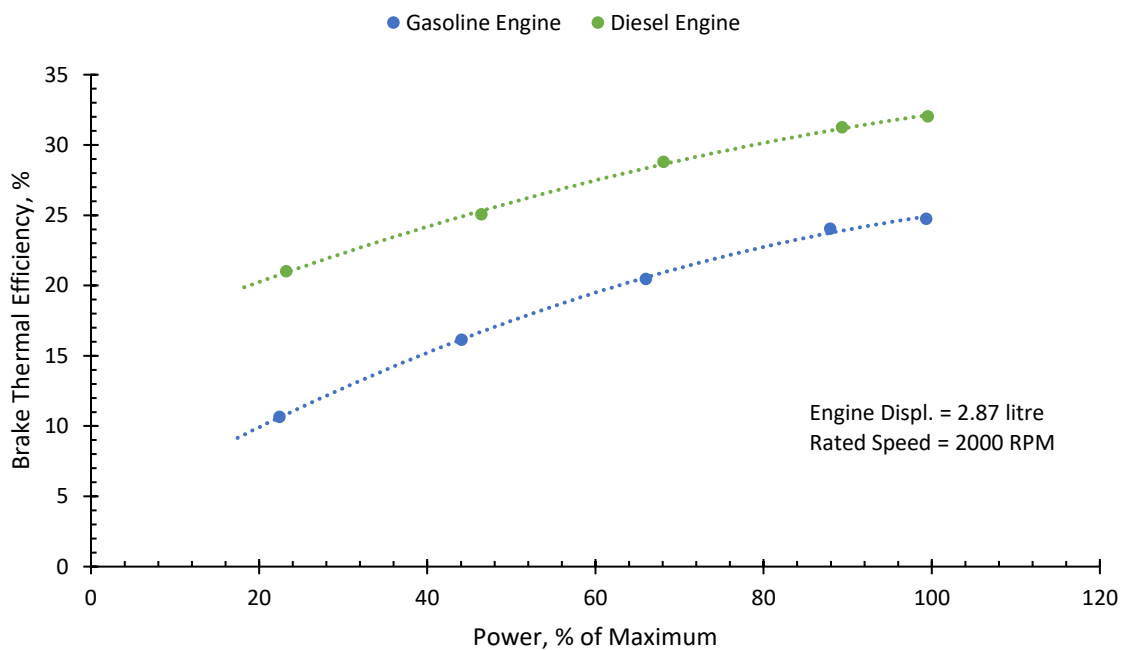


Figure 38. Brake thermal efficiencies of spark ignition and compression ignition engines

The operational data during the morning hours at maximum load and steady conditions was used for estimating the maximum possible performance. During steady operation, the cooling output and fuel use shows that the engine that operating efficiency was around 20% as presented in Figure 39. However, the daily average engine efficiency for this unit was found to be much lower due to low load operation and unsteady conditions during the entire day operation.

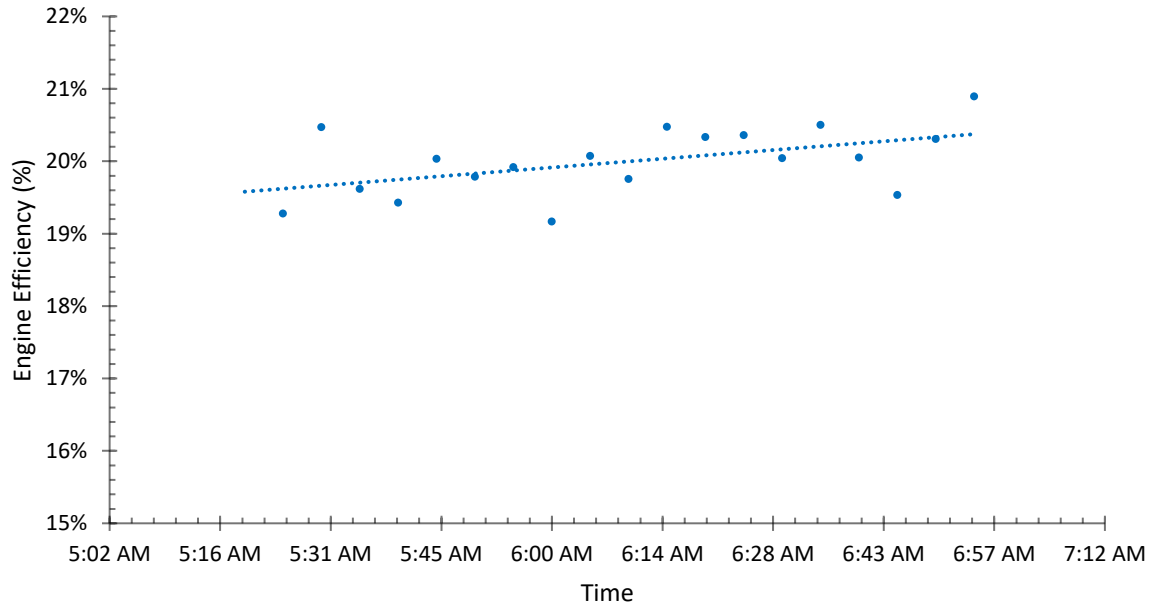


Figure 39. Engine efficiency at full load on 1<sup>st</sup> July-2014

Table 9 shows the summary of the data for maximum load operation of GEHP3. The system operated at a COP<sub>unit</sub> of 1.18 under full load conditions during summer. The average load on the engine during such days of operation was found to be about 65%. The engine efficiency is found to be comparable to the performance of a gasoline engine as shown in Figure 38 [65]. An overall higher performance could have been achieved if the engine was loaded to its rated capacity during operation and thus operating at maximum efficiencies.

Table 9. Maximum load operation performance

Ambient temperature (°C)	Energy from fuel (Wh)	Compressor power (W)	Cooling (Wh)	Overall efficiency	Engine efficiency	COP <sub>Unit</sub>	Average engine load
23.6	22570	3916	26516	17.4%	19.9%	1.18	65%

Table 10 shows the average seasonal performance from the recorded operation data from June-2014 to March-2015. Based on linear extrapolation the maximum COP<sub>unit</sub> of about 1.8 is possible for GEHP3 if the engine is loaded optimally to run at 25% efficiency all the time. In contrast, the achievable COP<sub>unit</sub> at 25 °C indoor temperature and 23.9 °C outdoor temperature was reported as 1.64 by the GRHP manufacturer at 100% cooling capacity.

Table 10. Case for maximum possible average COP<sub>unit</sub>

Description	GEHP #1	GEHP #2	GEHP #3	GEHP #4
<b>Sample data overall efficiency</b>	10.51%	8.40%	9.93%	9.3%
<b>Engine efficiency (assume transmission efficiency - 0.95, compressor efficiency -0.92)</b>	12.03%	9.61%	11.36%	10.64%
<b>Average COP<sub>unit</sub></b>	0.63	0.30	0.71	0.36
<b>Predicted COP<sub>unit</sub> with 25% engine efficiency.</b>	1.50	0.89	1.79	0.97

### 3.10 Economic Analysis

To understand the economic performance of GEHP units and compare them with conventional electric heat pumps, the marginal running cost of cooling for the FPU office was estimated using the average cost of electricity and natural gas. The cost of running the air handling units and auxiliary components was excluded because they are the same for both systems. The measured average COP<sub>unit</sub> values were used to obtain the missing data that was not captured due to issues of connectivity and breakdowns. The statistical approximation was used to adjust the reported values to account for such incidences. A financial model for the levelized cost of electricity was developed for natural gas based combined cycle power plant with a life of 25 years to compare the cost of electricity supply from natural gas combined cycle plant. It is found that the cost of electricity supply from such a plant was around 8 ¢/kWh in the range of the reported national average LCOE [67].

- The marginal cost of electricity is taken as the average unit price based on the ‘September 2014 Bill’ provided by FPU, which was 10.27 ¢/kWh.
- The cost of natural gas is based on the fuel price of 39.14 ¢/therm taken from the consumer tariff. Fixed charges are ignored for the calculation of the cost of natural gas.

The total running cost of providing cooling during the study period is presented in Appendix Table C.4. The natural gas consumption and electricity used came from the measured values of energy use during the study months.

### **3.11 Performance of GEHP vs. EHP**

A comparison of the running costs of a GEHP and an electric heat pump was carried out by using the same electricity tariff as mentioned in section 3.10. The actual delivered cost for natural gas in Florida for 2013 was used to estimate the operating costs for GEHP units. A building energy model was developed using Carrier HAP® 4.6 to estimate the comparative performance of an electric heat pump for DeBary, Okaloosa, and Plant City locations assuming similar buildings. HAP considers all the building elements such as walls, fenestrations, roofs, skylights, lights, people, electrical equipment, non-electrical equipment, infiltration, floors, and partitions considering the TOD and time-of-year factors. HAP uses Transfer Function Methodology (TFM) for its calculations. Conduction, convection, and radiation are the main drivers of heat transfer, and all the heat balance equations are used to derive Transfer Function Coefficients. Noticeable limitation of using HAP is that the source code is inaccessible to the users. However, less number of input parameters and fast convergence compared to other commercial tools make this program useful for the current study [68].

#### **3.11.1 DeBary Building Model**

The DeBary model was developed using the building characteristics to model the cooling performance and compared to the actual performance recorded during the monitoring period. As the model assumes distinct separations between the seven thermal zones, the influence of open walls and thermal loads for each of the four heat pump systems cannot be replicated effectively, which explains the deviations in the simulation results. The use of yearly averaged data also adds to this deviation of results from the actual. However, the results presented were found to be within acceptable industry norms, once the complexity of all the variables was considered.



The building model (Figure 40) includes seven thermal zones air-conditioned by four GEHP units. The seven thermal zones are shown in Figure 41 represented by different colors. GEHP1 and GEHP4 each condition a single zone, whereas GEHP3 conditions two zones and GEHP2 conditions three thermal zones. Due to the nature of the indoor equipment's operation, the energy utilized by the indoor units was excluded from the economic comparison for both technologies providing the same amount of cooling. However, the economic comparison includes the operation of the fans in the outdoor units in addition to the compressors.

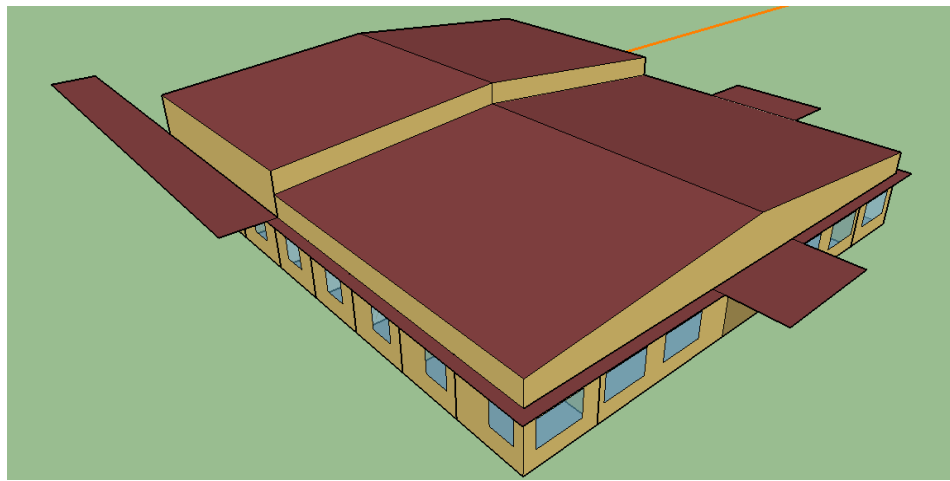


Figure 40. Model developed for study building

GEHP3 demonstrates the best performance among all the units. However, due to the variability in operation, the COP fluctuates significantly and makes a comparison with the model meaningless, as the gas engine efficiency varies with the load as shown in Figure 39. The field operation involves running the unit at different loads resulting in different efficiencies. The available HVAC design and prediction tools, such as HAP and NREL-OpenStudio cannot replicate such operation with accuracy. The limitations are due to the absence of an accurate model of a gas heat pump in these codes. The equivalent electrical heat pump model was used to provide the economic performance of the same building at the same location. For this comparison, the following models were developed for GEHPs of the same capacities as those in operation at the site (4x8 TR).

1. EER 9.2 EHP (Appendix Table C.5)

2. EER 11.8 EHP (Appendix Table C.6)
3. EER 12.8 EHP (Appendix Table C.7)
4. EER 15.0 EHP (Appendix Table C.8)



Figure 41. Seven thermal zones air-conditioned by four GEHP units

Simulation results of these models were then used to predict the electricity use for cooling/heating produced by the outdoor units alone. The details of the results are provided in Appendix Tables C.5 to C.8.

### 3.11.2 Economic Analysis

Comparative results of the actual vs. modeled EHP energy costs is presented in Figure 42, for the months recorded during the study. The measured GEHP costs of running lie between EHP systems with EER-9.2 and EER-11.8 during the study period. However, the estimated operating costs were higher during winter (December-January-15). The Higher operating costs were due to the reduced efficiencies of the oversized GEHPs at small loads as seen during the winter months in Figure 42. It is to be noted that the modeled EHP system used a 25-year average weather information and thus had a smoother simulated

profile as compared to the actual measurements in this study. The supporting cost comparison of providing the cooling for the period of this study for actual and predicted EHP system is given in Appendix C.11.

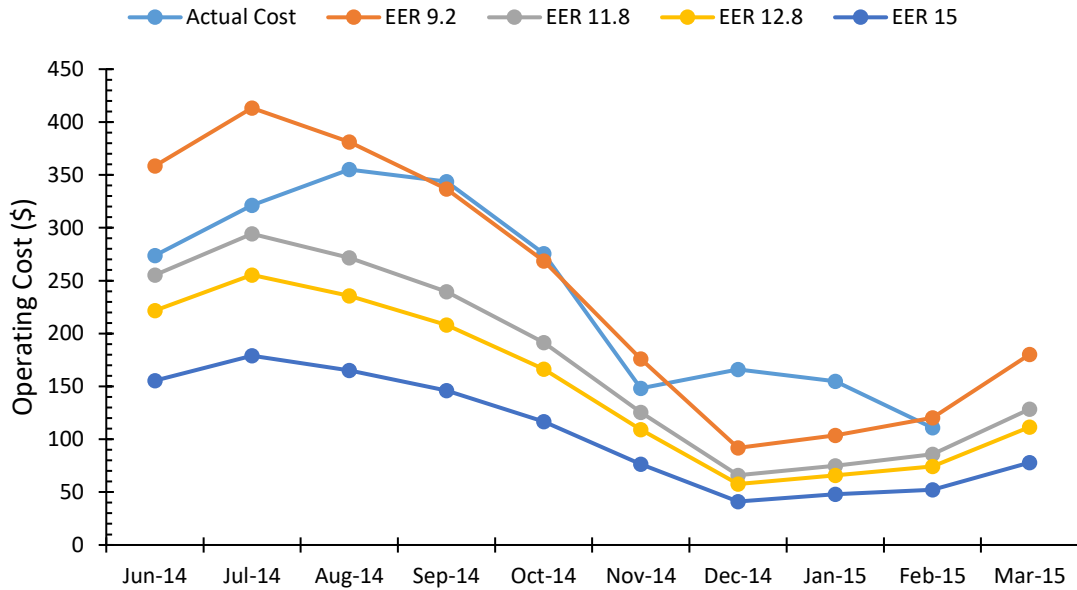


Figure 42. Cost comparison of actual vs. modeled systems

### 3.12 Performance Prediction at Okaloosa, FL and Plant City, FL

The performance of the same building model and load conditions was studied for the two other locations namely Okaloosa, and Plant City, FL. However, there were concerns about the utilization of this data due to the absence of complete information about these sites and irreproducibility of system capacities. The predicted running costs for all three locations considering similar buildings and heat pump units are shown in Figure 43.

It was predicted that the operating cost would be lower for Okaloosa as compared to the other two locations, primarily due to the ambient temperatures. This gap in performance was observed to be lower during the summer months of June-August 2014 due to similar weather conditions at the three locations. The simulation results of the models are presented in Appendix Tables C.5, C.9, and C.10 for DeBary, Okaloosa, and Plant City respectively.

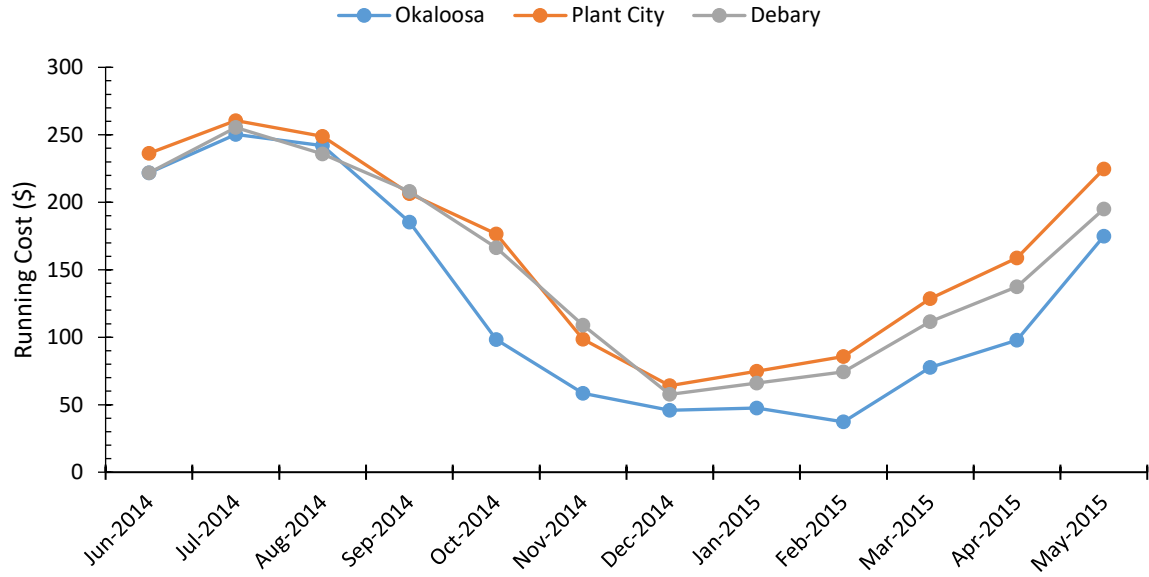


Figure 43. Operating costs (\$) of similar systems and loads as DeBary for Okaloosa and Plant City

### 3.13 Summary and Discussion

The operational data of the four GEHP units installed at the site was recorded for ten months and analyzed to determine the performance of these units. The average  $COP_{unit}$  determined for the four GEHP units differed significantly from each other, primarily due to different loading conditions for each of these systems. It is worth highlighting that the part-load operation of the SI engine affects the overall efficiency of the GEHP units significantly. The overall efficiency varies considerably during the year and during different times of the day.

The field testing done during the 2014 summer season reflects a significantly lower COP achieved from the operation of the GEHP units. The operation of VRF GEHP is significantly different from typical EHPs as the system runs intermittently delivering cooling and goes to idle when the indoor temperatures are lower than the set temperatures. This allows an on-off control strategy and thereby engaging and disengaging compressor many times in a day. Although the variable speed compressor allows a better control of the cooling delivery in the indoor zones, the impact of the part-load operation on the overall  $COP_{unit}$  is higher due to the lower fuel efficiency of the engine. Therefore, proper sizing of the engine and compressor capacities to match the load is crucial for achieving a better overall  $COP_{unit}$  for GEHPs.

It is evident that design engineers oversize the HVAC system to minimize the risk of underperforming on the comfort side for the customer. However, in doing so, they end up penalizing the owner with higher upfront cost as well as higher maintenance and energy use costs [69]–[71]. The situation is amplified significantly when one looks from a single building to a region, and further to a power utility level resulting in much steeper demand profiles during peak energy hours.

## **Chapter 4 Integration of Cooling Thermal Energy Storage in Commercial Buildings**

Thermal Energy Storage for HVAC in commercial buildings can improve power utility profiles and reduce baseload power plant capacity requirements for a region or state [35], [37], [72]. This chapter describes a detailed analysis and benefits of integrating cooling thermal energy storage in buildings for consumers and utilities.

### **4.1 Benefits of Adopting Thermal Energy Storage**

Thermal Energy Storage (TES) is used to bridge the gap between energy generation and energy use [73]. Buildings represent a major area where decentralized storage systems can make a significant impact on the utility load profile. Using TES for buildings can help optimize peak demands and energy costs. With TES for air-conditioning, large compressors and chillers (sized to meet peak load) can be replaced by smaller capacities [74]. Thus, use of TES facilitates proper sizing of HVAC systems for optimum capacities to improve performance. Optimum sized equipment requires fewer start/stop cycles resulting in reduced operating costs [75], [76]. It is evident that TES benefits both the demand and generation sides.

#### **4.1.1 Benefits to Power Generators**

The adoption of building TES can help limit the ramp challenges faced by utility power plants from off-peak to peak power demand, which also reduces the operation and maintenance challenges. At the utility scale, this results in shifting the operation hours and capacities of power plants to cooler ambient conditions at night when generation efficiencies are higher [56]. Energy storage in both demand side and generation side have a similar impact on the utility depending on the penetration and availability of right technology [8].

#### 4.1.2 Thermal Energy Storage for Air-conditioning

There are three main types of thermal energy storage:

1. Sensible heat
2. Latent heat
3. Thermochemical heat
  - a. Chemical reaction
  - b. Sorption systems

Selection of storage media depends on parameters like energy density, heat transfer between the HTF and storage material, mechanical and chemical stability, compatibility between storage material and the container, and cyclic.

Criteria for TES design are maximum load, nominal temperature, specific storage capacity, operational strategy and efficient integration in the system. TES systems can be active which use mechanical means to transfer heat or passive, which use natural forces such as gravity and buoyancy to transfer heat (Figure 44). Such systems can be further classified as direct or indirect systems depending on whether the storage media is used as working fluid or not.

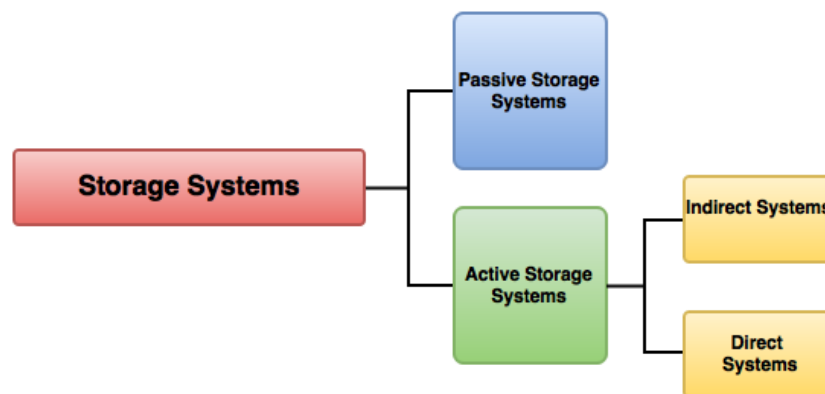


Figure 44. Classification of storage systems [73]

- Direct systems for cooling TES include Chilled Water or Water-Glycol as the working fluid;
- Indirect systems include ice as the Phase Change Material (PCM) storage.

In a chilled water storage, the supply fluid can be at 2 to 8 °C temperature to charge the storage tank which gives a storage density of around 30-40 kJ/m<sup>3</sup> [77]. However, the energy density of ice storage is about 4-5 times that of water storage (Latent storage vs. sensible storage), but it also requires much lower charging and evaporating temperatures, which in turn affects the following:

- TES system efficiencies;
- Dispatch capabilities - charge/discharge cycle delays;
- Cost of storage;
- Sizing limitations for commercial application.

#### **4.2 Research Methodology - Thermal Energy Storage for Peak Reduction**

This research is broken into sub-tasks to meet the objectives (Figure 45):

1. Identify and model a reference standard commercial building using EnergyPlus to obtain reference energy use profiles;
2. Develop a thermal energy storage model with size and cost optimization for the base case of a building's air-conditioning demand;
3. Develop control strategy for TES use for a select utility area with TOD rates in effect;
4. Quantify the economic benefits of TES for building energy with TOD rates;
5. Identify locations to test the variability of the simulation results for different weather conditions;
6. Obtain or simulate a power grid profile under reference utility supply conditions;
7. Analyze the potential benefits to a utility due to the adoption of TES at a utility scale.

##### **4.2.1 Location and Case**

1. Locations identified for the detailed analysis are Tampa, New York, Denver, Los Angeles, with Time-Of-Use electricity tariff rates;



2. Standard DOE reference building models are used to integrate thermal storage technologies so that other researchers and future studies can further explore the work;
3. Performance of a standard reference building with HVAC without and with TES system is compared;
4. Weather data and energy profile data for the select cases are used as input to the optimization model for a TES system with emphasis on the minimum operational cost of electricity.

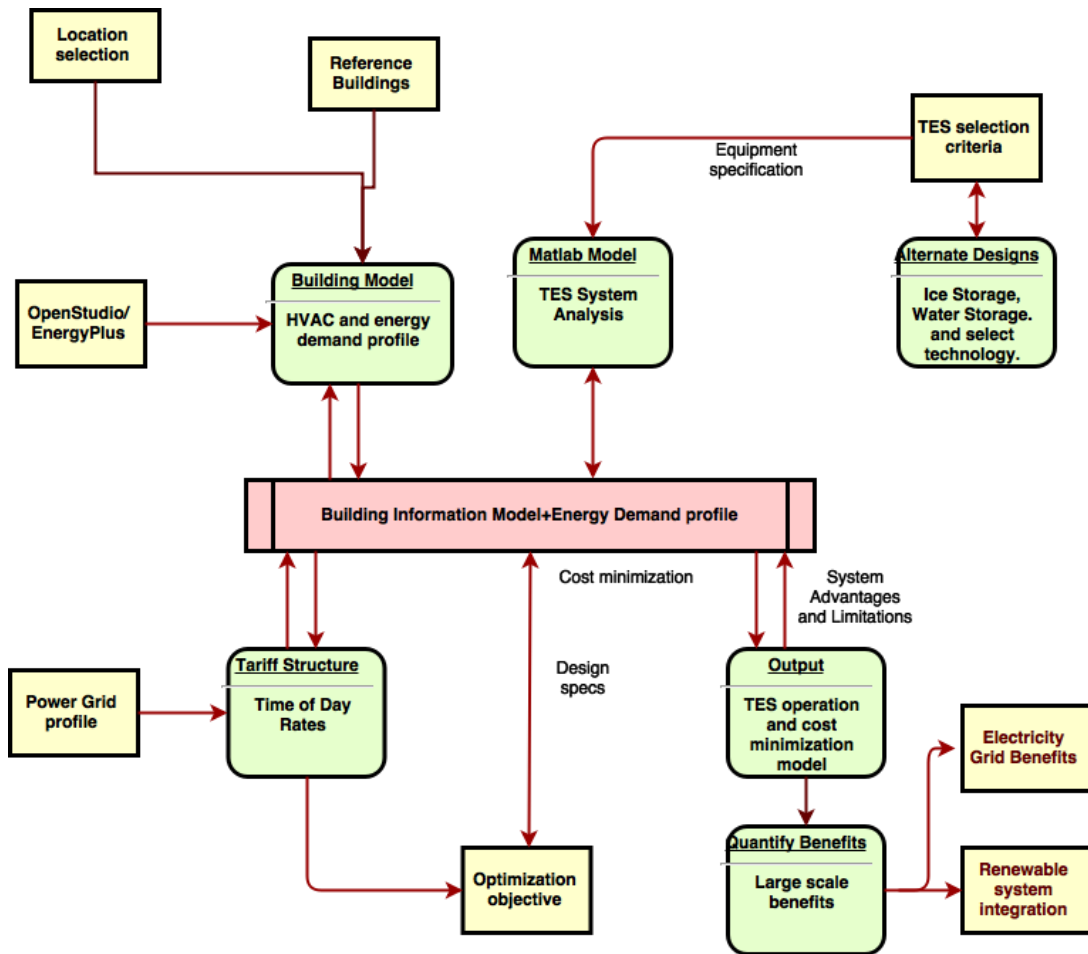


Figure 45. Study components for TES use for building

### 4.3 Building Energy Modeling

Building Energy Modelling (BEM) has come a long way towards its integration with other tools for HVAC system simulations and sizing. The field involves the use of software to design building model based on variables and predict energy use including HVAC systems to satisfy loads within a building. To

standardize the research and development in these fields, DOE has suggested reference commercial building designs which allow scientific comparison of energy models [78]. There are many energy performance analysis models available such as Carrier HAP [79], Trane TRACE 700, DOE-2, eQuest, EnergyPlus [80], ESP-r, IDA ICE [81], TRNSYS [82], HVACSIM+ [83], VA114, SIMBAD [84], OpenStudio [85]. In this study, we used EnergyPlus due to its long development history supported by the US DOE and its global acceptance by engineers and researchers.

DOE standard reference building is modeled for simulation and HVAC sizing using EnergyPlus, OpenStudio [80], [86]–[88]. Although EnergyPlus includes the Thermal Energy Storage object, there is not much available in the literature that can be used to model TES in buildings matching local tariff and weather conditions strategically. Ihm et al. [89] developed three ice storage models that were integrated into EnergyPlus. However, many control strategies are not easy to implement within EnergyPlus, and hence we have used EnergyPlus Runtime Language (Erl) to implement EMS control algorithms necessary for the operation of TES according to the TOD pricing implemented in the identified cities [88]. The model file for EnergyPlus is an ASCII text file saved as Input Data File (IDF). Ihm et al. highlighted the limitation of using native control strategies in EnergyPlus with respect to ice storage system for a small building[89]. Our current research has expanded the scope of work by including chilled water storage systems and implementing a strategic control of the operation.

#### **4.3.1 Building Information Model for Reference Building**

A DOE standard Large Office Building model (Figure 46) is used to implement the two commercially available storage solutions for implementing a control strategy. The reference large office building is characterized by the following features [90].

The chilled water loop (Figure 50) consists of two chillers configured in parallel operation to provide cooling through VAV boxes with reheat. The chilled water, after gaining heat from the user side, is circulated back to the chillers by the supply pumps thus completing the loop.

Table 11. Building characteristics for EnergyPlus model

Building Parameters	Details
Shape	Rectangle with aspect ratio 1.5
Number of Floors	12
Floor Area	46,320 m <sup>2</sup> (498,588 ft <sup>2</sup> )
Window to Wall Ratio	38%
Infiltration	0.4 cfm/ft <sup>2</sup>
Chiller	Two water cooled chillers
Lights	10.76 W/m <sup>2</sup>
People	2397
Elevators	12 @25 HP, 91% motor efficiency
Air Loops	VAV with Reheat
Plant Loops	Supply hot water, heating system, cooling system, and cooling tower system
Boiler	Gas fired
Total Number of Zones	19

The operation of the chillers is triggered when they sense demand from the user side. The change in temperature of the return chilled water dictates the desired chiller capacity to meet the outlet chilled water temperatures. The reference building with the above conditions has a typical occupancy for a week as shown in Figure 47. Figures 48 and 49 show the simulated profile of electricity used by chiller in the building model during a year and for a typical day in summer and winter respectively.

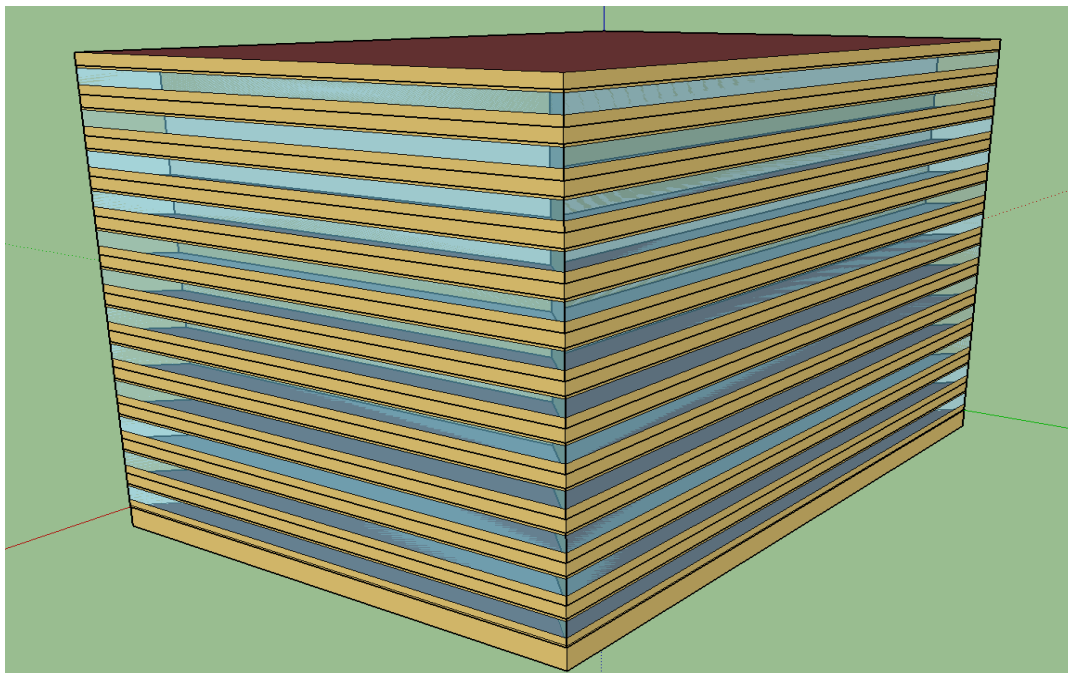


Figure 46. DOE reference large office building

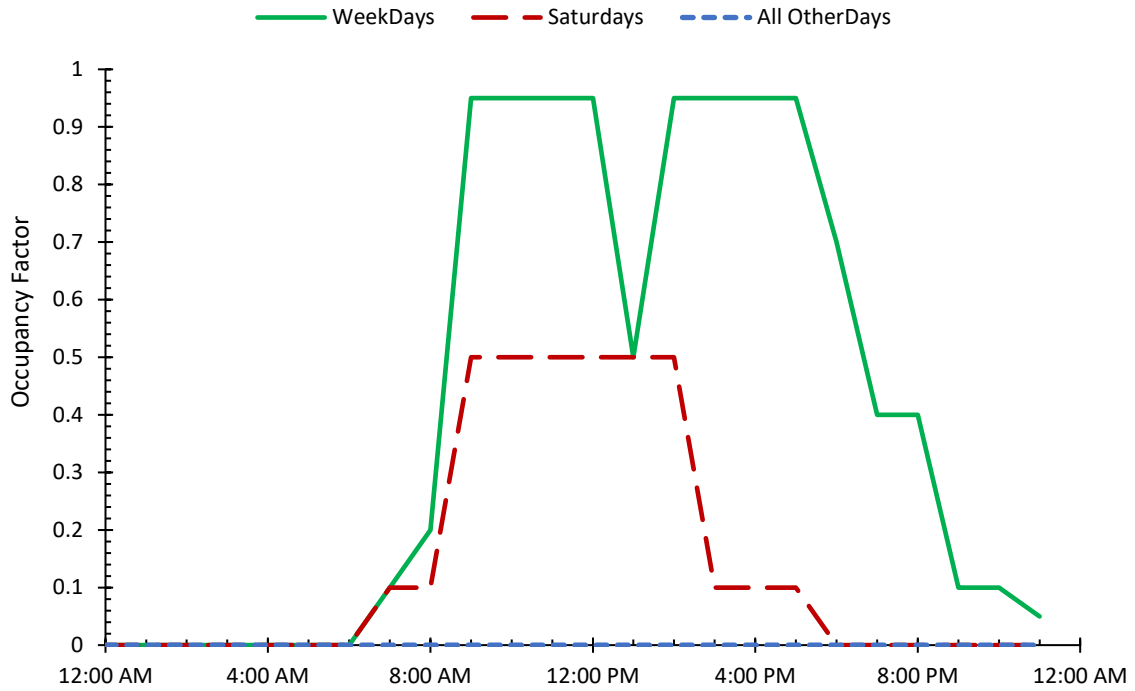


Figure 47. Occupancy definition for the building

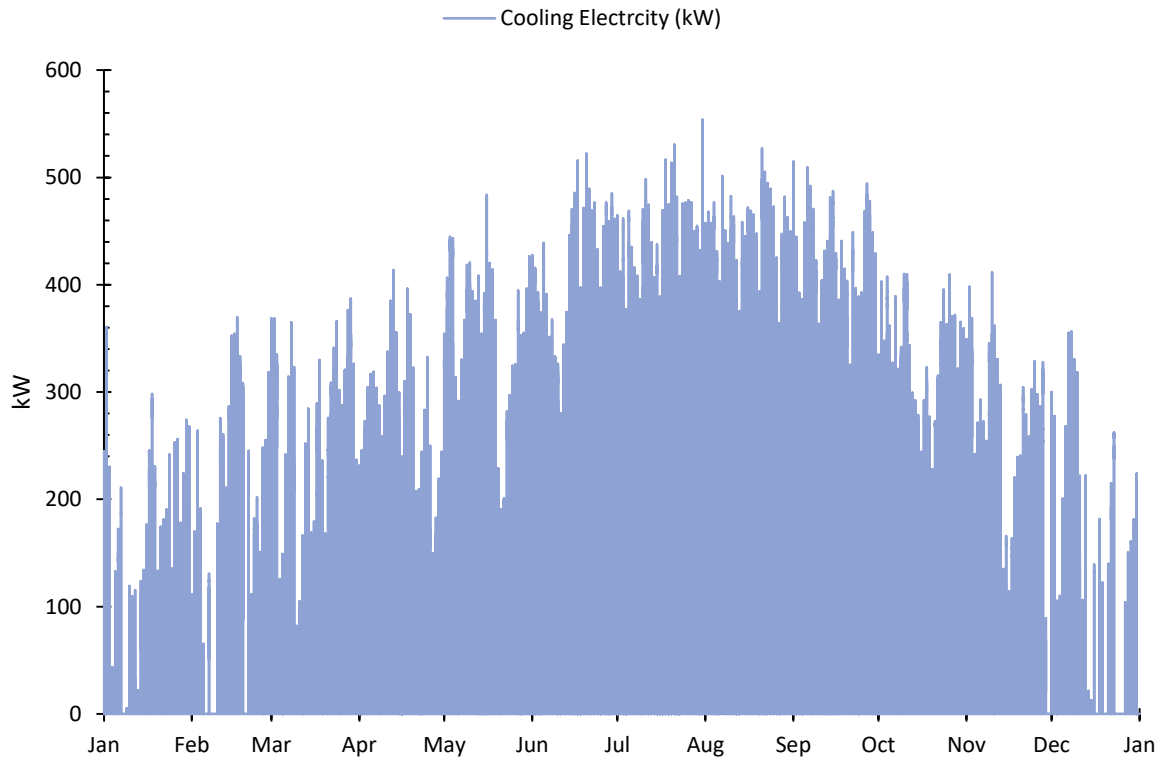


Figure 48. Annual cooling electricity

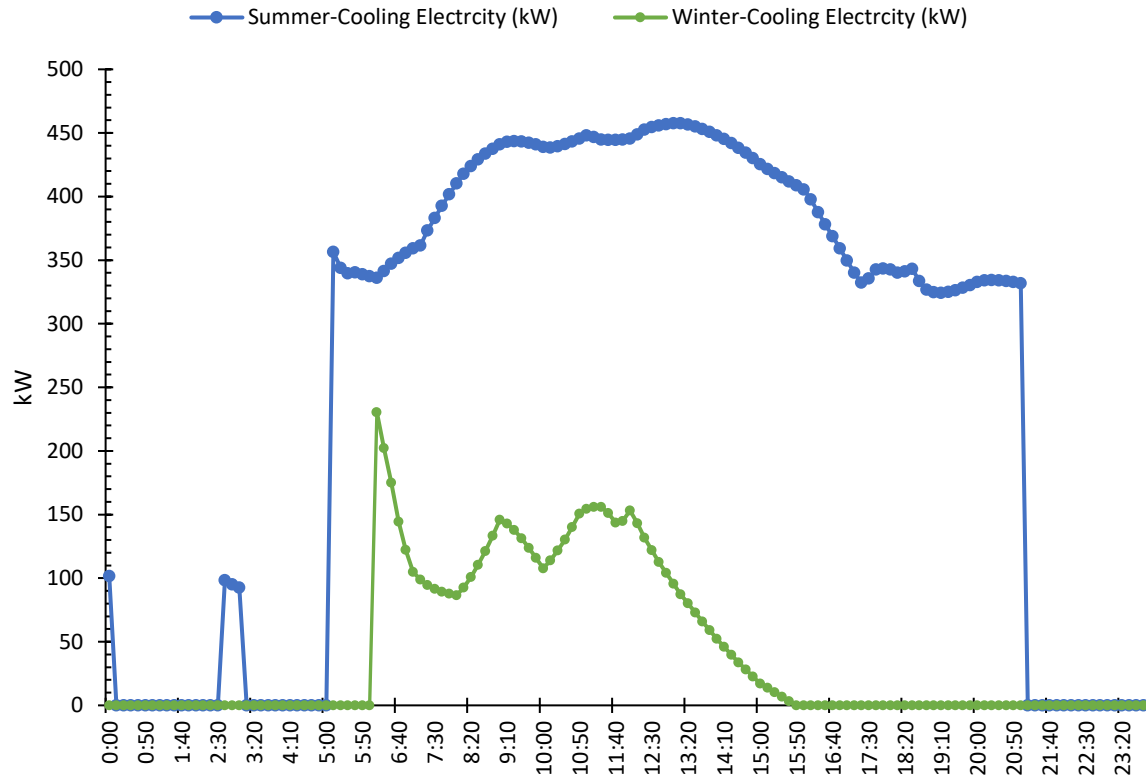


Figure 49. Typical daily cooling electricity demand in a building during summer and winter

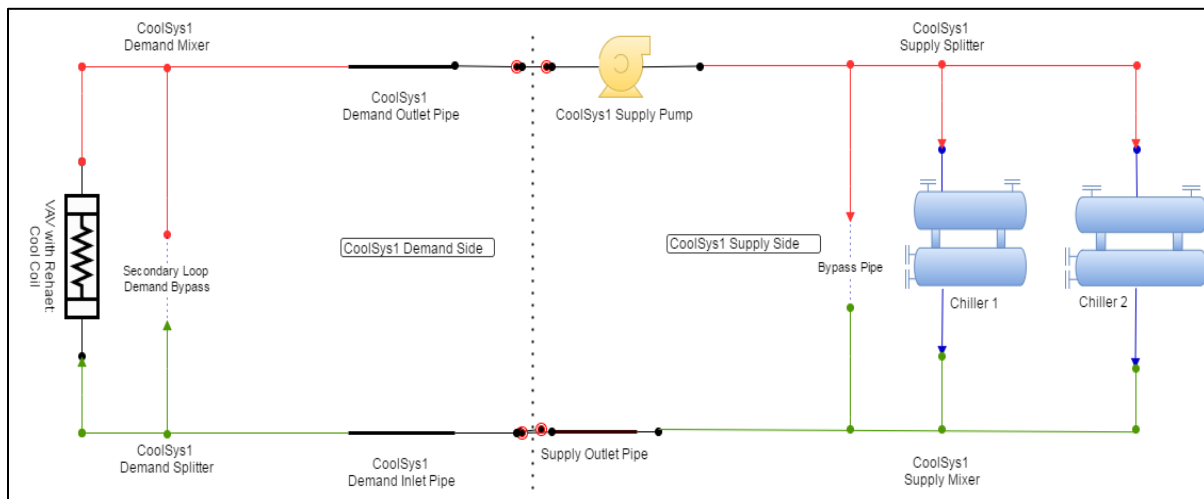


Figure 50. Chilled water cooling loop

#### 4.3.2 Model Operation Requirements

The reference DOE large office building model is characterized by a chilled water plant loop consisting of two chillers of equal capacity. The reference model is modified to integrate three thermal storage systems, i.e., ice storage, and chilled water mixed and stratified tank systems. Chiller operates

upon demand from the demand side of the plant loop (Figure 50). However, during times of no load, this control did not function the way expected, and the storage tank charging was not initiated. The native control does not provide much flexibility in the operation of the storage system especially during peak and off-peak demands. Due to this limitation, alternate configurations in this study are proposed.

#### 4.3.3 Cost Minimization

The electricity rate structure that affects most of the operating costs is usually in a block format to allow higher price when the generating costs are higher i.e. during peak hours. The higher price of electricity is due to the unavailability of the baseload power generation capacities so that the utilities have to either use expensive peaking units or purchase from the grid. Tampa, FL was selected for the cost minimization objective. For the selected commercial building of the selected size, the applicable tariff was found to be under the category of 'General Service-Demand (optional)-GSDT' where the consumers' past one-year consumption is more than 9 MW [91]. The following tariff structure and peak hours' definition were used for simulation purposes.

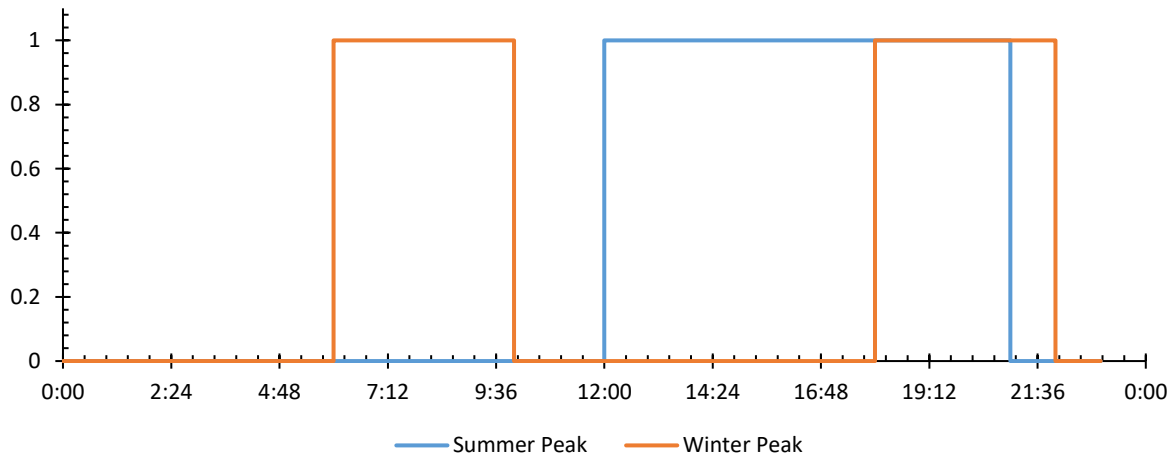


Figure 51. Two-season peak pricing window for Tampa

The Utility has defined peak hours for two seasons in blocks, shown in Figure 51. Weekends and holidays are not included in the peak pricing. The rates include demand charges and energy charges defined in blocks along with monthly fixed charges and state taxes.

Table 12. GSDT consumer electricity rates for Tampa, FL

Monthly Charges (\$)	Peak Energy Charges (¢/kWh)	Off-Peak Energy Charges (¢/kWh)	Peak Demand Charges (\$/kW)	Off-Peak Demand Charges (\$/kW)	Capacity Charges (\$/kW)	Fuel Cost Adjustment Peak (¢/kWh)	Cost Adjustment Off-Peak (¢/kWh)	Fuel Cost Adjustment Off-Peak (¢/kWh)	Energy Conservation & Environment (¢/kWh)	Taxes (%)
30.0	2.898	1.046	6.13	3.12	0.53	3.937	3.564	1.079	2.5641	

#### 4.3.4 Control Requirements

The model has a conventional chilled water loop and hot water loop for supplying the air conditioning requirements. The ice and chilled water storage systems once coupled with the existing system on the supply side of the chiller were configured to respond to peak and off-peak load conditions. However, due to the control strategy requiring a mix of operation where the storage tank operate with chiller at times while only supply during other and completely off sometimes even when there is a demand. A more flexible but also direct control strategy was needed. The reference building model is modified to include a storage system and an EMS using Erl program to implement such control. The EMS overrides the native control system of EnergyPlus wherever needed. The EMS controls make use of existing sensors, program, subroutines and actuators to provide a new set of values to the variables. The following three cold thermal storage systems are investigated in the current work:

- Ice tank [92];
- Chilled water mixed tank storage [93];
- Chilled water stratified tank storage [94], [95];

The size of the storage in each case was found iteratively using the JEPlus batch simulation tool to match the building demand [96].

#### 4.4 Modified Plant Loop Description

The above three storage systems modeled for the base reference building use a chilled water loop for the storage tank, a pump, and one or two heat exchangers depending on chilled water or ice tank systems. Ice storage model loop components and configuration deployed to enable the use of EMS to override the native control in EnergyPlus when needed are:

1. Plant loop uses ethylene glycol as the heat transfer fluid, and its flow rate is set very low which minimizes the thermal lag in the loop.
2. The pump head is kept very low to keep the pumping energy low in the overall cooling plant operation.
3. A heat exchanger (HX) is used to transfer heat between the fluids from the chiller and storage tank. The heat exchanger is located after the chillers on the supply outlet branch.
4. A very small virtual night load profile is added in parallel to the demand side chilled water loop with a binary operation mode. The load value is set to unity during nights and thus provides the required flow request for the chillers during nighttime for charging the storage tanks.

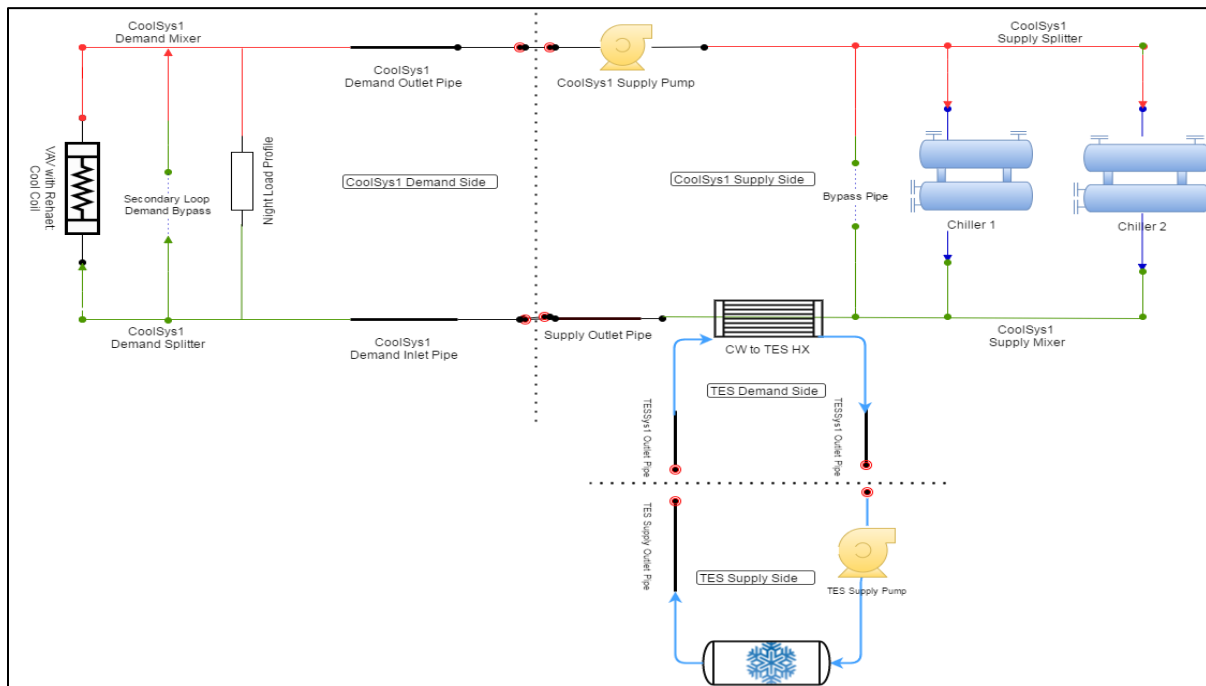


Figure 52. Ice storage loop configuration

During the operation when the storage tank has to be charged or discharged, the HX is activated while it remains inactive during the rest of the hours. The HX behaves like a cooling coil during discharging and like a heater during charging for the chilled water in the primary plant loop.



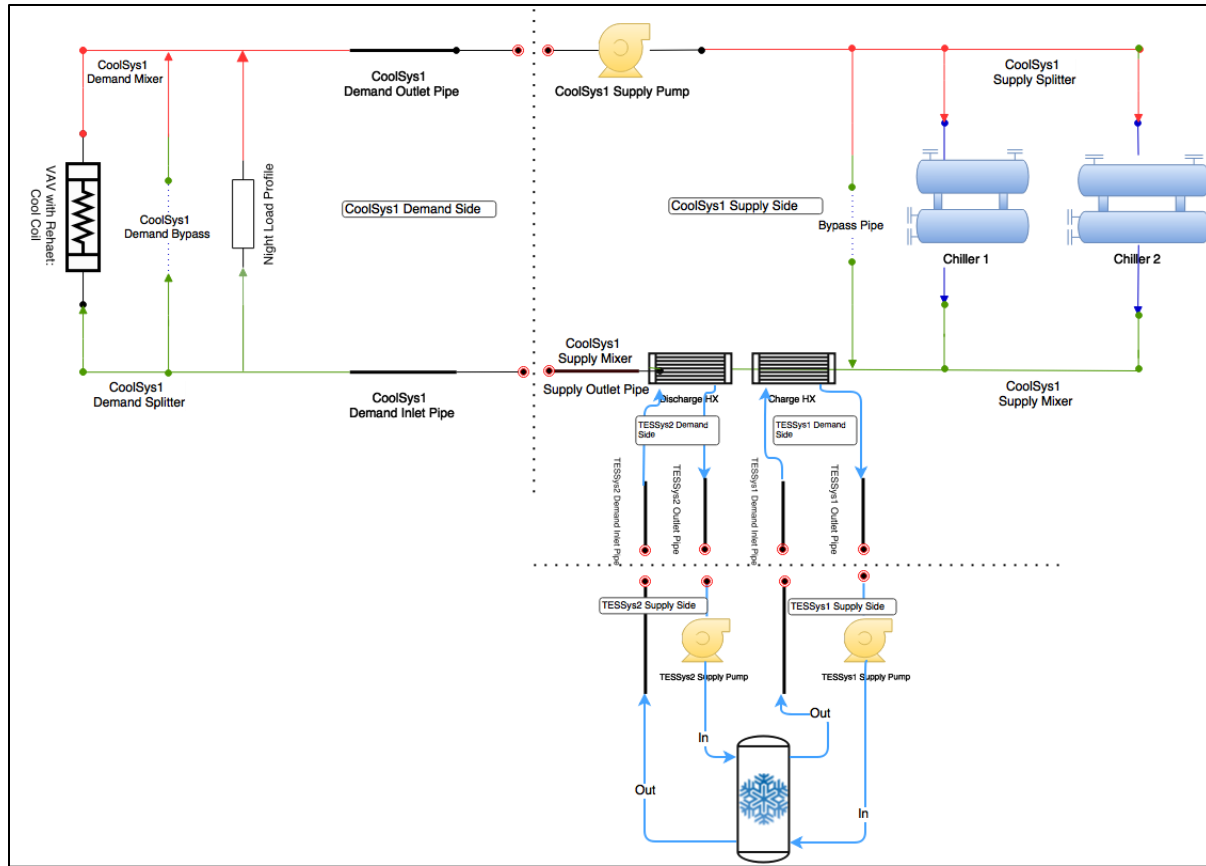


Figure 53. Chilled water storage loop configuration

Chilled-water tank storage loop components and configuration for the mixed tank and stratified tank models are:

1. Plant loop uses water as the heat transfer fluid, and its flow rate is set very low which minimize the thermal lag in the loop.
2. The pump head is kept very low so that the pumping energy is low in overall cooling plant operation.
3. Two separate HX's are used, one for charging the storage tank and the other for discharging storage tank for enabling heat transfer. This is because the storage tank model for chilled water tank has separate openings for charging and discharging. The position of heat exchangers is after the chillers on the supply outlet branch.

4. A very small virtual night load profile is added in parallel to the demand side chilled water loop with a binary operation mode. The night load value is set to unity during nights and thus provides the required flow request for the chillers during nighttime for charging the storage tanks.

During the charging or discharging modes for chilled water storage models, the respective HX's are activated, and both are activated during simultaneous operation. The set point temperature at the target node is manipulated to provide the needed temperature of chilled water from the chillers for charging, discharging or direct cooling using the EMS program.

#### **4.4.1 Control Strategy**

There are two aspects of control (1) tactical control that defines how the operation of the chiller and storage tank is controlled and (2) strategical control that defines when to apply the appropriate tactical control. The tactical control is set using the system parameters for meeting the current demand while the strategic control is setup based on the external variables like the TOD, peak energy window, and so forth. A literature review by Sun et al. [97] covered the possible load shifting control strategies for different storage solutions like building thermal mass, PCM and active thermal storage.

The strategical control is set by identifying the time windows most suitable for chiller operation or storage operation based on the electricity pricing without compromising on comfort.

The current study explores the use of EMS based control as part of the EnergyPlus program to develop tactical control subroutines which are defined in Table 13. EMS sensors and actuators are used to detect the input condition necessary to make the decision for the correct values for actuators based the program definition. EMS sensors are system nodes providing instantaneous values for schedule, cooling coil load, status, or temperature of storage tanks. The EMS program uses the sensed parameters to set the values for the actuators at select system nodes. The equipment operates to meet the setpoint temperatures based on the new set of values on these nodes. The chiller setpoint is set at the cooling

system outlet node which is manipulated by such EMS Actuator. Likewise, the outlet of storage tank acts as the actuator controlled setpoint for charging or discharging the tank.

Table 13. Tactical control functions

Function	Tactical Control State	EMS Routine Ice storage	EMS Routine CW Storage
Chiller Only	1.0	ApplyChillerOnlyFunction	
Ice Only	2.0	ApplyIceOnlyFunction	ApplyDischargeOnlyFunction
Chiller and Ice	3.0	ApplyChillerAndIceFunction	ApplyChillerAndDischargeFunction
Freeze	4.0	ApplyFreezeFunction	ApplyChargeFunction
Freeze and Cool	5.0	ApplyFreezeAndCoolFunction	ApplyChargeAndCoolFunction
Off	6.0	ApplyOffFunction	
Control Not Set	0.0	(catch a logical error)	
Control Error	-1.0	(catch schedule gaps)	

The HX's for meeting the requirements of the corresponding system nodes become active or inactive to control when the heat transfer occurs. In the case of chilled water storage model, two HX's are used, and hence additional actuator was needed to control charging or discharging operation.

The algorithm used for this control in chilled water storage tank is detailed in the flowchart in Figure 54. A similar control algorithm is used for ice storage tank where the tank storage status is captured using ice tank charge fraction instead of temperature that provides a more accurate indicator for decisions. However, as this variable is not generated for the model used in chilled water storage objects, the average storage tank temperature is used as a decision variable. Optimal values of the control variables like the tank capacity, cut off temperatures for charge/discharge and chiller operation are identified using parametric study by varying these variables and determine the best solution that meets the setpoint.

#### 4.4.2 System Sizing for Demand Side Management

System sizing in EnergyPlus primarily focusses on meeting all the cooling and heating demand for a design day. The designed chiller capacity is always more than the total cooling demand during other days, which results in part load operation during those days. The effect of oversizing and part load operation of HVAC systems is a critical issue for the HVAC engineers [76].

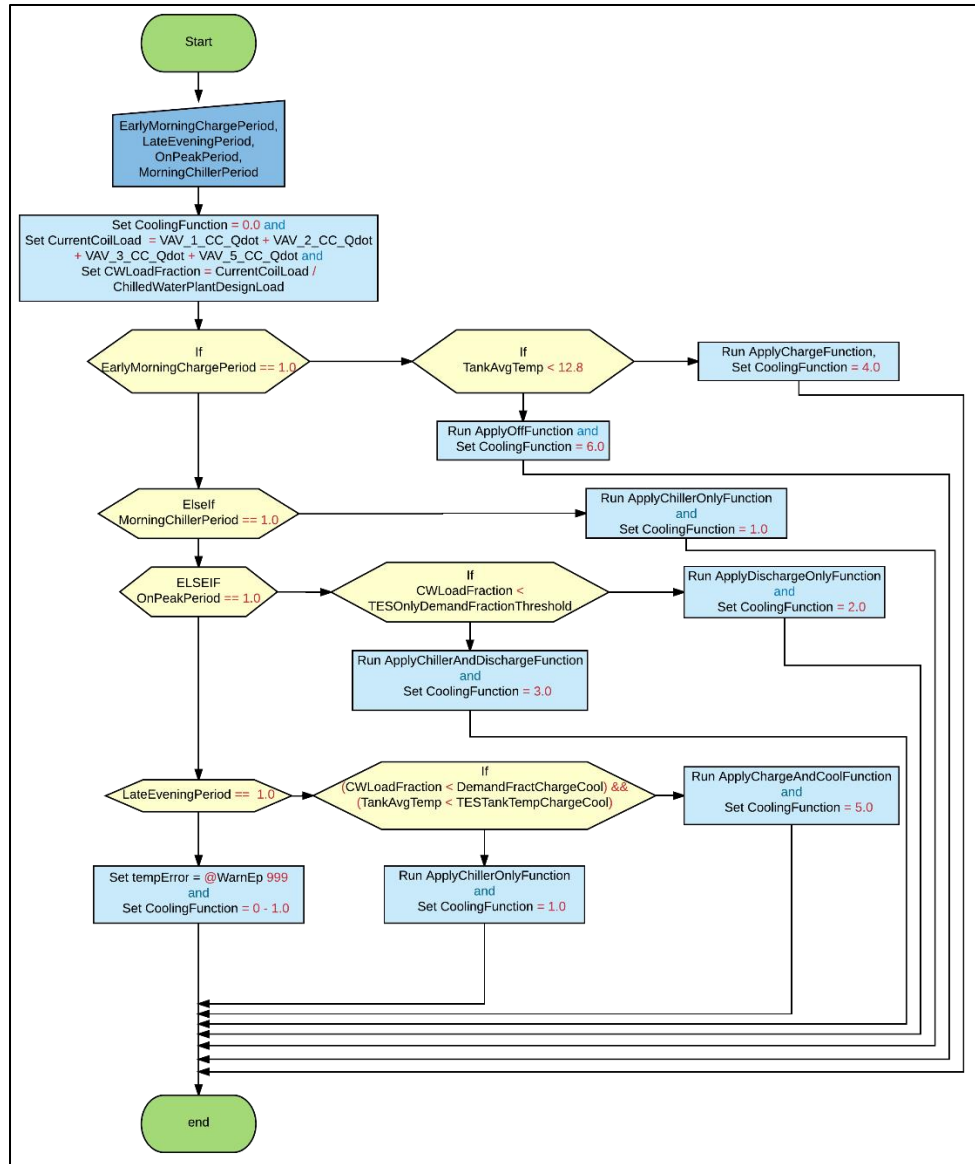


Figure 54. Control strategy algorithm

For optimum sizing of the chillers for cooling a compromise between comfort and energy use is required. Many studies focus on finding this balance for different systems as reported by Facci et al. and Ruan et al. [98], [99].

#### 4.5 Performance with New Configuration

In EnergyPlus, chiller parameters include the variable 'sizing factor' that represents the relative capacity of the chiller with respect to automatically sized chiller capacity. Two chillers with sizing factor of 0.5 were considered to satisfy the total cooling demand required so that each chiller shares the load

equally. However, the chiller capacities increased when the thermal storage system was implemented for the same cooling demand and chiller-sizing factor of 0.5. Figure 55 shows the operation of storage loop heat exchangers in response to the control states and the energy transfer rates during charging and discharging and discharging from the TES tank as a response to control states.

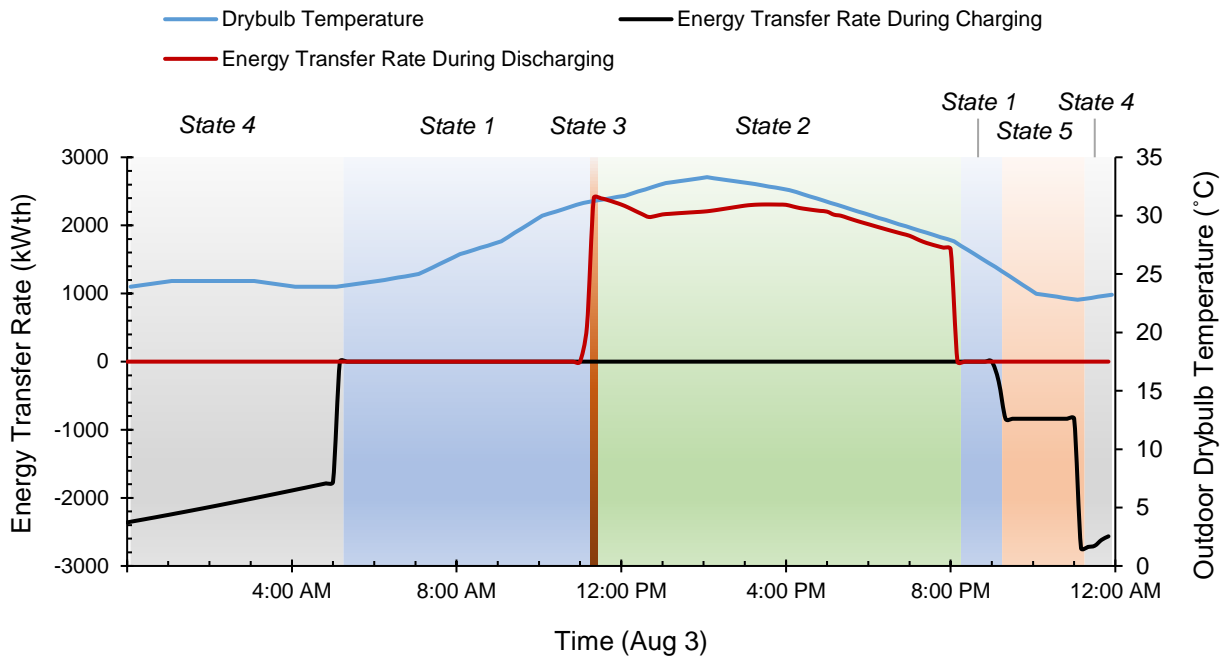


Figure 55. Charging and discharging heat transfer

#### 4.6 Optimization of the System Size for Storage

In this study, JEPlus was used to find the optimal chiller capacity required for the large building model for the selected location [96], [100]. There are many optimization algorithms mainly classified under either iterative or heuristic and when combined, give us hybrid optimization techniques. These techniques also fall under groups like single or multiple objectives. A JEPlus+EA tool based on Non-dominated Sorting Genetic Algorithm II (NSGA-II) which is a Multi-Objective Genetic Algorithms (MOGAs) is used for identifying the optimum parameters that minimize the operation cost for the building models with storage [101].

Optimal system sizing for a minimum cost of cooling was identified using an evolutionary algorithm. The objective function is subject to a constraint of total unmet hours for the annual simulation.

The objective function is defined for minimizing the operating costs along with lower cooling electricity. The reduction of chiller capacity not only provides upfront capital savings but also improves part load operations.

#### 4.6.1 Ice Storage Model Optimization

The ice storage model was optimized using the above algorithm and varying the following parameters:

- Sizing parameters
  - Tank capacity [GJ]
  - Chiller Sizing Factor
- Control parameters
  - Storage only threshold
  - Design load [W]

The maximum acceptable unmet hours for the whole facility were set at 100 hrs. The storage only threshold is the level of storage that is used as a decision variable in the control strategy. The optimization results from JEPlus runs for the ice storage model are provided in Figures 56 and 57. Figure D.1 provides additional results from the JEPlus simulation.

The best economic option results from a tradeoff between storage capacity and the annual cost of operation. The results from optimization gave the best solutions, which include a chiller sizing factor of 0.2 with a storage capacity of 40 GJ. Any further reduction in energy use by controlling the design parameters and stricter control strategy resulted in higher unmet hours which were not desirable, thus did not pass the constraint set for acceptable solutions.

A comparison between achieved average chiller PLR and unmet hours of the best solution models and the total annual electricity cost also found that the highest PLR was obtained with chiller sizing factors from 0.2 for minimum operating costs among the population. As the objective is to meet the cooling

requirement while minimizing costs, a secondary objective was to size the system as small as possible. The system with smaller storage tank and smaller chiller capacity with the most effective strategic control parameters were found to have a storage tank capacity of 40 GJ and a chiller sizing factor of 0.2.

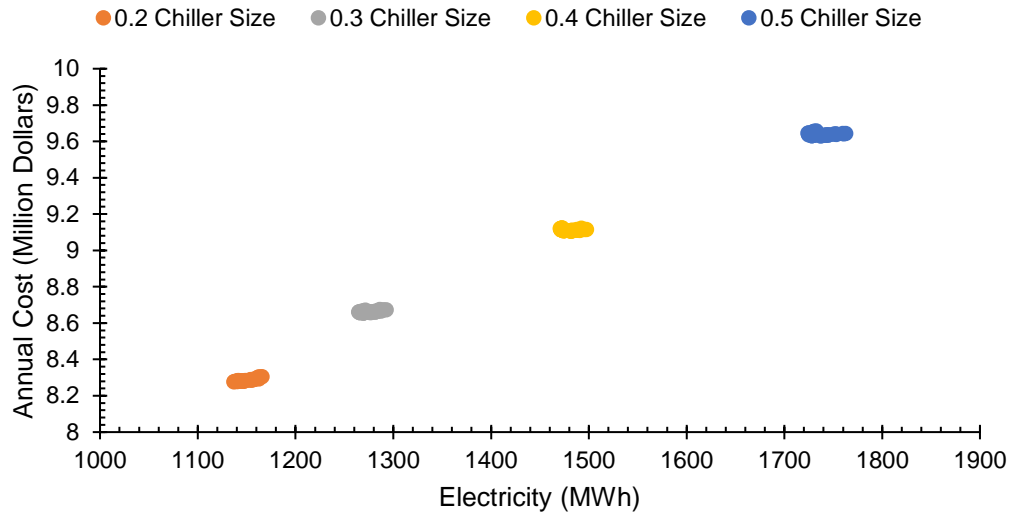


Figure 56. Optimization result: annual cost vs. annual cooling electricity

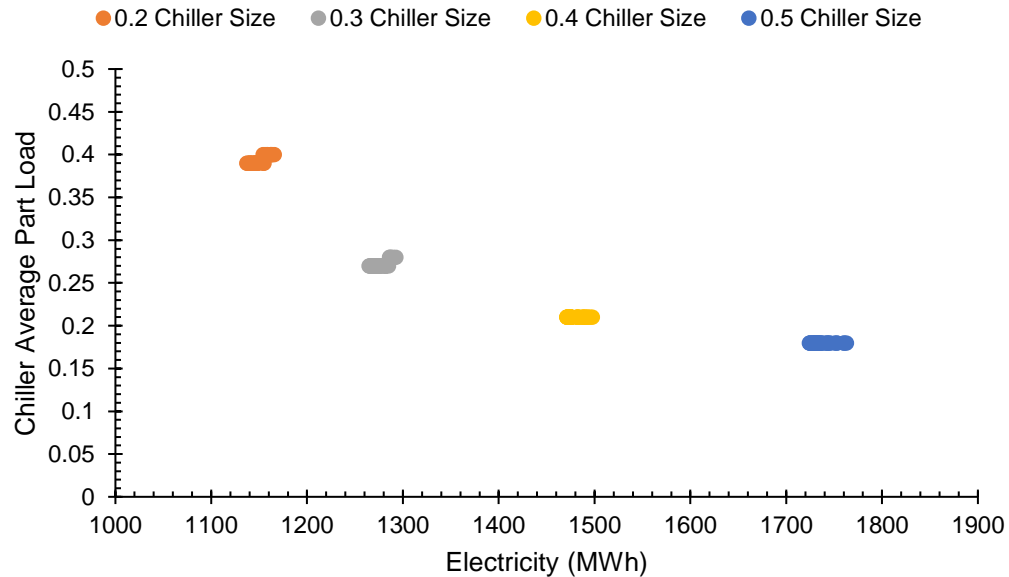


Figure 57. Optimization result: average part load ratio vs. annual electricity

#### 4.6.2 System Optimization for Chilled Water Mixed and Stratified Tank Storage

The two chilled water storage based models being similar in working fluid and configuration were optimized for the following parameters:

- Sizing parameters
  - Tank volume [m<sup>3</sup>]
  - Chiller sizing factor
- Control parameters
  - Storage only threshold
  - Design load [W]

The optimization results for the chilled water mixed storage tank and stratified tank models are provided in Figure D.2 and D.3. The best solution for both chilled water thermal storage with minimum cost and within the comfort was identified to have a tank volume of 3000 m<sup>3</sup> (~ 45 GJ) and a chiller sizing factor of 0.2. The overall operation cost of the mixed storage tank model was higher than the stratified tank model by about 7%.

#### 4.7 Results After System Optimization

A reduction in peak cooling electricity of between 25-78 % was achieved from the three storage system models as detailed in Table 14. However, the ratio of the annual cooling electricity to the total electricity was comparable in all models (~17%), which is dependent on the equipment efficiencies.

Table 14. Annual simulation results of optimized configuration

Model	Chiller Capacity [kW]	Chiller Avg. PLR []	Annual Cooling Electricity [kWh]	Annual Peak Cooling Elec. [kWh]	Annual Electricity [kWh]	Total cost for Electricity [\$]
Reference Building	2372	0.19	1429251	608320	7077663	582,557
ICE Tank	1164	0.40	1168596	451727	6459729	515,759
CW Mixed Tank	1397	0.31	1282699	424933	6620501	518,613
CW Stratified Tank	1397	0.33	1269337	130448	6549139	483,936

The typical daily operation for the four models is shown in Figures 58, 59 and 60 highlighting the chiller operation cycles, chiller PLR, and pumping power. During peak hours with high cooling demand, the chillers are in the 'OFF' state when full storage discharge is in effect, while, for partial storage, both chiller and storage discharge are operating.



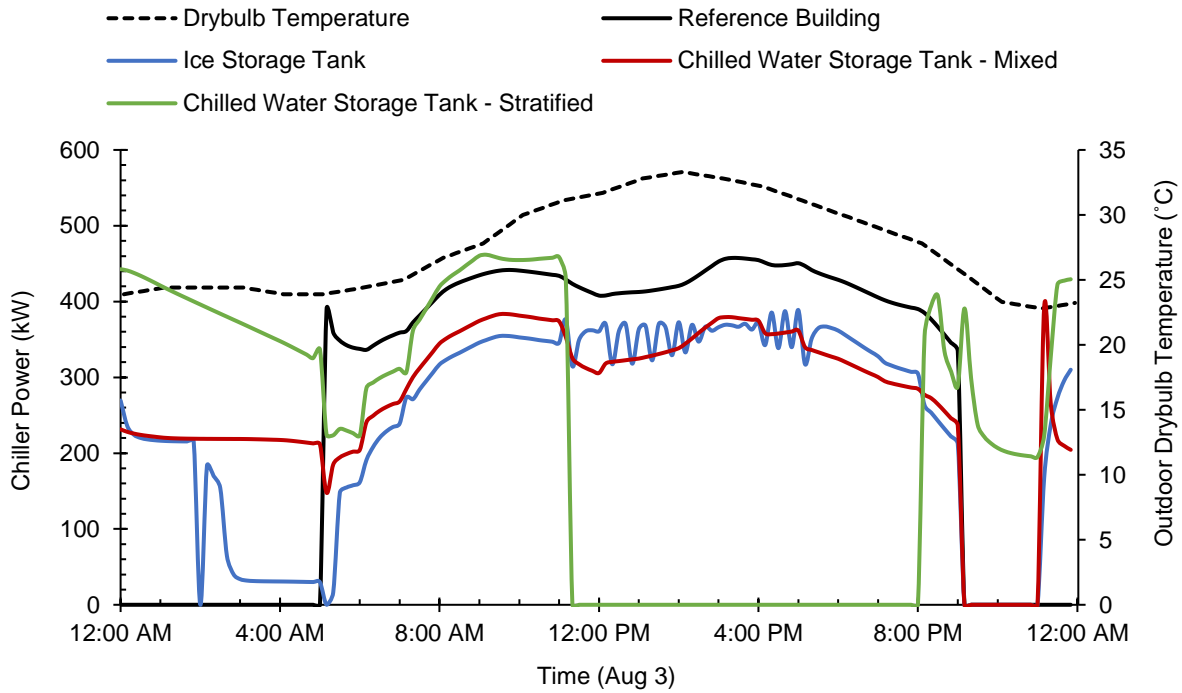


Figure 58. Chiller power after optimizing the three models

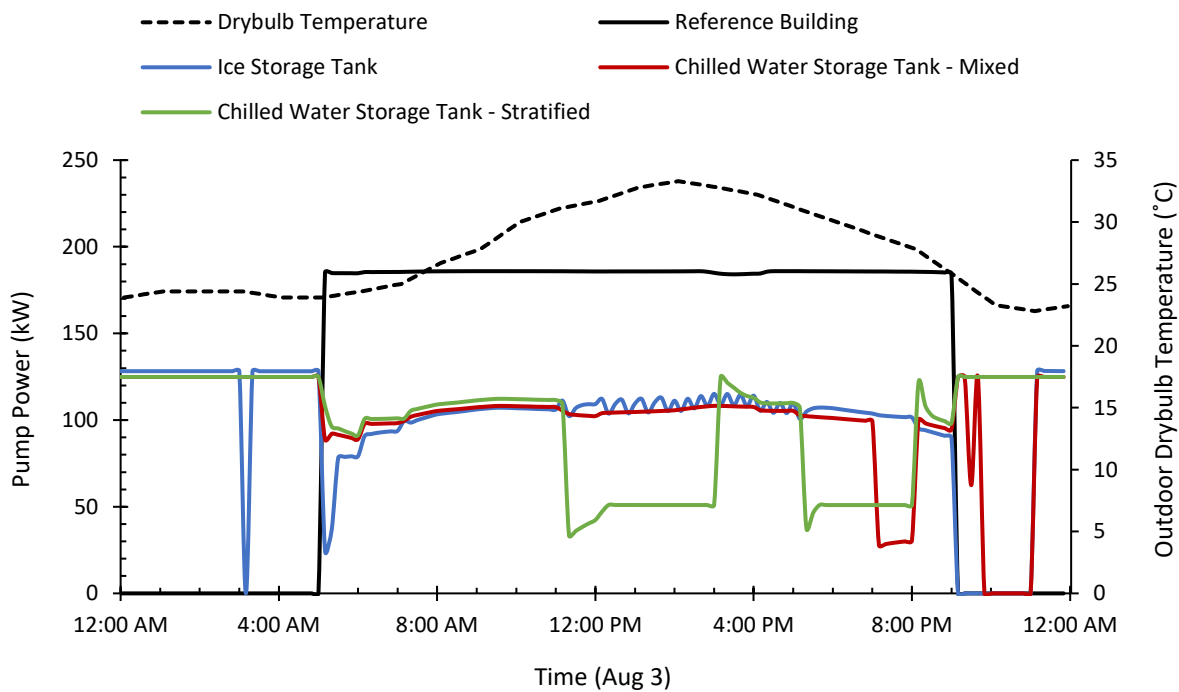


Figure 59. Pumping power after optimizing the storage models

The maximum pumping power for the day was reduced from 230 kW (before system optimization) to ~125 kW. The pumping power during peak hours was reduced significantly due to the shifted load from

chillers to storage. The resized chillers were found to operate with higher part-load-ratios, resulting in capacity reduction and optimal loading throughout the day.

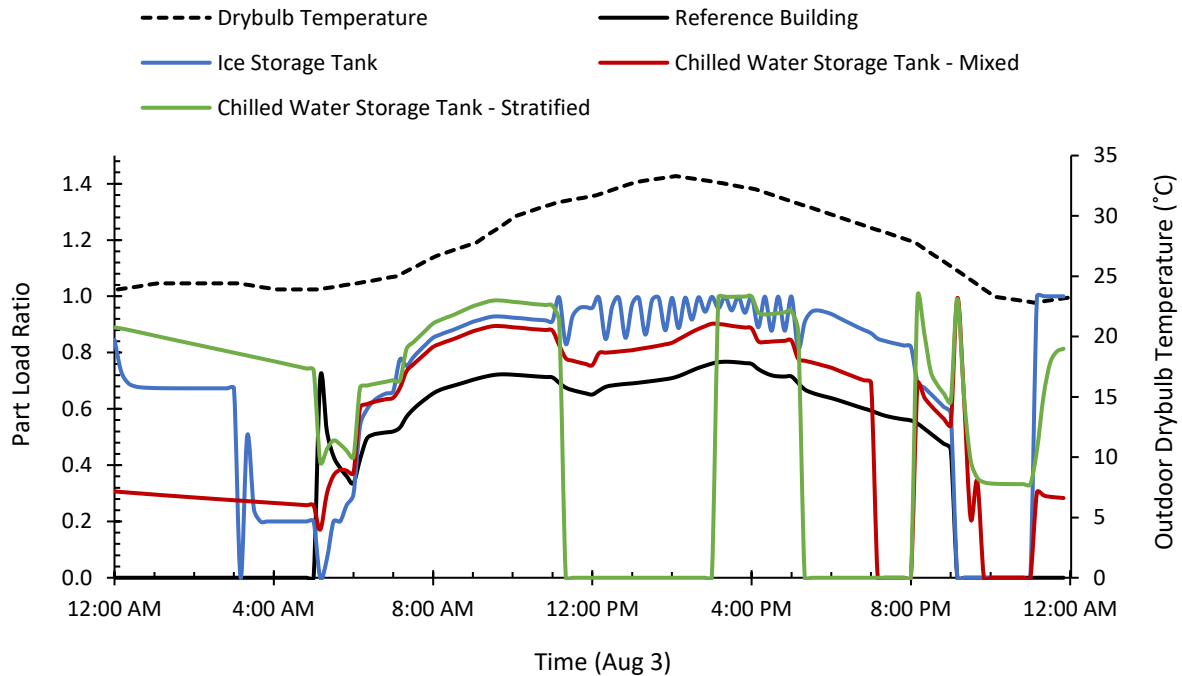


Figure 60. Chiller part load ratios after optimizing the storage models

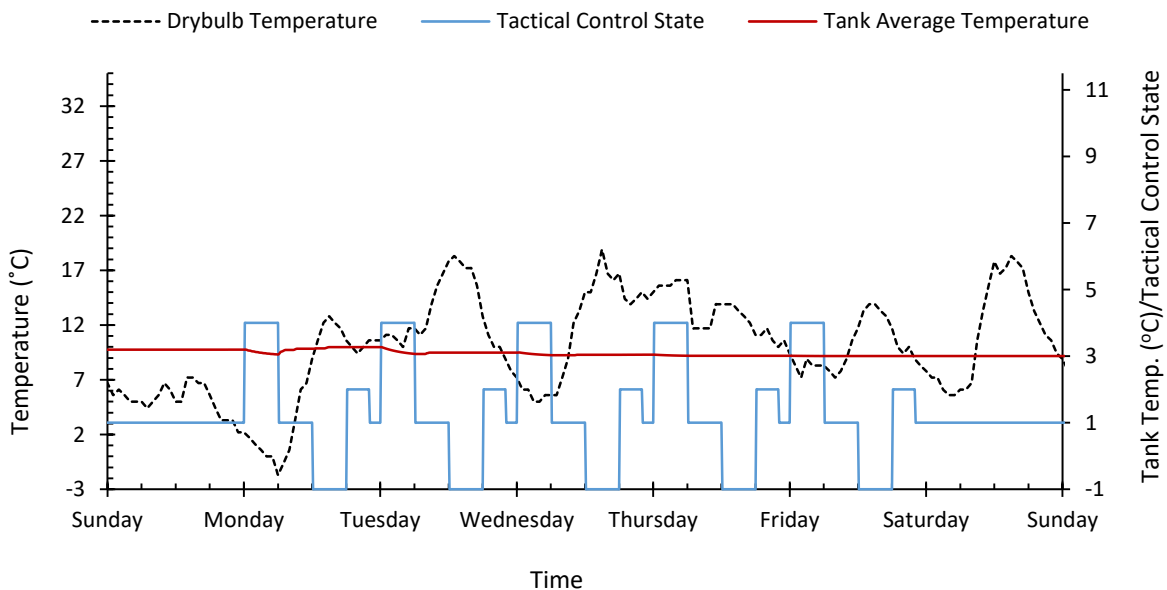


Figure 61. Week operation in winter (8-15<sup>th</sup> January)

Figures 61 and 62 show the operation of the storage tank during a weekly run for winter, mid-summer, and peak summer, highlighting the change in storage tank temperature with control state. In

colder days, the storage tank temperature hardly changes due to very low demand for cooling, while a significant use from the storage tank is observed during peak summer days.

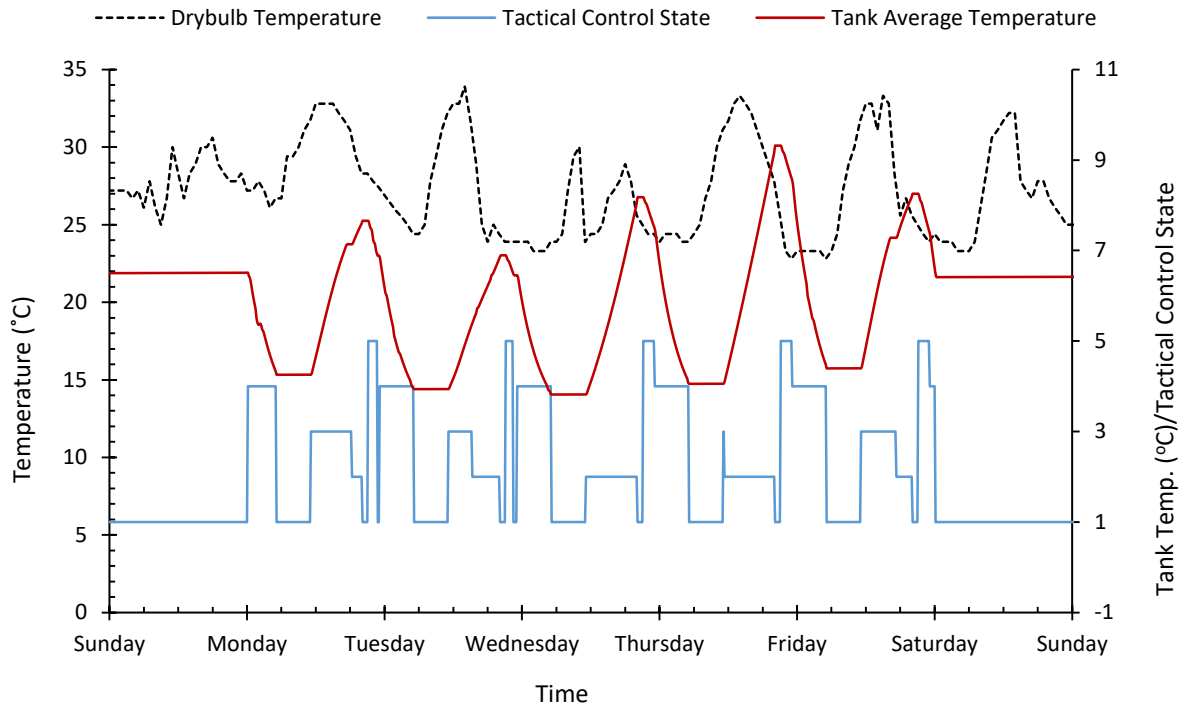


Figure 62. Week operation peak summer (30<sup>th</sup> July – 6<sup>th</sup> August)

#### 4.8 Economic Comparison and Discussion: Optimal TES System for Commercial Buildings

The operation costs of the three storage based plants with the same capacity chillers as the reference building's chilled water plant was found to be much higher due to the additional losses and cyclic inefficiency of TES. However, once the three models were optimized with cost minimization as the objective function, the three models produce an overall electricity cost reduction of 10-17% as compared to the original system (Figure 63), and cooling electricity reduction was about 7-10% resulting from smaller chillers operating at higher part loads. In contrast, the resulting peak electricity shifted was about 25-78% from the base model. The use of storage not only facilitates shifting the energy use to off-peak hours but also allows downsizing of the chillers, thereby reducing daily peak demand. The annual operating cost reduction potential by using ice storage tank of 40 GJ was found to be around 11.5%, while for a chilled water storage tank of 3000 m<sup>3</sup>(~45 GJ), it is projected to be about 17% using the proposed control strategy.

Although the use of chilled water TES is a good option for peak shifting, it has a limitation of larger footprint with a temperature differential of about 8.3°C and a storage volume of 0.43 m<sup>3</sup>/ton-hour. Ice based storage for HVAC has a smaller footprint of about 0.09 m<sup>3</sup>/ton-hour [102]. It is estimated that North America will have about 20% share of the global installed thermal energy storage capacity by 2020 [103].

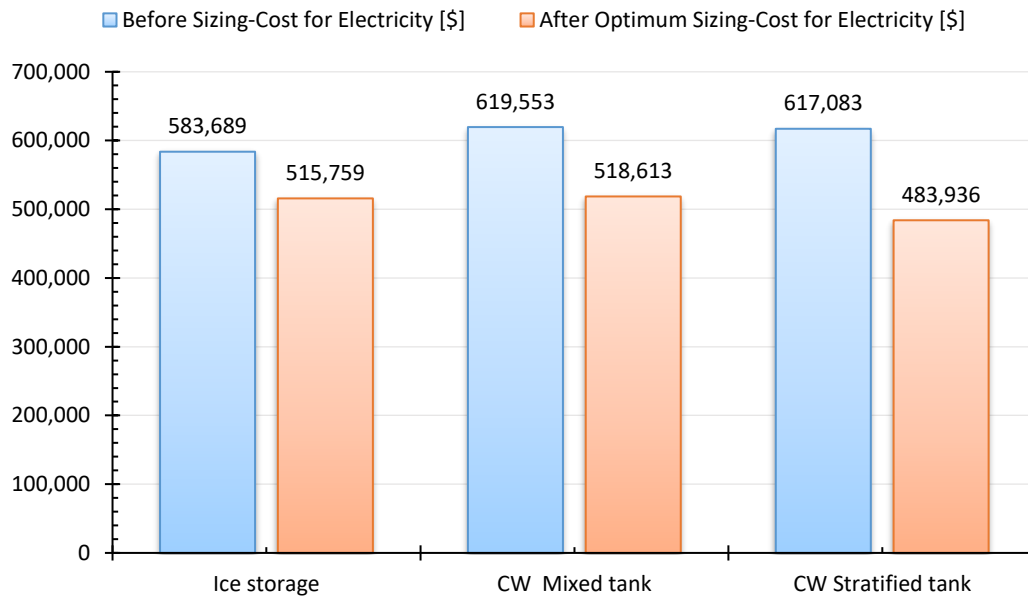


Figure 63. Reduction in annual cost of electricity after optimizing

The developed models were used for the following cities with different weather conditions but similar loading conditions:

- Tampa
- Los Angeles
- Denver
- New York

Figure 64 shows the total electricity used for the office building under different weather conditions in the selected locations. As expected, electricity use is highest in Tampa followed by Los Angeles, New York and Denver respectively. In terms of the cost of operation for the entire office, the overall energy cost is compared in Figure 65. The total cost is highest for Tampa and lowest for Denver.

However, the cost of electricity of New York is higher than Los Angeles due to the overall higher peak electricity consumption in contrast to lower total electricity consumption.

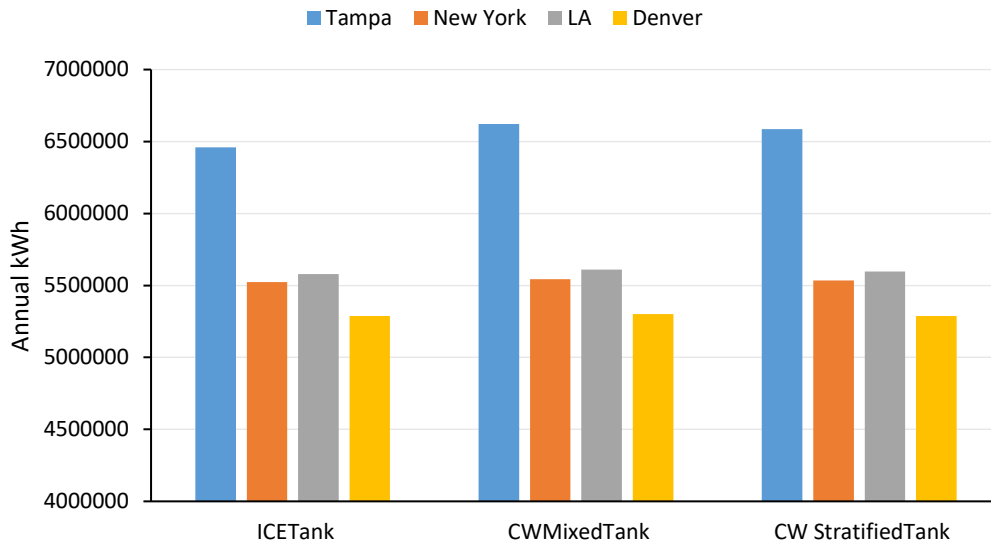


Figure 64. Annual electricity use from three models for selected locations

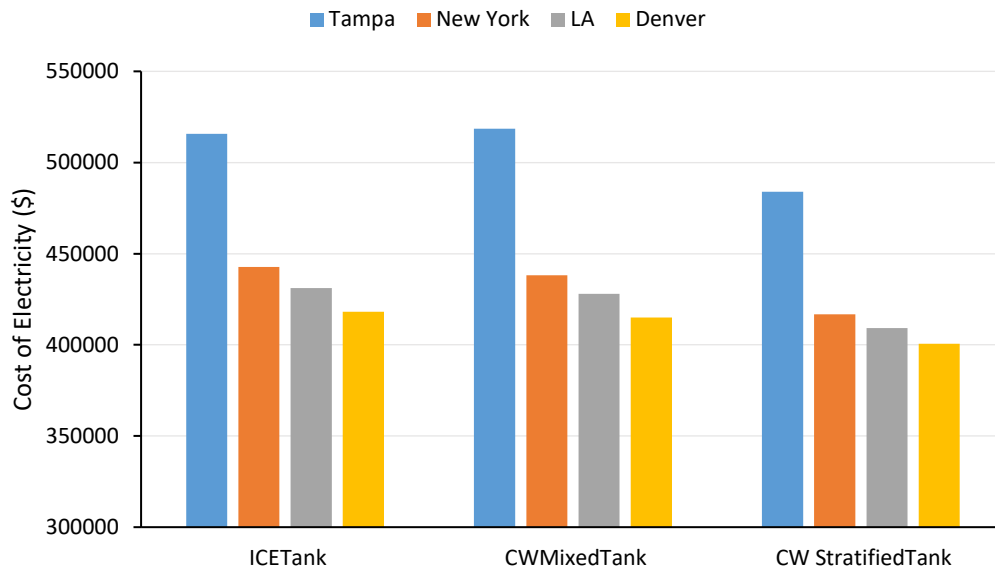


Figure 65. Annual cost of electricity use from three models for selected locations

The overall CO<sub>2</sub> emissions from the large office building were also compared and were found to be highest for Tampa (~8100 tons) and lowest for Denver (~6600 tons). Similarly, the water use for heat rejection was ~18000 m<sup>3</sup> for Tampa and lowest of ~7500 m<sup>3</sup> for Denver. The following chapter looks at the impact if TES can be deployed at large scale on a Utility profile.

## Chapter 5 Impact of Adopting Thermal Energy Storage in Buildings

### 5.1 Tampa Utility Generation and Demand Analysis

Based on the power generation data from TECO, the electric utility of Tampa, for 2013, it was observed that the average summer generation capacity included about 59% generation from base-load power plants, 38% from intermediate natural gas combined cycle power plants and 2.6% from peak generation units. However, the total generation capacity corresponding to the three categories of power plants was 40% for base load, 37% of intermediate load and 23% of peak load power plants. Interestingly, the average fuel cost (¢/kWh) of the peak power plants was about 86% higher than the base-load power plant with an average capacity factor of 4.2% vs. 83% for the base-load plants [8]. Figure 66 shows the respective capacity utilization of the three categories of a power plant with the peaking units in orange color, where the size of the bubble is the relative capacity of each type of units.

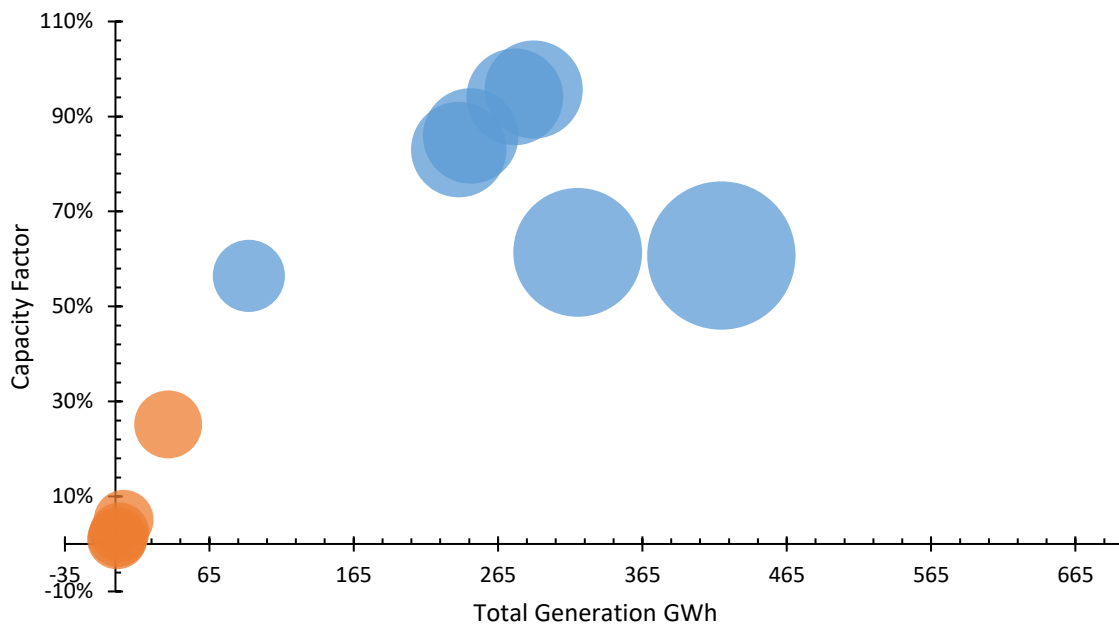


Figure 66. Generation capacity utilization in summer-2013, Tampa

The mismatch in utility generation capacities among the three categories of power plants is primarily due to the coincidental and non-coincidental peak demand from all the consumers. Figures 67 and 68 shows the monthly power profile of January-2013 and August-2013 months of Tampa Electric Company. The coincidental winter peak for January was 2563 MW at 7:00 pm (January 9th, 2013) while during summer the coincidental peak was 3873 MW at 5:00 pm (August 13th, 2013). The two peak values are in the defined peak intervals for peak electricity rate for the Time-of-Use (TOU) customers [104].

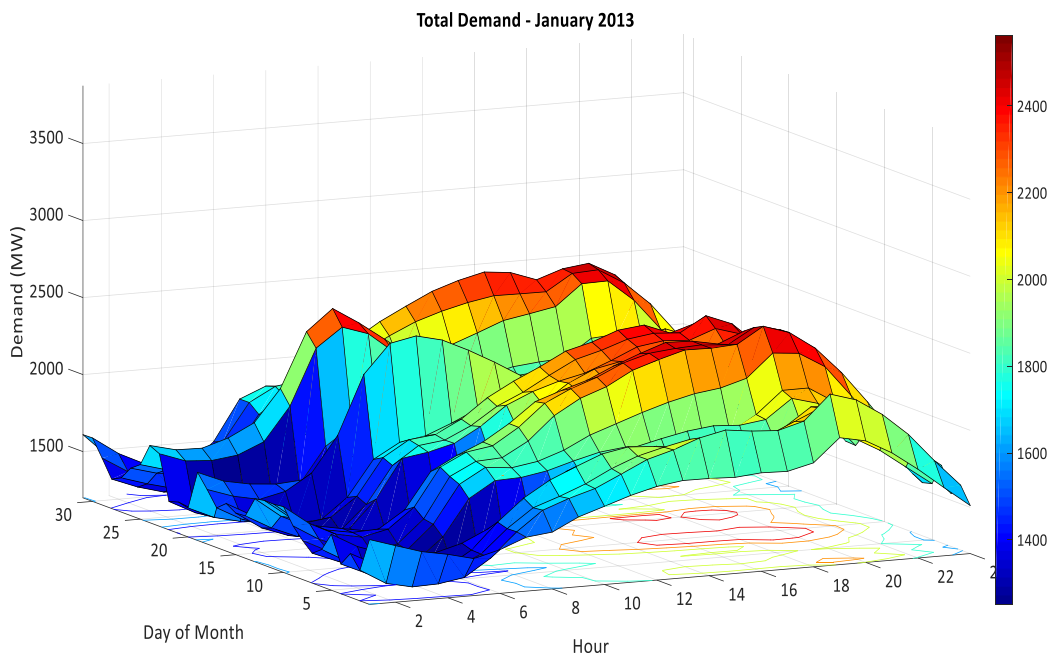


Figure 67. Utility load profile for January-2013

### 5.1.1 Benefits of Peak Demand Shifting from Commercial Buildings

According to EIA survey of the US commercial buildings (CBECS-2012), the electricity and natural gas accounted for 93% of total energy consumed in buildings with electricity at 61% and natural gas at 32% [105]. Commercial buildings have different energy use patterns based on activity, building design, floor area, and size. EIA survey aggregated commercial buildings into fourteen principal building activity types based on their primary activity. Office, warehouse, storage, service and mercantile buildings were most prevalent and occupied about 51.6% of total floor space [105]. However, energy use in commercial

buildings by air conditioning, cooling, and refrigeration in Southern Atlantic region is about 44% of the overall energy use, while 37.3% (Figure 69) of the overall electricity use [106].

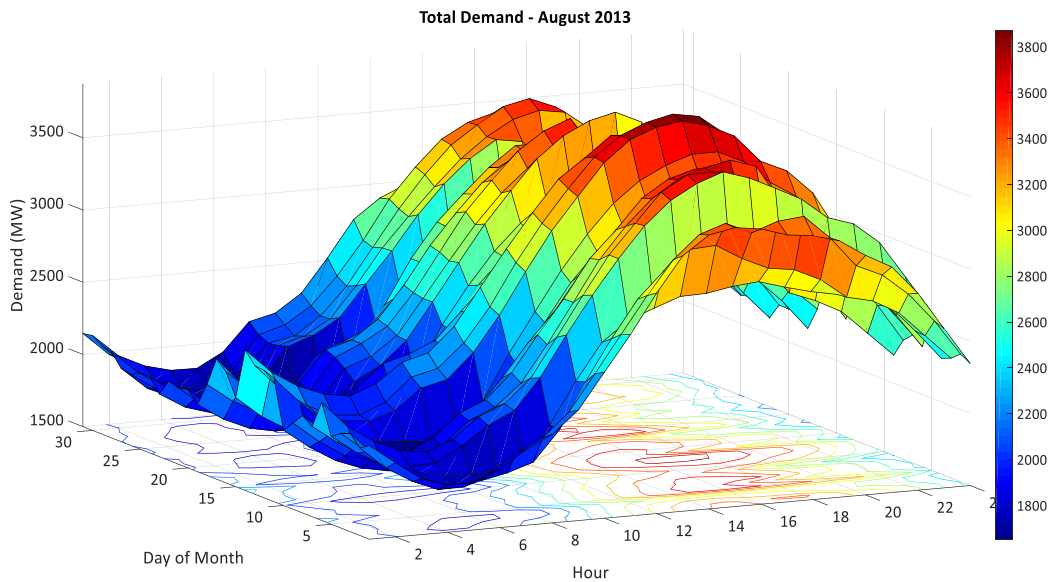


Figure 68. Utility load profile for August-2013

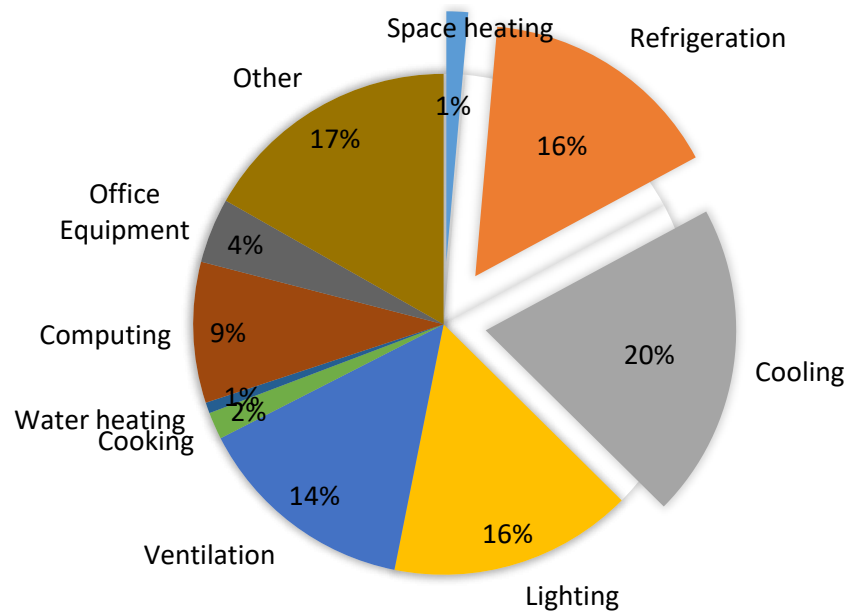


Figure 69. Electricity consumption by end-use in all buildings in South Atlantic Region, 2012, US-EIA

Demand side management can have a significant impact on the utility power supply quality when implemented in a large number of buildings. To quantify such impact, the results of the adoption of TES in one building analyzed in Chapter 4 is scaled up to represent a utility level penetration. Demand-side



energy efficiency measures and peak shifting strategies help reduce the investments in power generation, transmission, and distribution infrastructure, which allows a utility to save money through avoided capital cost. The avoided cost of DSM measures can be of significant value to both utilities and consumers.

## 5.2 TES Adoption Impact on Regional Demand Profile

Accurately predicting the impact of electricity use by each building with TES in a region would require measuring real-time data which economically not viable. Hence, the average energy use in the US commercial building sector was used to establish this relationship. On the average, 40% of total electricity in the US is used by buildings [107].

Fifteen DOE reference commercial building models were used which account for 86% of all the building types in the U.S. The national average population of all buildings types based on EIA estimates [105]. The representative count of reference building models and their population share is shown in Table 15 below.

Table 15. Commercial building share based on activity

Type of Building	Number of buildings	Representative number of buildings
Full-Service Restaurant	7	455
Hospital	2	130
Large Hotel	1	65
Large Office	8	520
Medium Office	8	520
Out Patient	2	130
Primary School	4	260
Quick Service Restaurant	4	260
Secondary School	3	195
Small Hotel	2	130
Small Office	13	845
Stand Alone Retail	7	455
Strip Mall	5	325
Super Market	8	520
Warehouse	12	780

Yearly simulation of all the commercial building models using 2013 weather data was done to get the overall demand from buildings. The total electricity demand for a selected day (Aug. 13th, 2013) from

large office buildings contributed to about 40% of the total electricity demand while the remaining 60% was collectively from the remaining fifteen building types (Figure 70). This electricity demand profile was used to estimate the optimum scale factor for matching the total electricity usage from all fifteen buildings with the utility demand. An iterative linear interpolation of the total building energy demand for the peak day of August (13th August 2013) found that a scale factor of 65 matches within 3% of the total utility demand from buildings (Figure 70). The calculated population mix of building types that contribute to equal electricity demand from commercial buildings for TECO region is given in Table 15.

The analysis shows that the ratio of the peak to average demand from all commercial buildings for TECO is about 1.5 which is lower than the reported 1.78 for entire South Eastern Region [108]. The difference can be attributed to statistical assumptions for such calculations. Even if all building construction types and ages are considered for demand calculation, the diversity in the peak and average load would be higher, thus supporting the case for TES in the buildings.

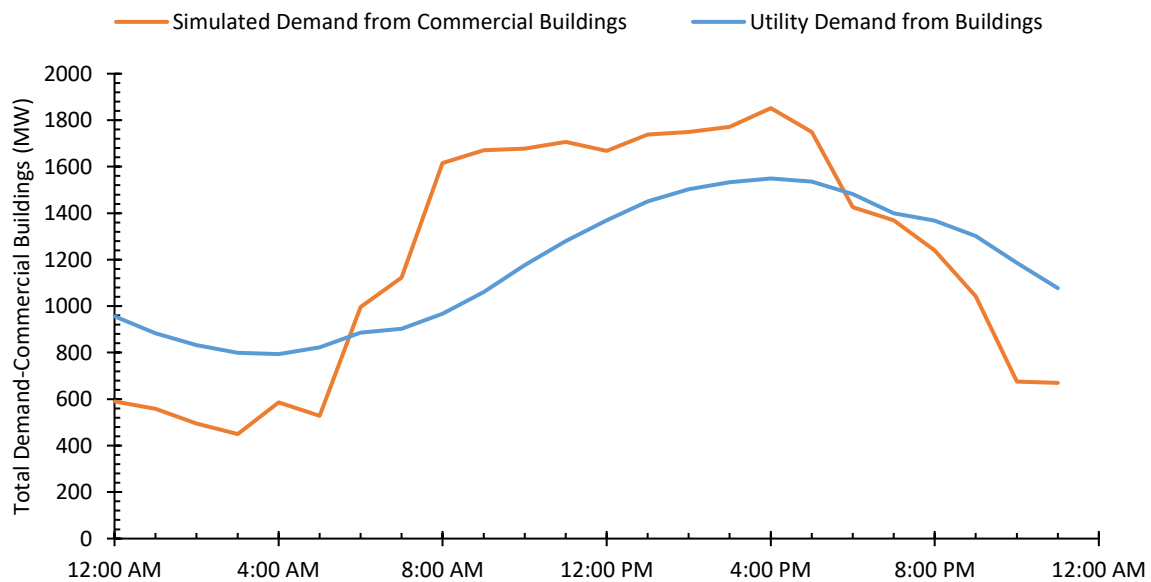


Figure 70. Aggregate building electricity demand on 13<sup>th</sup> August-2013, Tampa, FL

As observed in Section 4.6, the aggregated peak-shifting of 25-78% from buildings with thermal storage could be achieved. A simple conservative peak-shifting scenario of 25% -75% during peak summer time between 12:00 pm to 9:00 pm would mean a reduction of average 450 MW to 1.3 GW of peak

generation capacity. The mode of operation to achieve such a reduction is by utilizing either 'partial storage control - peak demand limiting' or 'partial storage - load leveling' or 'full storage control,' approaches for building TES [97].

If daily peak-load shifting in all commercial buildings for Tampa is implemented successfully using TES, a much flatter demand will be seen by the utility. To demonstrate it, TES with 90% storage cycling efficiency was assumed, and the following scenarios of 25%, 50%, 75%, and full peak shifting were projected as shown in Figures 71 to 74. Implementing and achieving 100% peak shifting in all commercial buildings using TES would mean an increase in the off-peak demand of about 2050 MW, much higher than the present peak demand as depicted in (Figure 71). Similarly, a 75% peak shifting would result in a maximum off-peak daily demand to about 1800 MW about the same as the current peak demand (Figure 74). An aggregate peak reduction of 25% and 50% would mean a favorable peak demand reduction while leveling the day peaks and increasing the off-peak demand to match the base load requirement from buildings.

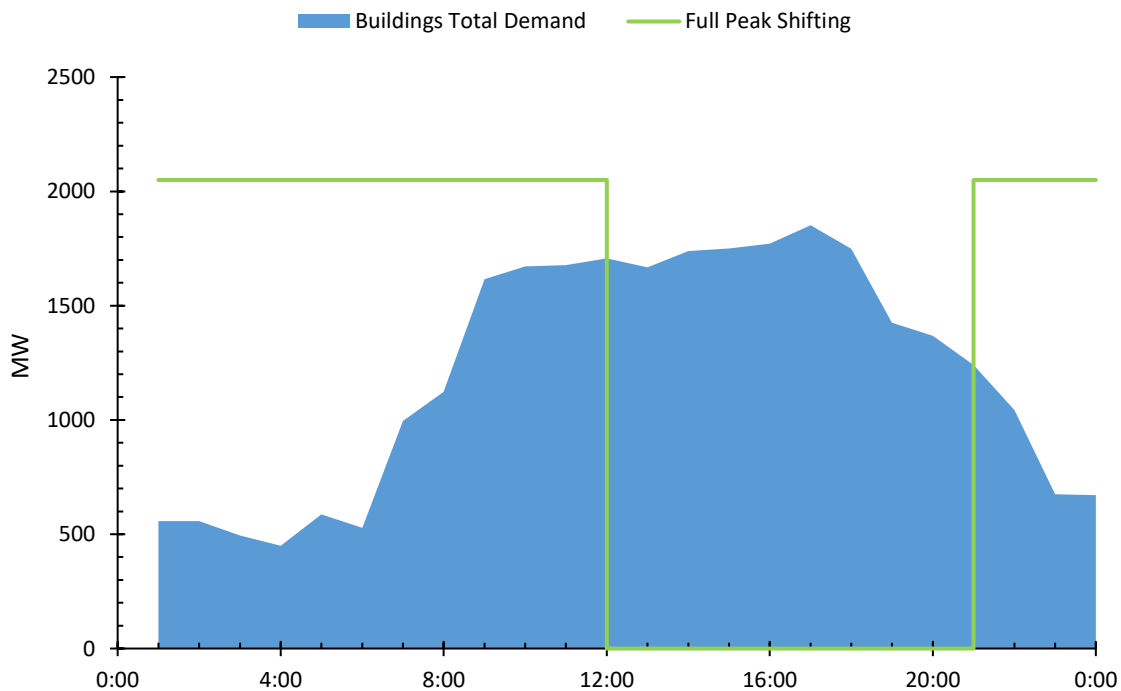


Figure 71. Building full peak shifting scenario

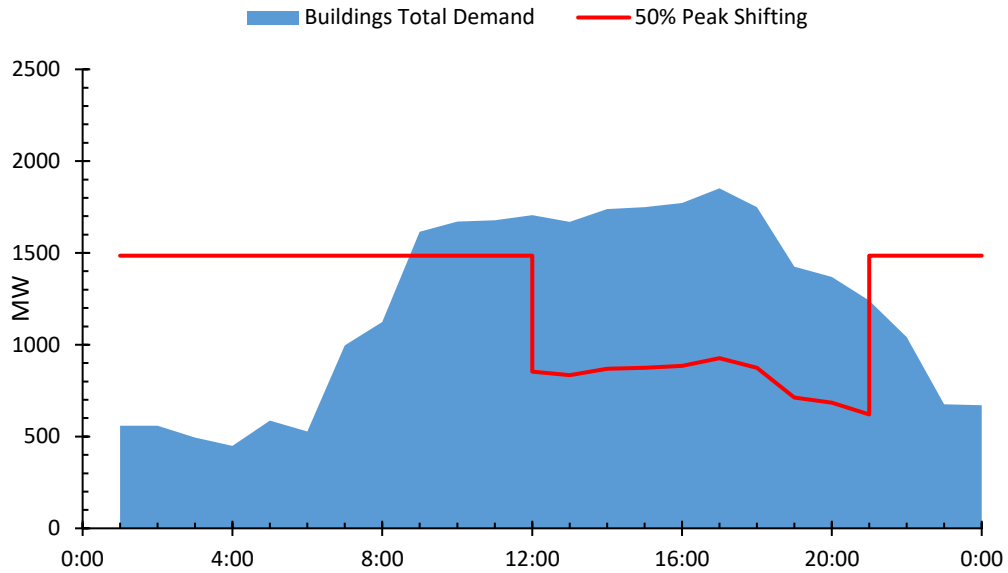


Figure 72. Partial control- 50% peak shifting scenario

Figure 72 presents the scenario with 50% peak is shifted for all commercial buildings resulting in a peak demand reduction by 367 MW.

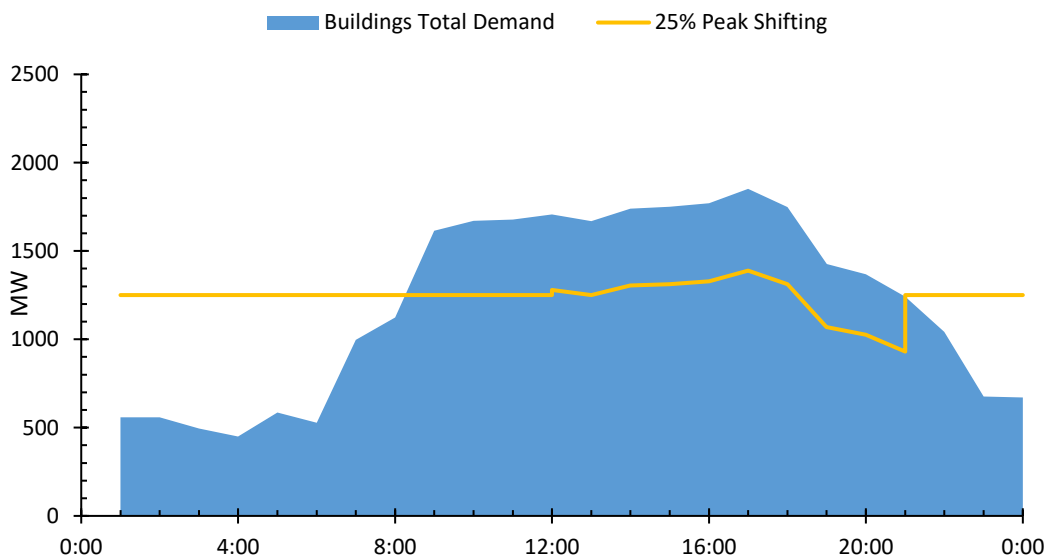


Figure 73. Load levelling scenario

A conservative 25% load leveling would reduce the peak demand to 1389 MW during peak hours resulting in lowest peak demand for commercial buildings (Figure 73). Load leveling by 25% peak shifting is ideal for achieving the best case for all commercial buildings in Tampa region, as it would result in higher

overall capacity factors for all utility power plants. Such improvement in capacity utilization is ideal for utility business and also for generation scheduling.

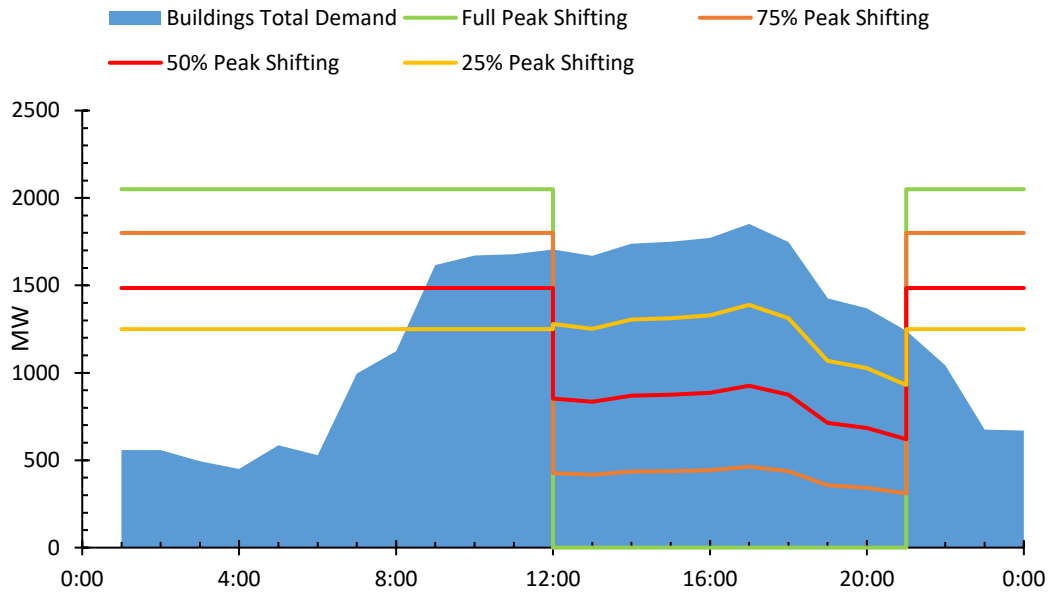


Figure 74. All scenarios of peak load shifting in buildings

### 5.3 Benefits of Storage to Power Grid and Renewable Energy Systems

Demand and supply of a power system require balancing of grid voltage and, frequency within an acceptable range. System operators face a challenge of matching the demand and supply for a continuous, reliable operation. The addition of variable generators (VG) to the grid result in an imbalance in the grid frequency and voltage. Renewables or VG have two important characteristics [109] that affect the quality of the electric grid:

- Variability - the output of variable generators like solar and wind is dependent on the available resources that result in variability over time.
- Uncertainty - the availability of the primary resource and its magnitude is difficult to predict and has a high uncertainty that conventional power plants during power generation.

The cost of integration of wind and solar includes additional ramping requirements to meet the load due to the intermittency of the renewable resources and the operation of power plants kept online

to balance the added uncertainty. Various studies reported these costs [110]. The overall cost of wind variability was found to be less than 0.5 cents/kWh in 2008, and most of the reported findings showed forecasting errors and uncertainties contributed the highest. It is possible that such forecasting errors follow under or over-commitments from baseloads power plants and result in outages. System operators under these conditions would rely on high-cost online power plants or purchase expensive energy from available utilities. Additionally, they even pay customers to cut down their load.

Due to the limitations of system capabilities and renewable generation, VG's are expected to face curtailment during periods of high generation and low demands. Storage provides an option to avoid curtailment of renewable generation by bridging the gap between VG supply and demand. This provides the potential for increased flexibility in the grid. Grid flexibility can be increased by adoption these options [111]:

1. Supply and Reserve Sharing- Aggregation of demand and supply makes it easier to deal with demand variations without adding new infrastructure;
2. Flexible generation- Updating and adding new conventional generation that has increased ramping range and load following capabilities;
3. Demand flexibility - Including demand side management by introducing smart grid and demand response to short-term load shifting and demand curtailment;
4. VG curtailment - Overbuilding renewable capacities will attract curtailment but, provide an option for operating reserves and allow reduced load on base load units that presently provide operating reserves;
5. New demand- Adding flexible and controllable loads that can use renewable generation. The use of electrical vehicles and plug-in hybrids has a large-scale potential for providing contingency reserves;

6. Electricity storage - Centralized or decentralized storage provides a buffer for utilizing VG generation by providing flexibility in demand. Various technologies can be deployed for balancing RE generation and demand by providing time shifting and frequency support.

### **5.3.1 Energy Storage Applications**

Energy storage applications are classified into three categories based on the discharge capabilities:

1. Power Quality- Help with frequency control and transient stability. Technologies for these are flywheel, capacitors, and superconducting magnetic energy storage;
2. Bridging Power - Providing a buffer for ramping capacities. Batteries like lead-acid, nickel-cadmium and lithium-ion provide rapid response to the demand;
3. Energy Management - Load leveling using thermal storage, pumped hydro storage, compressed air energy storage, and high-energy batteries like sodium-sulfur, sodium-nickel chloride batteries.

### **5.3.2 Thermal Energy Storage Value for Grid**

The cyclic efficiency of thermal energy storage is one of the major criteria while selecting suitable applications of TES. Electricity conversion from high-quality energy to lower quality energy incurs losses. Thermal energy (although it is a lower quality energy) can be stored with high cyclic efficiency. Thus, TES in solar power plants can operate at higher efficiency than electricity storage technologies. Similarly, distributed TES can have extremely high cyclic efficiencies in cooling applications. The power demand from building cooling can be levelized and shifted to off-peak hours by using chilled water or ice storage [111].

### **5.3.3 Renewable Generation from Solar**

The variability in a renewable generation for 2 MW solar PV power plant in four selected cities for summer days is shown in Figure 75. The power generation profiles for the selected cities are based on

simulated results obtained using System Advisor Model [112]. The total generation for Denver is found to vary significantly during two consecutive summer days of July, while, a small variation is observed for Tampa and New York. In contrast, the generation profile of Los Angeles is almost equivalent. Such variability in renewable generation is a major concern for utilities with increasing penetration of solar generation.

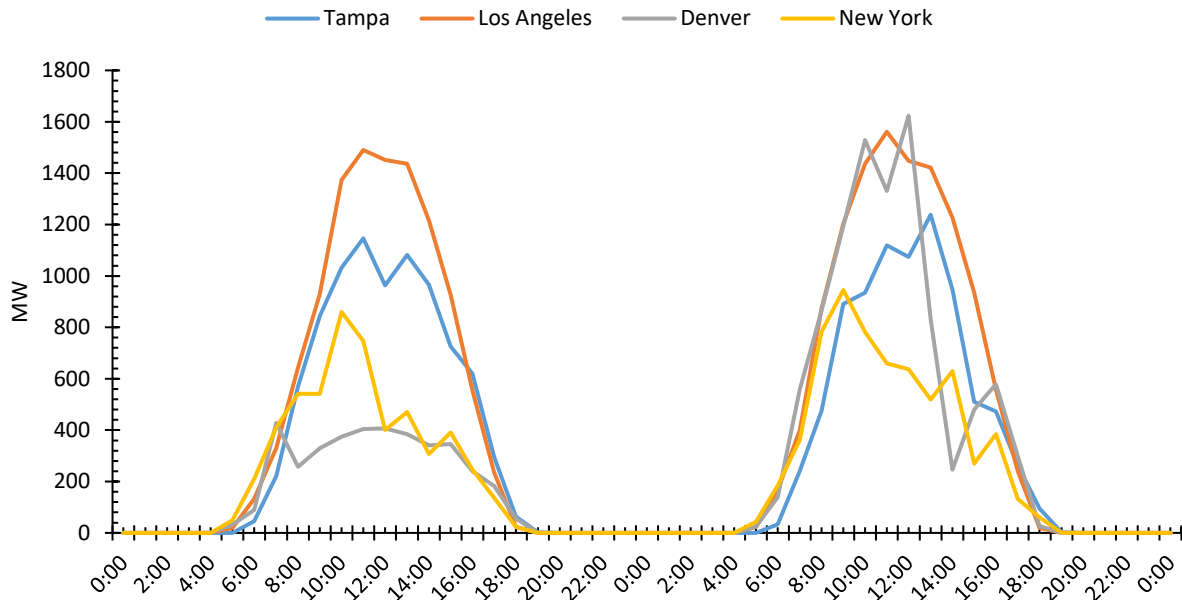


Figure 75. Variability in solar generation in four locations

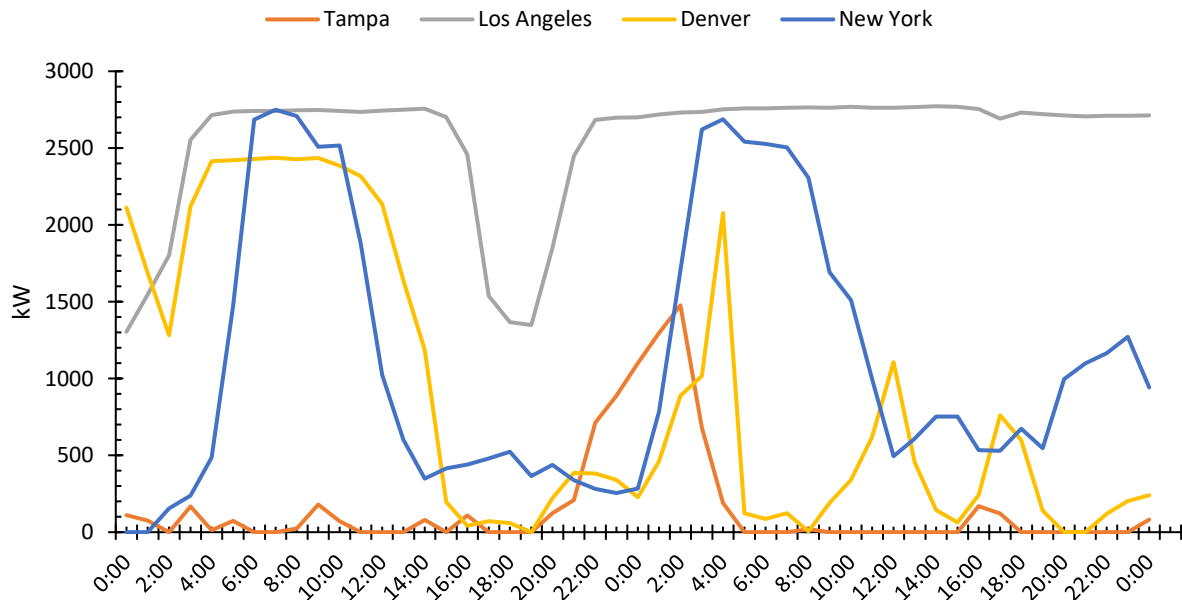


Figure 76. Variability in wind generation in four locations



Wind energy resources for two consecutive summer days were also simulated using System Advisor Model (Figure 76). The uncertainty and variation in generation from same capacity wind turbine in the four location pose greater challenge for utility and system operator in scheduling supply from these generation plants. Unlike solar power generation, wind resource is usually available during day and night. However, the forecast and scheduling of wind generation is still a challenge for system operators.

In the US, both solar and wind power installed capacities are expected to grow in future. This increase would enhance the peak generation from such sources. Introducing thermal energy storage or electrical storage would ensure improved grid performance by providing flexible demand for renewable generation.

## Chapter 6 Conclusion

### 6.1 Summary

Buildings contribute significantly to the power demand for the electrical utilities. Use of natural gas as an alternate fuel and thermal energy storage for cooling of buildings were studied for their potential to reduce the peak demand for the utilities and their economic impact on consumers and utilities. In both cases, the optimum performance of the system significantly depends on the sizing of the system matching the demand. The alternate fuel systems for cooling the buildings are Gas Engine-driven Heat Pumps or GEHP. The following summarizes the main findings.

1. The SI engines running the field deployed GEHPs were found to be oversized compared to the load they serve and, therefore, operate at very low fuel efficiencies. The average load on the engines in operation is about 25% of the rated full capacity. At such low loads, the fuel efficiency of the engine can dip to one-third of the maximum efficiency as determined from an analysis of the efficiency at rated output.
2. The average economic performance of the GEHP units in operation in this study was lower than EER 11.8 but higher than EER 9.2 equivalent electrical heat pumps. However, it was observed that during the full load operation, the units performed at a  $COP_{unit}$  close to 1.18.

Use of thermal energy storage for cooling of buildings was modeled in EnergyPlus. An operational strategy for using TES based on ice or chilled water storage was developed based TOD rates that would provide an economic benefit to the consumers as well as a peak demand reduction for the utilities. The following were the findings of the modeling analysis for using chilled water and an ice storage for building cooling.

1. The research found that using TES for all or a part of the peak demand due to chillers in a large office and the commercial buildings can result in overall cost reduction of 10-17% for the consumers and an annual peak shifting of 25-78%.
2. The economic benefit to consumers depends on the time-of-day rates. The analysis was made based on the applicable time of day rates in Tampa.
3. If 25% of all commercial buildings peak electricity during summer is shifted to off-peak durations in Tampa, a reduction of 463 MW in peak demand is possible for Tampa, thus reducing the peak generator requirement by that amount.
4. Reducing the peak demand improves the generation efficiency for a utility by not having to use lower efficiency peaking units. This benefit was discussed in the dissertation, but not quantified as the extent of improvement would depend on the peak size and duration, and peaking units capacities and efficiencies.

We analyzed the effect of renewable generation on the grid and found that intermitted nature or solar energy and the wind introduces uncertainty in the grid for which the utility has to keep some reserve capacity to overcome the fluctuations. We studied how TES would overcome this potential problem due to renewable energy.

## **6.2 Conclusions and Recommendations**

Alternate fuels for cooling and using thermal energy storage can play a significant role in shaping the demand profile for a utility. However, switching to alternate fuel would require more efficient operation of such systems to compete with the electrical HVAC equipment.

It was found experimentally from this research that for a typical commercial building, a natural gas-based HVAC system can be a good alternative to conventional HVAC system, but its performance would suffer drastically if the system size were not matched to the load. With oversized equipment in practice, engine natural gas heat pumps (GEHP) on average operate at lower than the rated full capacity.

The loss of efficiency due to the part-load operation is significant in these combustion engines. A higher load operation is recommended to ensure high-efficiency performance of these systems by coupling them with other auxiliary applications during low load conditions, such as water heating, process heat or thermal storage.

Using TES for cooling in buildings provides an opportunity to optimize the system size for better performance. The consumers can benefit financially if they opt for electricity rates with different peak and off-peak pricing. Utilities need to provide such incentives to encourage consumers to install TES in buildings as part of demand side management.

Utilities benefit greatly by distributed TES in buildings, however, utilities could also take advantage of a large-scale deployment of the TES solution for reducing the peak power demands from the region they serve and at the same time providing a buffer for intermittent renewable generation capacities. TES would provide an opportunity for current and future peak-load plant capacity addition. TES integration could help optimize the generation by allowing higher PLF operation of peak-load plants. With constantly increasing non-schedulable renewable energy generation, this becomes even more crucial for utilities to adopt centralized storage for generation or TES for building and other consumers.

In this study, EnergyPlus was used for analysis of the benefits from TES in a commercial building. EnergyPlus has built-in models for chillers built in the software. However, they are not adequate to model ice storage. With some modification, EnergyPlus can be used for ice storage, but if additional models for chillers for low temperature are added, that will improve the applicability of EnergyPlus to ice storage. Following conclusions can be drawn from the study of TES using ice or chilled water for building cooling:

1. Utility support in the form of rebates and subsidies and time of day electricity rates is important for motivating consumers to adopt TES in buildings for cooling.
2. Although energy is lost from TES, it can still be advantageous to the utility by efficiency gains in generation and to the consumer by time of day rates and other incentives.

3. TES effectively overcome the transients in the grid introduced by the intermittent nature of solar and wind energy. However, there is a need to develop advanced, robust dynamic controls to in order to adapt the system operation.

The two research areas that would help to develop operation and control of buildings HVAC systems to support utility grid are:

1. Dynamic control of thermal storage operation in response to hourly pricing
2. Dispatch strategy for distributed storage in the smart grid.

## List of References

- [1] P. Gadonneix, Y. D. Kim, K. Meyers, G. Ward, and C. Frei, "World Energy Resources 2013," 2013.
- [2] International Energy Agency, "Electricity Access Database 2014," *World Energy Outlook*, 2014. .
- [3] International Energy Agency, "Energy Access Database 2014," *World Energy Outlook*, 2014. .
- [4] U.S. Energy Information Agency, "International Energy Outlook 2013," 2013.
- [5] U. S. DoE, "2011 Buildings Energy Databook," *Energy Effic. Renew. Energy Dep.*, p. 286, 2011.
- [6] California Independent System Operator, "Demand response and energy efficiency roadmap:," 2013.
- [7] R. Turvey, "Peak-Load Pricing," *J. Polit. Econ.*, vol. 76, no. 1, pp. 101–113, 1968.
- [8] B. E. Osterman-burgess, D. Y. Goswami, and E. K. Stefanakos, "Economic Performance of Thermal Energy Storage Integrated With Natural Gas Combined Cycle Power Plants," *ASME*, pp. 1–12, 2015.
- [9] L. F. Cabeza and A. de Gracia, *Thermal energy storage (TES) systems for cooling in residential buildings*. Elsevier, 2015.
- [10] J. M. Calm, "Heat pumps in the USA," *Int. J. Refrig.*, vol. 10, no. 4, pp. 190–196, Jul. 1987.
- [11] G. Daniel, M. J. Anderson, W. Schmid, and M. Tokumitsu, "Performance of selected synthetic lubricants in industrial heat pumps," *J. Heat Recover. Syst.*, vol. 2, no. 4, pp. 359–368, Jan. 1982.
- [12] C. O. Perera and M. S. Rahman, "Heat Pump Dehumidifier Drying of Food," *Trends Food Sci. Technol.*, vol. 8, no. 3, pp. 75–79, Mar. 1997.
- [13] M. S. Rahman, C. O. Perera, and C. Thebaud, "Desorption isotherm and heat pump drying kinetics of peas," *Food Res. Int.*, vol. 30, no. 7, pp. 485–491, 1998.
- [14] J. Brenn, P. Soltic, and C. Bach, "Comparison of natural gas driven heat pumps and electrically driven heat pumps with conventional systems for building heating purposes," *Energy Build.*, vol. 42, no. 6, pp. 904–908, Jun. 2010.
- [15] H. J. Laue, "9 Heat pumps," *Heinloth, K. (ed.). SpringerMaterials -The Landolt-Börnstein Database*, vol. VIII/3C, p. 22, 2005.
- [16] Z. Qi, "Advances on air conditioning and heat pump system in electric vehicles – A review," *Renew. Sustain. Energy Rev.*, vol. 38, pp. 754–764, Oct. 2014.
- [17] *2009 ASHRAE Handbook: Fundamentals*. Atlanta, GA, USA: American society of heating, refrigerating and air-conditioning engineers, 2009.
- [18] G. Ding, "Recent developments in simulation techniques for vapour-compression refrigeration systems," *Int. J. Refrig.*, vol. 30, no. 7, pp. 1119–1133, Nov. 2007.

- [19] R. Best and W. Rivera, "A review of thermal cooling systems," *Appl. Therm. Eng.*, vol. 75, pp. 1162–1175, Jan. 2015.
- [20] L. A. Chidambaram, A. S. Ramana, G. Kamaraj, and R. Velraj, "Review of solar cooling methods and thermal storage options," *Renew. Sustain. Energy Rev.*, vol. 15, no. 6, pp. 3220–3228, Aug. 2011.
- [21] L. N. Lauerhass and D. F. Rudd, "On the thermodynamics of the chemical heat pump," *Chem. Eng. Sci.*, vol. 36, no. 5, pp. 803–807, Jan. 1981.
- [22] A. Hepbasli, Z. Erbay, F. Icier, N. Colak, and E. Hancioglu, "A review of gas engine driven heat pumps (GEHPs) for residential and industrial applications," *Renew. Sustain. Energy Rev.*, vol. 13, no. 1, pp. 85–99, Jan. 2009.
- [23] Z. Lian, S. R. Park, W. Huang, Y. J. Baik, and Y. Yao, "Conception of combination of gas-engine-driven heat pump and water-loop heat pump system," *Int. J. Refrig.*, vol. 28, no. 6, pp. 810–819, Sep. 2005.
- [24] M. D. D'Accadia, "Survey on GHP technology," *ASME Adv. Energy Syst. Proc.*, vol. 504, p. 1, 1998.
- [25] D. D. Colosimo, "Introduction to engine-driven heat pumps.," *ASHRAE Trans.*, vol. 93(CONF-87, 1987.
- [26] R. R. Zhang, X. S. Lu, S. Z. Li, W. S. Lin, and A. Z. Gu, "Analysis on the heating performance of a gas engine driven air to water heat pump based on a steady-state model," *Energy Convers. Manag.*, vol. 46, no. 11–12, pp. 1714–1730, Jul. 2005.
- [27] M. J. McDonough and S. Lafaille, "Natural-Gas-Engine-Driven Heat Pumps," Waltham, MA, p. 4, Aug-2012.
- [28] R. Lazzarin and M. Noro, "District heating and gas engine heat pump: Economic analysis based on a case study," *Appl. Therm. Eng.*, vol. 26, no. 2–3, pp. 193–199, Feb. 2006.
- [29] S. Sanaye, M. A. Meybodi, and M. Chahartaghi, "Modeling and economic analysis of gas engine heat pumps for residential and commercial buildings in various climate regions of Iran," *Energy Build.*, vol. 42, no. 7, pp. 1129–1138, Jul. 2010.
- [30] A. Ficarella and D. Laforgia, "Energy conservation in alcohol distillery with the application of pinch technology," *Energy Convers. Manag.*, vol. 40, no. 14, pp. 1495–1514, Sep. 1999.
- [31] S. Gopiya Naik, D. K. Khatod, and M. P. Sharma, "Optimal allocation of combined DG and capacitor for real power loss minimization in distribution networks," *Int. J. Electr. Power Energy Syst.*, vol. 53, pp. 967–973, Dec. 2013.
- [32] M. a. Rosen, "Energy efficiency and sustainable development," *IEEE Technol. Soc. Mag.*, vol. 15, no. 4, 1996.
- [33] DOE/EIA, "Annual Energy Review 2011," Washington D.C., 2012.
- [34] D. R. Laybourn, "The Benefits Of Thermal Energy Storage For Cooling Commercial Buildings," *IEEE*, pp. 4–5, 1985.
- [35] R. Parameshwaran, S. Kalaiselvam, S. Harikrishnan, and A. Elayaperumal, "Sustainable thermal energy storage technologies for buildings: A review," *Renew. Sustain. Energy Rev.*, vol. 16, no. 5, pp. 2394–2433, Jun. 2012.

- [36] M. R. Anisur, M. A. Kibria, M. H. Mahfuz, R. Saidur, and I. H. S. C. Metselaar, "Analysis of a thermal energy storage system for air cooling–heating application through cylindrical tube," *Energy Convers. Manag.*, vol. 76, pp. 732–737, Dec. 2013.
- [37] P. Arce, M. Medrano, A. Gil, E. Oró, and L. F. Cabeza, "Overview of thermal energy storage (TES) potential energy savings and climate change mitigation in Spain and Europe," *Appl. Energy*, vol. 88, no. 8, pp. 2764–2774, Aug. 2011.
- [38] A. A. Al-Abidi, S. Bin Mat, K. Sopian, M. Y. Sulaiman, C. H. Lim, and A. Th, "Review of thermal energy storage for air conditioning systems," *Renew. Sustain. Energy Rev.*, vol. 16, no. 8, pp. 5802–5819, Oct. 2012.
- [39] A. Saito, "Recent advances in research on cold thermal energy storage," *Int. J. Refrig.*, vol. 25, no. 2, pp. 177–189, Mar. 2002.
- [40] a. Campoccia, L. Dusonchet, E. Telaretti, and G. Zizzo, "Economic impact of ice thermal energy storage systems in residential buildings in presence of double-tariffs contracts for electricity," *2009 6th Int. Conf. Eur. Energy Mark. EEM 2009*, 2009.
- [41] S. M. Hasnain, "Review on sustainable thermal energy storage technologies, Part II: cool thermal storage," *Energy Convers. Manag.*, vol. 39, no. 11, pp. 1139–1153, Aug. 1998.
- [42] M. J. Sebzali, B. Ameer, and H. J. Hussain, "Comparison of energy performance and economics of chilled water thermal storage and conventional air-conditioning systems," *Energy Build.*, vol. 69, pp. 237–250, Feb. 2014.
- [43] G. P. Henze, C. Felsmann, and G. Knabe, "Evaluation of optimal control for active and passive building thermal storage," *Int. J. Therm. Sci.*, vol. 43, no. 2, pp. 173–183, Feb. 2004.
- [44] Z. Zhang, W. D. Turner, and P. E. Qiang, "A method to determine the optimal tank size for a chilled water storage system under a time-of-use electricity rate structure," 2010.
- [45] G. P. Henze, M. Krarti, and M. J. Brandemuehl, "Guidelines for improved performance of ice storage systems," *Energy Build.*, vol. 35, no. 2, pp. 111–127, Feb. 2003.
- [46] B. Soediono, "Reducing Energy Costs and Peak Electrical Demand through Optimal Control of Building Thermal Storage," *J. Chem. Inf. Model.*, vol. 53, p. 160, 1989.
- [47] B. Rismanchi, R. Saidur, H. H. Masjuki, and T. M. I. Mahlia, "Modeling and simulation to determine the potential energy savings by implementing cold thermal energy storage system in office buildings," *Energy Convers. Manag.*, vol. 75, pp. 152–161, Nov. 2013.
- [48] S. Sanaye and M. Hekmatian, "Ice thermal energy storage (ITES) for air-conditioning application in full and partial load operating modes," *Int. J. Refrig.*, vol. 66, pp. 181–197, Jun. 2016.
- [49] M. O. Abdullah, L. P. Yij, E. Junaidi, G. Tambi, and M. A. Mustapha, "Electricity cost saving comparison due to tariff change and ice thermal storage (ITS) usage based on a hybrid centrifugal-ITS system for buildings: A university district cooling perspective," *Energy Build.*, vol. 67, pp. 70–78, Dec. 2013.
- [50] F. Sehar, S. Rahman, and M. Pipattanasomporn, "Impacts of ice storage on electrical energy consumptions in office buildings," *Energy Build.*, vol. 51, pp. 255–262, Aug. 2012.



- [51] Z. (Jerry) Yu, G. Huang, F. Haghighat, H. Li, and G. Zhang, "Control strategies for integration of thermal energy storage into buildings: State-of-the-art review," *Energy Build.*, vol. 106, pp. 203–215, May 2015.
- [52] V. de Oliveira, J. Jäschke, and S. Skogestad, "Optimal operation of energy storage in buildings: Use of the hot water system," *J. Energy Storage*, vol. 5, pp. 102–112, Dec. 2015.
- [53] N. Vulic, M. Patil, Y. Zou, S. H. Amilineni, C. B. Honsberg, and M. Stephen, "Matching AC Loads to Solar Peak Production Using Thermal Energy Storage in Building Cooling Systems – A Case Study at Arizona State," pp. 1504–1509, 2014.
- [54] USGBC, "LEED v4 for Building Design and Construction." U.S. Green Building Council, p. 160, 2017.
- [55] M. MacCracken, "Thermal Energy Storage in Sustainable Buildings," *ASHRAE J.*, no. September, pp. S2–S5, 2004.
- [56] J. Patterson, P. Kulkarni, M. Smith, and N. Deller, "Source Energy and Environmental Impacts of Thermal Energy Storage," 1996.
- [57] B. W. Jones and R. Powell, "Evaluation of distributed building thermal energy storage in conjunction with wind and solar electric power generation," *Renew. Energy*, vol. 74, pp. 699–707, Feb. 2015.
- [58] C. W. Sohn, F. H. Holcomb, D. J. Sondeno, and J. M. Stephens, "Field-Tested Cooling Performance of Gas-Engine-Driven Heat Pumps," *ASHRAE J.*, p. 8, 2008.
- [59] E. Lemmon, M. Huber, and M. McLinden, "NIST Standard Reference Database 23: REFPROP version 9.0," *Ref. Data Program, Natl. Inst. Stand. Technol.*, 2010.
- [60] E. W. Lemmon, M. L. Huber, and M. O. McLinden, "NIST standard reference database 23: Reference fluid thermodynamic and transport properties-REFPROP," *REFPROP*. National Institute of Standards and Technology, Standard Reference Data Program, Gaithersburg, 2013.
- [61] H. W. Coleman and W. G. Steele, *Experimental Uncertainty Analysis for Engineers*. John Wiley, New York, 1989.
- [62] EIA, "Heat Content of Natural Gas Consumed," 2013. [Online]. Available: [http://www.eia.gov/dnav/ng/ng\\_cons\\_heat\\_a\\_epg0\\_vgth\\_btucf\\_a.htm](http://www.eia.gov/dnav/ng/ng_cons_heat_a_epg0_vgth_btucf_a.htm). [Accessed: 20-Aug-2014].
- [63] A. Zaltash, R. Linkous, R. Wetherington, P. Gephegan, and E. Vineyard, "Performance of Gas-Engine Driven Heat Pump Unit," 2009.
- [64] N. Ishii, M. Yamamura, S. Muramatsu, S. Yamamoto, and M. Sakai, "Mechanical Efficiency of a Variable Speed Scroll Compressor," 1990.
- [65] C. E. Goering, M. L. Stone, D. W. Smith, and P. K. Turnquist, "Compression Ignition Engines," in *Off-road vehicle engineering principles*, St. Joseph, Michigan: American Society of Agricultural and Biological Engineers, 2006.
- [66] "Annual Energy Outlook 2015: Levelized Cost and Levelized Avoided Cost of New Generation Resources," Washington D.C., 2015.

- [67] F. P. & L. Company, "Schedule 9-Status Report and Specifications of Proposed Generating Facilities," 2016.
- [68] Carrier Software Systems, "HAP e-Help 004 - Transfer Function Methodology," 2005, pp. 1–9.
- [69] E. Djunaedy, K. van den Wymelenberg, B. Acker, and H. Thimmana, "Oversizing of HVAC system: Signatures and penalties," *Energy Build.*, vol. 43, no. 2–3, pp. 468–475, Feb. 2011.
- [70] D. Woradetchjumroen, Y. Yu, H. Li, D. Yu, and H. Yang, "Analysis of HVAC system oversizing in commercial buildings through field measurements," *Energy Build.*, vol. 69, pp. 131–143, Feb. 2014.
- [71] J. B. Cummings, C. R. Withers, and F. Solar, "Making the Case for Oversizing Variable-Capacity Heat Pumps Research Findings," pp. 42–54, 2014.
- [72] A. Arteconi, N. J. J. Hewitt, and F. Polonara, "Domestic demand-side management (DSM): Role of heat pumps and thermal energy storage (TES) systems," *Appl. Therm. Eng.*, vol. 51, no. 1–2, pp. 155–165, 2013.
- [73] L. F. Cabeza, I. Martorell, L. Miró, A. I. Fernández, and C. Barreneche, *Introduction to thermal energy storage (TES) systems*. Elsevier, 2015.
- [74] K. M. Powell, W. J. Cole, U. F. Ekarika, and T. F. Edgar, "Optimal chiller loading in a district cooling system with thermal energy storage," *Energy*, vol. 50, pp. 445–453, 2013.
- [75] D. Haeseldonckx, L. Peeters, L. Helsen, and W. D'haeseleer, "The impact of thermal storage on the operational behaviour of residential CHP facilities and the overall CO2 emissions," *Renew. Sustain. Energy Rev.*, vol. 11, no. 6, pp. 1227–1243, Aug. 2007.
- [76] R. Kamal, A. K. Narasimhan, C. Wickramaratne, A. Bhardwaj, D. Y. Goswami, E. K. Stefanakos, and H. A. Ingley, "Field performance of gas-engine driven heat pumps in a commercial building," *Int. J. Refrig.*, vol. 68, pp. 15–27, 2016.
- [77] W. Liu, X. Miao, J. Wang, X. Ma, G. Peng, and Z. Pan, "Applying 'thermal storage cooling tower' to shift on-peak electric energy demand of underground commercial building," *Asia-Pacific Power Energy Eng. Conf. APPEEC*, 2009.
- [78] U. S. D. of E. (DoE), "Commercial Reference Buildings." [Online]. Available: <http://energy.gov/eere/buildings/commercial-reference-buildings>. [Accessed: 09-Jun-2015].
- [79] U. Description and I. Procedures, "Carrier E20-II Design Software Hourly Analysis Program v4.60 Release Sheet." Carrier, 2012.
- [80] B. D. B. Crawley and L. K. Lawrie, "EnergyPlus : Energy Simulation Program," *Ashrae*, vol. 42, no. 4, pp. 49–56, 2000.
- [81] M. Vuolle and P. Sahlin, "IDA-ICE, 'IDA Indoor Climate and Energy Application 4.1.'" 2000.
- [82] S. A. Klein, "TRNSYS: A transient simulation program." Solar Energy Laboratory, University of Wisconsin, Madison, 1973.
- [83] C. Park, D. R. Clark, and G. E. Kelly, "An Overview of HVACSIM+, A Dynamic Building/HVAC/Control Systems Simulation Program," *Proc. 1st Annu. Build. Energy Simul. Conf.*, 1985.

- [84] A. Husaunndee, R. Lahrech, H. Vaezi-Nejad, and J. C. Visier, "SIMBAD A simulation toolbox for the design and test of HVAC control systems," *Proc. Fifth Int. IBPSA Conf. Build. Simul. 1997*, pp. 269–276, 1997.
- [85] M. Trčka and J. L. M. Hensen, "Overview of HVAC system simulation," *Autom. Constr.*, vol. 19, no. 2, pp. 93–99, Mar. 2010.
- [86] R. Guglielmetti, D. Macumber, and N. Long, "OpenStudio : An Open Source Integrated Analysis Platform Preprint," *12th Conf. Int. Build. Perform. Simul. Assoc.*, no. December, 2011.
- [87] D. B. Crawley, L. K. Lawrie, F. C. Winkelmann, W. F. Buhl, Y. J. Huang, C. O. Pedersen, R. K. Strand, R. J. Liesen, D. E. Fisher, M. J. Witte, and J. Glazer, "EnergyPlus: creating a new-generation building energy simulation program," *Energy Build.*, vol. 33, no. 4, pp. 319–331, 2001.
- [88] P. G. Ellis, P. A. Torcellini, and D. B. Crawley, "Simulation of Energy Management Systems in EnergyPlus," *NREL*, 2007.
- [89] P. Ihm, M. Krarti, and G. P. Henze, "Development of a thermal energy storage model for EnergyPlus," *Energy Build.*, vol. 36, no. 8, pp. 807–814, Aug. 2004.
- [90] M. Deru, K. Field, D. Studer, K. Benne, B. Griffith, P. Torcellini, B. Liu, M. Halverson, D. Winiarski, M. Rosenberg, M. Yazdanian, J. Huang, and D. Crawley, "Commercial Reference Building Models of the National Building Stock," 2011.
- [91] Tampa Electric Company, "Tampa Electricity Rate Schedules," Tampa, FL, 2014.
- [92] R. K. Strand, "Indirect Ice Storage System Simulation," University of Illinois at Urbana-Champaign, 1992.
- [93] U. S. Edwards, "10 CFR Part 430." 2010.
- [94] J. A. Duffie and W. A. Beckman, *Solar Engineering of Thermal Processes*. 1980.
- [95] B. J. Newton, "Modeling of Solar storage Tanks," University of Wisconsin, Madison, 1995.
- [96] Y. Zhang and I. Korolija, "Performing complex parametric simulations with jEPlus," *SET2010-9th Int. Conf. Sustain. Energy Technol.*, 2010.
- [97] Y. Sun, S. Wang, F. Xiao, and D. Gao, "Peak load shifting control using different cold thermal energy storage facilities in commercial buildings: A review," *Energy Convers. Manag.*, vol. 71, pp. 101–114, Jul. 2013.
- [98] Y. Ruan, Q. Liu, Z. Li, and J. Wu, "Optimization and analysis of Building Combined Cooling, Heating and Power (BCHP) plants with chilled ice thermal storage system," *Appl. Energy*, vol. 179, pp. 738–754, 2016.
- [99] A. L. Facci, L. Andreassi, S. Ubertini, and E. Sciubba, "Analysis of the Influence of Thermal Energy Storage on the Optimal Management of a Trigenation Plant," *Energy Procedia*, vol. 45, pp. 1295–1304, 2014.
- [100] Y. Zhang, "CIBSE ASHRAE Technical Symposium, Imperial College, London UK – 18 and 19 April 2012," *CIBSE ASHRAE Tech. Symp.*, no. April, pp. 1–12, 2012.
- [101] K. Deb, A. Pratap, S. Agarwal, and T. Meyarivan, "A fast and elitist multiobjective genetic algorithm: NSGA-II," *IEEE Trans. Evol. Comput.*, vol. 6, no. 2, pp. 182–197, 2002.

- [102] M. Rutberg, M. Hastbacka, A. Cooperman, and A. Bouza, "Thermal Energy Storage," *ASHRAE J.*, no. June, pp. 62–66, 2013.
- [103] PikeResearch, "Executive Summary : Thermal Energy Storage," 2012.
- [104] Tampa Electric Company, "Tampa Electricity Rate Schedules," Tampa, FL, 2014.
- [105] DOE/EIA, "Commercial Buildings Energy Consumption Survey (CBECS 2012)," *US Energy Information Administration*, 2016. [Online]. Available: <http://www.eia.gov/consumption/commercial/reports/2012/energyusage/>. [Accessed: 01-Jan-2016].
- [106] DOE/EIA, "Table E5. Electricity consumption (kWh) by end use, 2012 (CBECS)," 2016.
- [107] DOE/IEA, "U . S . Electricity Flow , 2015 quadrillion Btu," 2015.
- [108] DOE/EIA, "Peak-to-average electricity demand ratio rising in New England and many other U.S. regions," 2014. [Online]. Available: [http://www.eia.gov/todayinenergy/detail.php?id=15051#tabs\\_SpotPriceSlider-5](http://www.eia.gov/todayinenergy/detail.php?id=15051#tabs_SpotPriceSlider-5).
- [109] North American Electric Reliability Corporation, "Accommodating High Levels of Variable Generation," *North Am. Electr. Reliab. Corp.*, no. April, p. 104, 2009.
- [110] J. DeCesaro, K. Porter, and M. Milligan, "Wind Energy and Power System Operations: A Review of Wind Integration Studies to Date," *Electr. J.*, vol. 22, no. 10, pp. 34–43, 2009.
- [111] P. Denholm, E. Ela, B. Kirby, and M. Milligan, "The Role of Energy Storage with Renewable Electricity Generation The Role of Energy Storage with Renewable Electricity Generation," 2010.
- [112] NREL, "System Advisor Model." National Renewable Energy Laboratory, Denver, CO, 2016.


## Appendix A Abbreviations

AHU	- Air Handling Unit
BIM	- Building Information Modeling
CW	- Chilled Water
COP	- Coefficient of Performance
DOE	- Department of Energy
DSM	- Demand Side Management
EER	- Energy Efficiency Ratio
EEV	- Electronic Expansion Valve
EHP	- Electric Heat Pump
EMS	- Energy Management System
FPU	- Florida Public Utility
GEHP	- Gas Engine-driven Heat Pump
HVAC	- Heating Ventilation and Air-Conditioning
HX	- Heat Exchanger
HP	- Heat Pump
ISO	- Independent System Operator
LEED	- Leadership in Energy and Environmental Design
PLR/PLF	- Part Load Ratio/Part Load Factor
SI	- Spark Ignition
TES	- Thermal Energy Storage
TOU/TOD	- Time-of-Use/Time-of-Day
USGBC	- U.S. Green Building Council
VG	- Variable Generators

## Appendix B Copyright Permissions

The content of the Chapter 2 are previously published in International Journal of Refrigeration.

The permission from the publisher to use the content in this dissertation is provided below.



My Orders   My Library   My Profile   Welcome rajeev@mail.usf.edu   Log out | Help

My Orders > Orders > All Orders

### License Details

This Agreement between Rajeev Kamal ("You") and Elsevier ("Elsevier") consists of your license details and the terms and conditions provided by Elsevier and Copyright Clearance Center.

[printable details](#)

License Number	4039400401914
License date	Jan 26, 2017
Licensed Content Publisher	Elsevier
Licensed Content Publication	International Journal of Refrigeration
Licensed Content Title	Field performance of gas-engine driven heat pumps in a commercial building
Licensed Content Author	Rajeev Kamal,Arun Kumar Narasimhan,Chatura Wickramaratne,Abhinav Bhardwaj,D. Yogi Goswami,Elias K. Stefanakos,Herbert A. Ingle
Licensed Content Date	August 2016
Licensed Content Volume	68
Licensed Content Issue	n/a
Licensed Content Pages	13
Type of Use	reuse in a thesis/dissertation
Portion	full article
Format	both print and electronic
Are you the author of this Elsevier article?	Yes
Will you be translating?	No
Order reference number	
Title of your thesis/dissertation	Optimization and Performance Study of Select Heating Ventilation and Air Conditioning Technologies for Commercial Buildings
Expected completion date	May 2017
Estimated size (number of pages)	150
Elsevier VAT number	GB 494 6272 12
Requestor Location	Rajeev Kamal [REDACTED] TAMPA, FL 33613 United States Attn: Rajeev Kamal
Billing Type	Invoice
Billing address	Rajeev Kamal [REDACTED] TAMPA, FL 33613 United States Attn: Rajeev Kamal
Total	0.00 USD

[BACK](#)

Copyright © 2017 Copyright Clearance Center, Inc. All Rights Reserved. Privacy statement . Terms and Conditions . Comments? We would like to hear from you. E-mail us at [customer-care@copyright.com](mailto:customer-care@copyright.com)

### Appendix C Supporting Information for Chapter 3

Table C.1. Specification of sensors installed at DeBary, FL

Sensor Type	Sensor ID	Number	Model No:	Manufacturer	Measurement range
Watt-meter	FCU1	W1/-	PC5-020E2	Ohio Semitronics	0-3000 W
Watt-meter	FCU2	W2/-	PC5-002E2	Ohio Semitronics	0-1000 W
Watt-meter	FCU3	W3/-	PC5-020E2	Ohio Semitronics	0-3000 W
Watt-meter	FCU4	W4/-	PC5-020E2	Ohio Semitronics	0-3000 W
Watt-meter	FCU5	W5/-	PC5-020E2	Ohio Semitronics	0-3000 W
Watt-meter	FCU6	W6/-	PC5-107E2	Ohio Semitronics	0-500 W
Watt-meter	FCU7	W7/-	PC5-107E2	Ohio Semitronics	0-500 W
Watt-meter	GEHP1	W8/-	PC5-119E2	Ohio Semitronics	0-5000 W
Watt-meter	GEHP2	W9/-	PC5-119E2	Ohio Semitronics	0-5000 W
Watt-meter	GEHP3	W10/-	PC5-119E2	Ohio Semitronics	0-5000 W
Watt-meter	GEHP4	W11/-	PC5-119E2	Ohio Semitronics	0-5000 W
Flow-meter	REF1	Ref1	Optimass 1300	Krohne	50-1000 kg/hr.
Flow-meter	REF2	Ref2	Optimass 1300	Krohne	50-1000 kg/hr.
Flow-meter	REF3	Ref3	Optimass 1300	Krohne	50-1000 kg/hr.
Flow-meter	REF4	Ref4	Optimass 1300	Krohne	50-1000 kg/hr.
Temperature	FCU1	T1/-	RHP-2W44-Nist	Dwyer Instruments	(-)4 - 140
Temperature	FCU2	T2/-	RHP-2W44-Nist	Dwyer Instruments	(-)4 - 140
Temperature	FCU3	T3/-	RHP-2W44-Nist	Dwyer Instruments	(-)4 - 140
Temperature	FCU4	T4/-	RHP-2W44-Nist	Dwyer Instruments	(-)4 - 140
Temperature	FCU5	T5/-	RHP-2W44-Nist	Dwyer Instruments	(-)4 - 140
Temperature	FCU6	T6/-	RHP-2W44-Nist	Dwyer Instruments	(-)4 - 140
Temperature	FCU7	T7/-	RHP-2W44-Nist	Dwyer Instruments	(-)4 - 140
Temperature	AMB1	T8/-	RHP-2R11-NIST	Dwyer Instruments	(-)40 - 140
Humidity	FCU1	H1/-	RHP-2W44-Nist	Dwyer Instruments	0-100%
Humidity	FCU2	H2/-	RHP-2W44-Nist	Dwyer Instruments	0-100%
Humidity	FCU3	H3/-	RHP-2W44-Nist	Dwyer Instruments	0-100%
Humidity	FCU4	H4/-	RHP-2W44-Nist	Dwyer Instruments	0-100%
Humidity	FCU5	H5/-	RHP-2W44-Nist	Dwyer Instruments	0-100%
Humidity	FCU6	H6/-	RHP-2W44-Nist	Dwyer Instruments	0-100%
Humidity	FCU7	H7/-	RHP-2W44-Nist	Dwyer Instruments	0-100%
Humidity	AMB1	H8/-	RHP-2R11-NIST	Dwyer Instruments	0-100%
<b>Installed by AGDF</b>					
Natural Gas Meter	NG1	NGF1	R-275	-	Counter
Natural Gas Meter	NG2	NGF2	R-275	-	Counter
Natural Gas Meter	NG3	NGF3	R-275	-	Counter
Natural Gas Meter	NG4	NGF4	R-275	-	Counter
<b>Data Logging Equipment</b>					
DAQ Chassis	DAQ		cDAQ-9138	National Instruments	
Power supply	DC supply		NI PS-15	National Instruments	
Current input module 16 channel	Mod1,2		NI 9208	National Instruments	

## C.1 Data Collection of Operating Parameters

Operation data table 2014/10/13 15:26:03

File Graph Error/Avoidance Help

記録データ表示中 | 1秒 | File name: C:\Users\rajeev\Google Drive\USF Work\Heat Pump\Working\GHP data\Unit01\20140907\_1 ---

Time and date of displayed recorded data 2014- 9- 7 13:48:49 | 1 |

**Indoor unit data**

Connected IU. qty	1unit	Operating IU. qty	0unit	IU operation capacity	0.0kw	Connected IU. Capacity	22.4kw
補正データ要求	auto	冷却SCHs 補正データ	auto	加熱SCHs 補正データ	auto	Tc	0
Indoor unit No.	1	Unit / Stc	Mode	Airflow	Indirect	Direct	Temperature
0	Run	Cooling	Spare	0	23deg	29deg	25deg

**Outdoor unit data**

IU. type	DAIKIN-AISIN	O.U. capacity	28.0kw	Type	Multi	Mode	Fan	Air-condition	OFF	O.U. No.	255
Operation prohibit	OFF	Check/Normal	Normal	Avoidance	HP	LP	Discharge	Intake	HP Urgent	Frost	E/G temp.

INPUT		OUTPUT		Others		Recorded data	
E/G OP SW	ON	Compressor 1	OFF	Specified engine RPM	0min-1	Main software ver.	
HP SW	ON	Compressor 2	OFF	Actual engine RPM	0min-1	E/G software ver.	C
LP SW	OFF	Compressor 3	OFF	Engine igniter spark	10.0l	IF software ver.	I
High pressure	1.72MPa	Compressor 4	OFF	Requested calculated	0min-1	Outdoor unit multi-address	0
Low pressure	1.63MPa	4-way chqov. valve	OFF	Calculated engine RPK	0min-1	Gas type	13A
HP equiv. temp.	27deg	Output spare 1	OFF	Requested calculated	0min-1	Model code	D1
LP equiv. temp.	26deg	Fan airflow level	0	Calculated engine RPK	0min-1	Serial code	18A3314Ah
C/P 1 discharge tem	46deg	Heat ex. fan 1	0%	Suction superheating c	0deg	Indoor unit manufacturer code	DAIKIN-AISIN
C/P 2 discharge tem	47deg	Heat ex. fan 2	0%	Sub heat ex. outlet sup	19deg	Outdoor unit capacity	28.0kw
C/P 3 discharge tem	140deg	Heat ex. fan 3	0%	Outdoor supercooling c	0deg	Model type	Multi
C/P 4 discharge tem	140deg	E/G coolant pump	0%	Outdoor heat ex. super	0deg	Additional spec.	00000000B
C/P intake temp. 1	48deg	Throttle valve	110stp	Data spare 5	0	Serial No.	0 00000
C/P intake temp. 2	105deg	Fuel gas valve	700stp	Data spare 6	0	EEPROM DPSW 1	00000001B
Liquid pipe temp.	29deg	Main heat ex. refriq. liquid	90stp	Silent mode	OFF	EEPROM DPSW 2	00000110B
Heat ex. liquid temp.	30deg	Sub heat ex. refriq. liquid	40stp	Compressor protect coi	OFF	EEPROM DPSW 3	00010000B
Sub heat ex. outlet te	45deg	Supercooling valve	40stp	Defrost control	OFF	EEPROM DPSW 4	10000000B
Accumulator outlet te	39deg	C/P capacity control valv	40stp	Cold district spec. oper	OFF	EEPROM DPSW 5	00000000B
Accumulator outlet te	105deg	Liquid flow control valve	0stp	Periodic inspection	I	EEPROM DPSW 6	00000000B
Supercooling heat ex	-40deg	Data spare 4	0	E/G operation hour	4005Hr	Remote monitoring address No.	255
Data spare 1	105	Compressor heater	OFF	Requesting power gen	0w	Air net address No.	255
Data spare 2	105	Drain heater	OFF	Actual power generatic	0w	Ex4 address No.	1
Data spare 3	105	Oil pan heater	OFF	Output 2		Outdoor multi-unit connected number	1unit
Outside temp.	35deg	Fuel gas valve 1	OFF	Oil return valve 1	OFF	BS unit connected number	0unit
E/G oil temp.	60deg	Fuel gas valve 2	OFF	Oil return valve 2	OFF	Low-noise address setting	0
E/G room temp.	51deg	Starter	OFF	Oil return valve 3	OFF	Cooling-Heating bundle address setting	0
E/G exhaust air temp	200deg	Starter transformer	OFF	Oil return valve 4	OFF	DIV terminal number	7unit
Starter voltage	0.0V	12VDC output permission	ON	Hot gas bypass valve	OFF	DIV zone number	0unit
Igniter voltage	0.0V	12VDC output permission	ON	Output spare 4	OFF	DIV BS unit number	0unit
Fuel gas valve outpu	OFF	Output data spare 1	0	Output spare 5	OFF	DIV outdoor unit number	4unit
Power supply phase	Single phase	Output data spare 2	0	Refriq. gas P supply va	OFF	Energy save level	255
R-S phase detection	ON			Output spare 9	OFF	Low-noise level	255
S-T phase detection	OFF			Oil return valve	OFF	Tc value	-128
T-R phase detection	OFF			Refriq. gas valve	ON	Te value	-128
E/G side spare input	ON			Output spare 2	OFF	Data spare 1	255
Silent mode external	OFF			Output spare 3	OFF	Data spare 2	255
Input spare 1	0			Output spare 6	OFF	Heating mode thermostat OFF indoor unit expansion	255
Input spare 2	0			Output spare 7	OFF	Heating mode stopped indoor unit expansion valve o	255
				Output spare 8	OFF	Heating mode hot air start high pressure value	3.55MPa
				Output spare 10	OFF	Heating mode indoor unit SC target temp.	-128
						Error log 1	3- 99   3261Hr
						Error log 2	5- 0   3132Hr

Figure C.1. Parameters recorded by GEHP data logger



FCU6W6	FCU7W7	GHP1W6	GHP2W6	GHP3W7	GHP4W7	REF1	REF2	REF3	REF4	NG1	NG2	NG3	NG4
4.423157	4.473888	35.53107	35.68597	37.28002	35.76137	9.703905	0.233516	0.505284	54.41324	406483.0	973206.0	996946.0	808055.0
4.523553	4.476182	35.43027	35.92856	37.30789	35.81546	9.702594	0.223517	0.499710	55.70209	406483.0	973206.0	996946.0	808055.0
4.434385	4.506260	35.43682	35.80808	37.17184	35.64663	9.685219	0.214502	0.490531	55.99861	406483.0	973206.0	996946.0	808055.0
4.503146	4.529044	35.44256	35.78022	37.19315	35.74006	9.698824	0.218928	0.494301	55.87026	406483.0	973206.0	996946.0	808055.0
4.409142	4.450284	35.47206	35.77612	37.18495	35.78596	9.707019	0.240892	0.515446	55.27674	406483.0	973206.0	996946.0	808055.0
4.445695	4.458480	35.34175	35.73760	37.14151	35.54009	9.709478	0.242040	0.500530	54.07493	406483.0	973206.0	996946.0	808055.0
4.532732	4.473068	35.43846	35.73432	37.26035	35.86873	9.708167	0.225320	0.506923	52.93131	406483.0	973206.0	996946.0	808055.0
4.432418	4.499294	35.43272	35.73350	37.19479	35.87529	9.707511	0.230566	0.487253	52.10306	406483.0	973206.0	996946.0	808055.0
4.497983	4.603952	35.56221	35.74908	37.30789	35.81136	9.704069	0.226140	0.497744	51.61689	406483.0	973206.0	996946.0	808055.0
4.406192	4.450776	35.49911	35.72531	37.16856	35.84169	9.785370	0.213519	0.495449	51.18219	406483.0	973206.0	996946.0	808055.0
4.464545	4.557647	35.51796	35.65646	37.07431	35.75563	12.55910	0.225976	0.497416	51.87981	406483.0	973206.0	996946.0	808055.0
4.526094	4.476019	35.40322	35.78759	37.23003	35.78432	17.15669	0.228271	0.490040	54.15672	406483.0	973206.0	996946.0	808055.0
4.432172	4.472740	35.49911	35.77858	37.24724	35.79743	21.45071	0.241384	0.491679	57.90573	406483.0	973206.0	996946.0	808055.0
4.452497	4.579857	35.35241	35.72121	37.10054	35.72449	22.23946	0.217944	0.498727	61.86685	406483.0	973206.0	996946.0	808055.0
4.460283	4.476756	35.52615	35.90315	37.21609	35.81218	20.38298	0.245154	0.506431	63.83249	406483.0	973206.0	996946.0	808055.0
4.426845	4.563958	35.44174	35.81792	37.24068	35.67859	17.90315	0.229746	0.494629	62.48644	406483.0	973206.0	996946.0	808055.0
4.501015	4.462578	35.36798	35.71301	37.16938	35.80071	15.63738	0.222042	0.506431	56.94504	406483.0	973206.0	996946.0	808055.0
4.439630	4.462086	35.53435	35.67941	37.16938	35.67286	14.46524	0.247121	0.509873	47.79608	406483.0	973206.0	996946.0	808055.0

Figure C.2. LabVIEW code front-end at the logging system

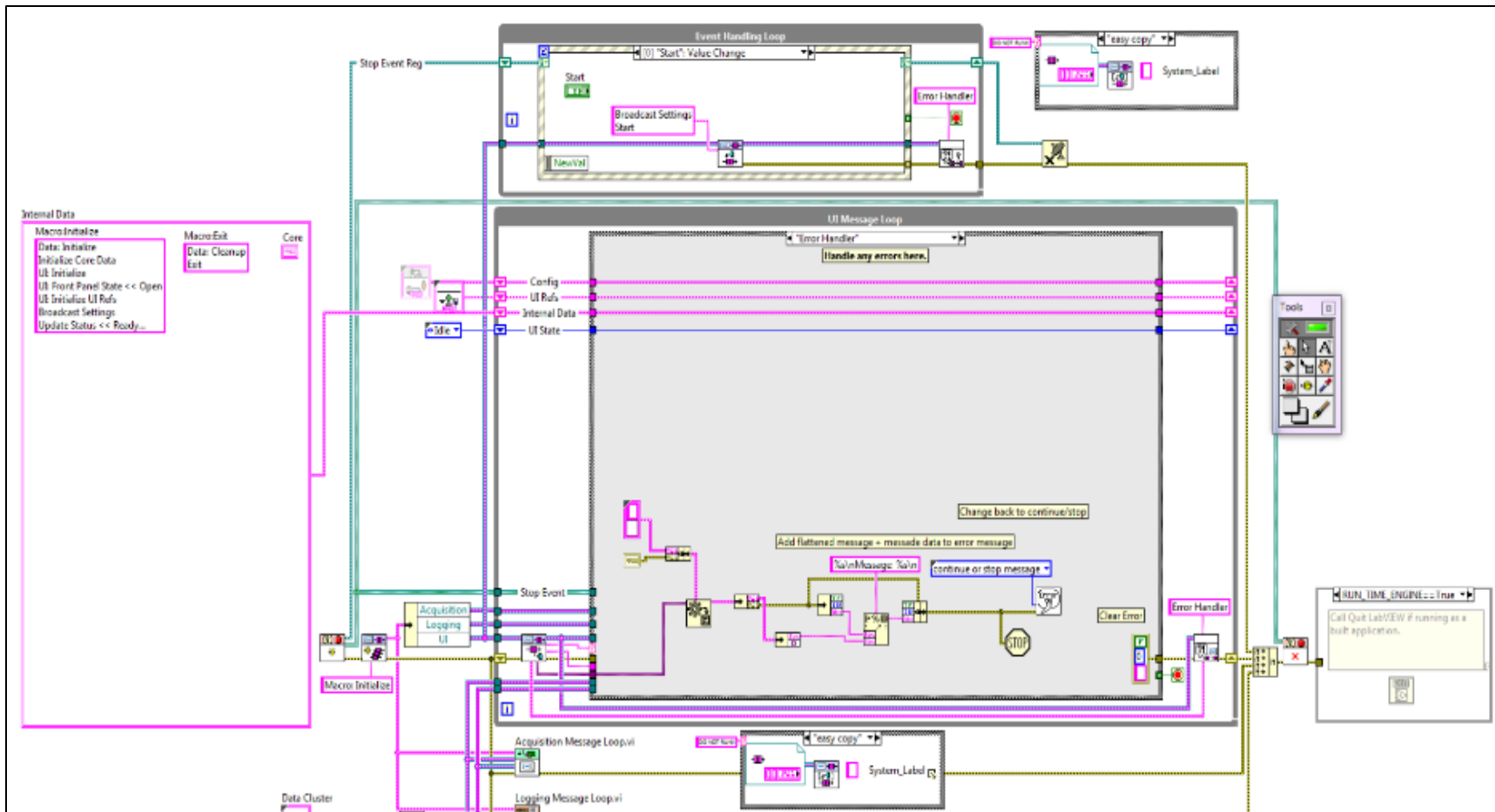


Figure C.3. LabVIEW back-end program logic

## C.2 Procedure of Processing Collected Data from GEHP Data Logger

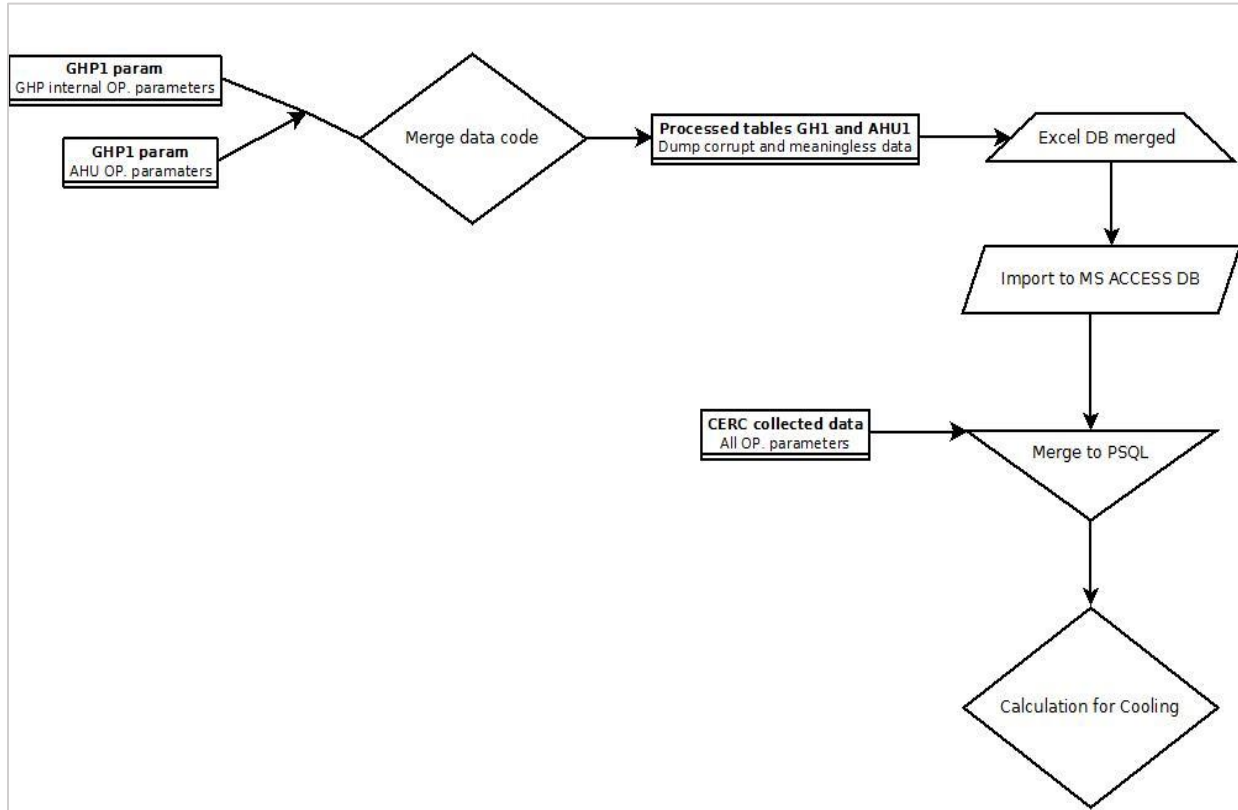


Figure C.4. Procedure for processing GEHP data files

The '\*.And' file formatted data conversion process involves a set of manual operations which are time-consuming steps with multiple tools. The following tools were employed to complete the process of migration of '\*.And' files to the server for use in calculations:

- MS Excel scripts
- MS Power Query
- FlowHeater v3.0
- PostgreSQL 9 query language
- Dreamcoder SQL DB tool
- EMS SQL Management Studio 1.2.0.18

Procedure steps involved in this data processing are:

1. Created working folders which have two folders for 'main' and 'ahu' and the CERC process file (excel with macros).
2. Using the 'GhpPcMonitor2006D\_Eng070123 port 4.exe', the source file is converted to respective .csv files for outdoor unit and indoor units provided by the manufacturer.
3. Move 24 files with same date to 'main' folder (i.e. 20140702\_005332.csv) and remaining 24 corresponding '\*\_NaiGp1.csv' files (i.e. 20140702\_005332\_NaiGp1.csv) to 'ahu' folder. Checking the file size to validate correct files for the units as in the table below. *(Special attention is given to ensure correct files are used as the data does not have any flags to differentiate between the GEHP units).*
4. Validation check of the correct file size of the GEHP units is as in the list below.

Table C.2. Validation of correct source files

Unit	File size (approx.)	2nd check
unit1	1561 kb	Visual inspection of data
unit2	1744 kb	NaiGP1 file has triple columns that of unit1 and unit4 (3 AHU data)
unit3	1653 kb	NaiGP1 file has double columns that of unit1 and unit4 (2 AHU data)
unit4	1561 kb	Visual inspection of data and parameter values

5. Using the CERCmacro.xls (macro enabled) file a power query code imports all the data from the outdoor units and indoor units in separate sheets named 'main' and 'ahu'. The M-code is attached as Appendix C.3 with this report.
6. The final table combining both the data sets from sheet 'main' and 'ahu' is populated using a macro run to merge the rows in the same order and fixing any timestamp formatting errors as shown in Figure C.5. The macro performs the following operations:
  - a. Copy the Main data from columns till the end on the right side and bottom to merge the sheet.
  - b. Next copy the ahu data from 'column 1' till the end and bottom.

- c. Insert a column before the first column and add the formula as =sum (b1+c1) and drag until the last value. Change the format of the value to custom 'yy-mm-dd hh-mm-ss AMPM' to generate complete timestamps.
  - d. Copy the header from the 'header' sheet to fix the headers according to SQL friendly format.
7. Name the Merged MS-DOS CSV file as GEHP#\_yyyy-mm-dd.csv where the unit number replaces '#' as in the main folder.

Once all the relevant CSV files are generated with data from each day, they are uploaded to PSQl server at USF using another tool named as 'Flow Heater v3' which maps the correct structure of the source and destination structures. Four tables with their respective data are generated in this process named as GEHP1, GEHP2, GEHP3 and GEHP4.



Table C.3. Measured performance data for 4 GEHP units

<b>GEHP1</b>							
	GHP1 NG (kWh)	Electricity use (kWh)	Electricity (kWh)	Cooling GEHP1 (kWh)	Cost NG (\$)	Cost Electricity (\$)	Total cost (\$)
June-14	3661	101	101	2478	48	10	58
July-14	3928	104	104	2541	52	11	62
August-14	4196	108	108	2727	55	11	66
September-14	3993	95	95	2543	52	10	62
October-14	2812	78	78	1378	37	8	45
November-14	1212	44	44	624	16	5	20
December-14	922	46	46	615	12	5	17
January-15	748	46	46	492	10	5	15
February-15	462	33	33	280	6	3	9
March-15	-	-	-	-	-	-	-
<b>GEHP2</b>							
	GEHP2 NG (kWh)	Electricity use (kWh)	Electricity (kWh)	Cooling GEHP1 (kWh)	Cost NG (\$)	Cost Electricity (\$)	Total cost (\$)
June-14	4245	104	104	0	56	11	66
July-14	4372	117	117	1687	57	12	69
August-14	5123	137	137	1511	67	14	81
September-14	5639	127	127	1613	74	13	87
October-14	5053	113	113	2188	66	12	78
November-14	3183	76	76	1357	42	8	50
December-14	4171	101	101	1085	55	10	65
January-15	4170	120	120	842	55	12	67
February-15	3129	88	88	588	41	9	50
March-15	5662	116	116	1737	74	12	86
<b>GEHP3</b>							
	GEHP3 NG (kWh)	Electricity use (kWh)	Electricity (kWh)	Cooling GEHP1 (kWh)	Cost NG (\$)	Cost Electricity (\$)	Total cost (\$)
June-14	5414	145	145	4586	71	15	86
July-14	5726	149	149	4525	75	15	91
August-14	6840	176	176	5044	90	18	108
September-14	7008	151	151	5042	92	16	108
October-14	5167	116	116	3947	68	12	80
November-14	2789	71	71	1911	37	7	44
December-14	3035	74	74	1863	40	8	47
January-15	2732	75	75	2055	36	8	44
February-15	1534	47	47	897	20	5	25
March-15	4585	97	97	2657	60	10	70
<b>GEHP4</b>							
	GEHP4 NG (kWh)	Electricity use (kWh)	Electricity (kWh)	Cooling GEHP1 (kWh)	Cost NG (\$)	Cost Electricity (\$)	Total cost (\$)
June-14	3780	92	92	1705	50	9	59
July-14	6179	130	130	2567	81	13	95
August-14	6155	133	133	2167	81	14	95
September-14	5378	109	109	1931	71	11	82
October-14	4488	96	96	1283	59	10	69
November-14	2035	52	52	681	27	5	32
December-14	2172	56	56	655	29	6	34
January-15	1791	40	40	0	24	4	28
February-15	1536	45	45	319	20	5	25
March-15	3737	81	81	565	49	8	57

Table C.4. Running costs calculated for the DeBary four GEHP units

	GEHP1 NG (kWh)	Electricity (kWh)	Cost NG (\$)	Cost Electricity (\$)	GEHP2 NG (kWh)	Electricity (kWh)	Cost NG (\$)	Cost Electricity (\$)
Jun-14	3661	101	49	10	4245	104	57	11
Jul-14	3928	104	52	11	4372	117	58	12
Aug-14	4196	108	56	11	5123	137	68	14
Sep-14	3993	95	53	10	5639	127	75	13
Oct-14	2812	78	38	8	5053	113	67	12
Nov-14	1212	44	16	5	3183	76	43	8
Dec-14	922	46	12	5	4171	101	56	10
Jan-15	748	46	10	5	4170	120	56	12
Feb-15	462	33	6	3	3129	88	42	9
Mar-15	-*	-	-	-	5662	116	76	12

\*The March data is not available due to Gas meter sensor failure in March 2015.

	GEHP3 NG (kWh)	Electricity (kWh)	Cost NG (\$)	Cost Electricity (\$)	GEHP4 NG (kWh)	Electricity (kWh)	Cost NG (\$)	Cost Electricity (\$)	Grand Total (\$)
Jun-14	5414	145	72	15	3780	92	50	9	274
Jul-14	5726	149	76	15	6179	130	83	13	321
Aug-14	6840	176	91	18	6155	133	82	14	355
Sep-14	7008	151	94	16	5378	109	72	11	344
Oct-14	5167	116	69	12	4488	96	60	10	276
Nov-14	2789	71	37	7	2035	52	27	5	148
Dec-14	3035	74	41	8	2172	56	29	6	166
Jan-15	2732	75	36	8	1791	40	24	4	155
Feb-15	1534	47	20	5	1536	45	21	5	111
Mar-15	4585	97	61	10	3737	79	50	8	217*

\*The March data is not available due to Gas meter sensor failure in March 2015.



Table C.5. Model results EER-9.2 EHP system

<b>GEHP1</b>								
	(kBTU)	(kBTU)	(kWh)	(kBTU)	(kBTU)	(kWh)	(kWh)	(\$)
Month	Terminal Cooling Coil Load	Terminal Cooling Eqpt Load	Terminal Unit Clg Input	Terminal Heating Coil Load	Terminal Heating Eqpt Load	Terminal Unit Htg Input	Terminal Fan	Cost
January	3324	3380	241	0	0	0	63	25
February	3778	3842	278	0	0	0	72	29
March	5214	5302	402	0	0	0	98	41
April	6024	6126	473	0	0	0	113	49
May	7508	7635	651	0	0	0	134	67
June	8151	8288	735	0	0	0	138	76
July	9086	9239	843	0	0	0	150	87
August	8648	8794	791	0	0	0	143	81
September	8072	8208	716	0	0	0	136	74
October	7234	7356	601	0	0	0	128	62
November	5414	5505	424	0	0	0	100	44
December	3199	3253	225	0	0	0	62	23
Total	75653	76929	6381	0	0	0	1339	656
<b>GEHP2</b>								
	(kBTU)	(kBTU)	(kWh)	(kBTU)	(kBTU)	(kWh)	(kWh)	(\$)
Month	Terminal Cooling Coil Load	Terminal Cooling Eqpt Load	Terminal Unit Clg Input	Terminal Heating Coil Load	Terminal Heating Eqpt Load	Terminal Unit Htg Input	Terminal Fan	Cost
January	3105	3570	234	280	321	28	98	27
February	3904	4489	295	21	22	2	110	31
March	5644	6489	451	1	1	0	177	46
April	6780	7796	552	0	0	0	236	57
May	8628	9921	761	0	0	0	311	78
June	9196	10574	836	0	0	0	328	86
July	10080	11590	938	0	0	0	353	96
August	9754	11216	899	0	0	0	335	92
September	8932	10271	803	0	0	0	301	83
October	7747	8908	665	0	0	0	249	68
November	5710	6565	463	3	3	0	165	48
December	2748	3159	200	133	149	12	81	22
Total	82228	94547	7096	437	497	42	2743	733
<b>GEHP3</b>								
	(kBTU)	(kBTU)	(kWh)	(kBTU)	(kBTU)	(kWh)	(kWh)	(\$)
Month	Terminal Cooling Coil Load	Terminal Cooling Eqpt Load	Terminal Unit Clg Input	Terminal Heating Coil Load	Terminal Heating Eqpt Load	Terminal Unit Htg Input	Terminal Fan	Cost
January	6164	6281	395	0	0	0	133	41
February	6623	6748	440	0	0	0	140	45
March	8877	9044	620	0	0	0	181	64
April	10411	10608	751	0	0	0	211	77
May	13097	13345	1056	0	0	0	242	108
June	14194	14463	1204	0	0	0	237	124
July	16190	16496	1420	0	0	0	259	146
August	14915	15196	1282	0	0	0	240	132
September	13665	13924	1139	0	0	0	227	117
October	11701	11922	903	0	0	0	212	93
November	8157	8311	585	0	0	0	162	60
December	5894	6005	366	0	0	0	129	38
Total	129889	132344	10162	0	0	0	2373	1044

Table C.5. Continued

GEHP4	(kBTU)	(kBTU)	(kWh)	(kBTU)	(kBTU)	(kWh)	(kWh)	(\$)
Month	Terminal Cooling Coil Load	Terminal Cooling Eqpt Load	Terminal Unit Clg Input	Terminal Heating Coil Load	Terminal Heating Eqpt Load	Terminal Unit Htg Input	Terminal Fan	Cost
January	1329	1440	101	111	115	10	33	11
February	2060	2232	157	0	0	0	49	16
March	3579	3879	282	0	0	0	86	29
April	4866	5274	390	0	0	0	119	40
May	6870	7446	604	0	0	0	159	62
June	7816	8472	715	0	0	0	169	73
July	8734	9466	822	0	0	0	184	84
August	7990	8660	739	0	0	0	169	76
September	6893	7471	618	0	0	0	149	63
October	5266	5708	445	0	0	0	118	46
November	3009	3262	242	0	0	0	70	25
December	1173	1271	87	43	44	4	28	9
Total	59586	64582	5202	154	159	14	1332	536

Table C.6. Model results EER-11.8 EHP system

<b>GEHP1</b>								
	(kBTU)	(kBTU)	(kWh)	(kBTU)	(kBTU)	(kWh)	(kWh)	(\$)
Month	Terminal Cooling Coil Load	Terminal Cooling Eqpt Load	Terminal Unit Clg Input	Terminal Heating Coil Load	Terminal Heating Eqpt Load	Terminal Unit Htg Input	Total Electricity	Cost
January	3324	3380	175	0	0	0	175	18
February	3778	3842	202	0	0	0	202	21
March	5214	5302	292	0	0	0	292	30
April	6024	6126	344	0	0	0	344	35
May	7508	7635	472	0	0	0	472	48
June	8151	8288	534	0	0	0	534	55
July	9086	9239	612	0	0	0	612	63
August	8648	8794	574	0	0	0	574	59
September	8072	8208	520	0	0	0	520	53
October	7234	7356	436	0	0	0	436	45
November	5414	5505	308	0	0	0	308	32
December	3199	3253	164	0	0	0	164	17
Total	75653	76929	4632	0	0	0	4632	476
<b>GEHP2</b>								
	(kBTU)	(kBTU)	(kWh)	(kBTU)	(kBTU)	(kWh)	(kWh)	(\$)
Month	Terminal Cooling Coil Load	Terminal Cooling Eqpt Load	Terminal Unit Clg Input	Terminal Heating Coil Load	Terminal Heating Eqpt Load	Terminal Unit Htg Input	Total Electricity	Cost
January	3105	3570	166	280	321	28	194	20
February	3904	4489	209	21	22	2	211	22
March	5644	6489	320	1	1	0	320	33
April	6780	7796	392	0	0	0	392	40
May	8628	9921	540	0	0	0	540	55
June	9196	10574	593	0	0	0	593	61
July	10080	11590	665	0	0	0	665	68
August	9754	11216	638	0	0	0	638	66
September	8932	10271	570	0	0	0	570	59
October	7747	8908	472	0	0	0	472	48
November	5710	6565	329	3	3	0	329	34
December	2748	3159	142	133	149	12	154	16
Total	82228	94547	5034	437	497	42	5076	522
<b>GEHP3</b>								
	(kBTU)	(kBTU)	(kWh)	(kBTU)	(kBTU)	(kWh)	(kWh)	(\$)
Month	Terminal Cooling Coil Load	Terminal Cooling Eqpt Load	Terminal Unit Clg Input	Terminal Heating Coil Load	Terminal Heating Eqpt Load	Terminal Unit Htg Input	Total Electricity	Cost
January	6164	6281	278	0	0	0	278	29
February	6623	6748	310	0	0	0	310	32
March	8877	9044	437	0	0	0	437	45
April	10411	10608	529	0	0	0	529	54
May	13097	13345	744	0	0	0	744	76
June	14194	14463	848	0	0	0	848	87
July	16190	16496	1000	0	0	0	1000	103
August	14915	15196	903	0	0	0	903	93
September	13665	13924	802	0	0	0	802	82
October	11701	11922	636	0	0	0	636	65
November	8157	8311	412	0	0	0	412	42
December	5894	6005	258	0	0	0	258	27
Total	129889	132344	7158	0	0	0	7158	735

Table C.6. Continued

GEHP4	(kBTU)	(kBTU)	(kWh)	(kBTU)	(kBTU)	(kWh)	(kWh)	(\$)
Month	Terminal Cooling Coil Load	Terminal Cooling Eqpt Load	Terminal Unit Clg Input	Terminal Heating Coil Load	Terminal Heating Eqpt Load	Terminal Unit Htg Input	Total Electricity	Cost
January	1329	1440	72	111	115	10	82	8
February	2060	2232	112	0	0	0	112	12
March	3579	3879	202	0	0	0	202	21
April	4866	5274	279	0	0	0	279	29
May	6870	7446	431	0	0	0	431	44
June	7816	8472	510	0	0	0	510	52
July	8734	9466	587	0	0	0	587	60
August	7990	8660	528	0	0	0	528	54
September	6893	7471	441	0	0	0	441	45
October	5266	5708	318	0	0	0	318	33
November	3009	3262	173	0	0	0	173	18
December	1173	1271	62	43	44	4	66	7
Total	59586	64582	3715	154	159	14	3729	383

Table C.7. Model results EER-12.8 EHP system

<b>GEHP1</b>								
	(kBTU)	(kBTU)	(kWh)	(kBTU)	(kBTU)	(kWh)	(kWh)	(\$)
Month	Terminal Cooling Coil Load	Terminal Cooling Eqpt Load	Terminal Unit Clg Input	Terminal Heating Coil Load	Terminal Heating Eqpt Load	Terminal Unit Htg Input	Total Electricity	Cost
January	3324	3380	153	0	0	0	153	16
February	3778	3842	177	0	0	0	177	18
March	5214	5302	256	0	0	0	256	26
April	6024	6126	301	0	0	0	301	31
May	7508	7635	414	0	0	0	414	43
June	8151	8288	468	0	0	0	468	48
July	9086	9239	537	0	0	0	537	55
August	8648	8794	503	0	0	0	503	52
September	8072	8208	456	0	0	0	456	47
October	7234	7356	383	0	0	0	383	39
November	5414	5505	270	0	0	0	270	28
December	3199	3253	144	0	0	0	144	15
Total	75653	76929	4061	0	0	0	4061	417
<b>GEHP2</b>								
	(kBTU)	(kBTU)	(kWh)	(kBTU)	(kBTU)	(kWh)	(kWh)	(\$)
Month	Terminal Cooling Coil Load	Terminal Cooling Eqpt Load	Terminal Unit Clg Input	Terminal Heating Coil Load	Terminal Heating Eqpt Load	Terminal Unit Htg Input	Total Electricity	Cost
January	3105	3570	144	280	321	31	175	18
February	3904	4489	181	21	22	2	183	19
March	5644	6489	277	1	1	0	277	28
April	6780	7796	339	0	0	0	339	35
May	8628	9921	468	0	0	0	468	48
June	9196	10574	514	0	0	0	514	53
July	10080	11590	576	0	0	0	576	59
August	9754	11216	552	0	0	0	552	57
September	8932	10271	493	0	0	0	493	51
October	7747	8908	409	0	0	0	409	42
November	5710	6565	285	3	3	0	285	29
December	2748	3159	123	133	149	13	136	14
Total	82228	94547	4361	437	497	46	4407	453
<b>GEHP3</b>								
	(kBTU)	(kBTU)	(kWh)	(kBTU)	(kBTU)	(kWh)	(kWh)	(\$)
Month	Terminal Cooling Coil Load	Terminal Cooling Eqpt Load	Terminal Unit Clg Input	Terminal Heating Coil Load	Terminal Heating Eqpt Load	Terminal Unit Htg Input	Total Electricity	Cost
January	6164	6281	240	0	0	0	240	25
February	6623	6748	267	0	0	0	267	27
March	8877	9044	377	0	0	0	377	39
April	10411	10608	456	0	0	0	456	47
May	13097	13345	642	0	0	0	642	66
June	14194	14463	732	0	0	0	732	75
July	16190	16496	863	0	0	0	863	89
August	14915	15196	780	0	0	0	780	80
September	13665	13924	693	0	0	0	693	71
October	11701	11922	549	0	0	0	549	56
November	8157	8311	356	0	0	0	356	37
December	5894	6005	223	0	0	0	223	23
Total	129889	132344	6178	0	0	0	6178	635

Table C.7. Continued

GEHP4	(kBTU)	(kBTU)	(kWh)	(kBTU)	(kBTU)	(kWh)	(kWh)	(\$)
Month	Terminal Cooling Coil Load	Terminal Cooling Eqpt Load	Terminal Unit Clg Input	Terminal Heating Coil Load	Terminal Heating Eqpt Load	Terminal Unit Htg Input	Total Electricity	Cost
January	1329	1440	63	111	115	11	74	8
February	2060	2232	97	0	0	0	97	10
March	3579	3879	175	0	0	0	175	18
April	4866	5274	242	0	0	0	242	25
May	6870	7446	375	0	0	0	375	39
June	7816	8472	444	0	0	0	444	46
July	8734	9466	510	0	0	0	510	52
August	7990	8660	459	0	0	0	459	47
September	6893	7471	384	0	0	0	384	39
October	5266	5708	277	0	0	0	277	28
November	3009	3262	150	0	0	0	150	15
December	1173	1271	54	43	44	4	58	6
Total	59586	64582	3230	154	159	15	3245	333

Table C.8. Model results EER-15.0 EHP system

<b>GEHP1</b>								
	(kBTU)	(kBTU)	(kWh)	(kBTU)	(kBTU)	(kWh)	(kWh)	(\$)
Month	Terminal Cooling Coil Load	Terminal Cooling Eqpt Load	Terminal Unit Clg Input	Terminal Heating Coil Load	Terminal Heating Eqpt Load	Terminal Unit Htg Input	Total Electricity	Cost
January	3324	3380	111	0	0	0	111	11
February	3778	3842	128	0	0	0	128	13
March	5214	5302	185	0	0	0	185	19
April	6024	6126	218	0	0	0	218	22
May	7508	7635	300	0	0	0	300	31
June	8151	8288	339	0	0	0	339	35
July	9086	9239	388	0	0	0	388	40
August	8648	8794	364	0	0	0	364	37
September	8072	8208	330	0	0	0	330	34
October	7234	7356	277	0	0	0	277	28
November	5414	5505	195	0	0	0	195	20
December	3199	3253	104	0	0	0	104	11
Total	75653	76929	2939	0	0	0	2939	302
<b>GEHP2</b>								
	(kBTU)	(kBTU)	(kWh)	(kBTU)	(kBTU)	(kWh)	(kWh)	(\$)
Month	Terminal Cooling Coil Load	Terminal Cooling Eqpt Load	Terminal Unit Clg Input	Terminal Heating Coil Load	Terminal Heating Eqpt Load	Terminal Unit Htg Input	Total Electricity	Cost
January	3105	3570	100	280	321	34	134	14
February	3904	4489	126	21	22	2	128	13
March	5644	6489	193	1	1	0	193	20
April	6780	7796	236	0	0	0	236	24
May	8628	9921	326	0	0	0	326	33
June	9196	10574	358	0	0	0	358	37
July	10080	11590	401	0	0	0	401	41
August	9754	11216	385	0	0	0	385	40
September	8932	10271	344	0	0	0	344	35
October	7747	8908	285	0	0	0	285	29
November	5710	6565	198	3	3	0	198	20
December	2748	3159	86	133	149	14	100	10
Total	82228	94547	3038	437	497	50	3088	317
<b>GEHP3</b>								
	(kBTU)	(kBTU)	(kWh)	(kBTU)	(kBTU)	(kWh)	(kWh)	(\$)
Month	Terminal Cooling Coil Load	Terminal Cooling Eqpt Load	Terminal Unit Clg Input	Terminal Heating Coil Load	Terminal Heating Eqpt Load	Terminal Unit Htg Input	Total Electricity	Cost
January	6164	6281	165	0	0	0	165	17
February	6623	6748	184	0	0	0	184	19
March	8877	9044	259	0	0	0	259	27
April	10411	10608	314	0	0	0	314	32
May	13097	13345	442	0	0	0	442	45
June	14194	14463	503	0	0	0	503	52
July	16190	16496	594	0	0	0	594	61
August	14915	15196	536	0	0	0	536	55
September	13665	13924	476	0	0	0	476	49
October	11701	11922	378	0	0	0	378	39
November	8157	8311	245	0	0	0	245	25
December	5894	6005	153	0	0	0	153	16
Total	129889	132344	4249	0	0	0	4249	437

Table C.8. Continued

GEHP4	(kBTU)	(kBTU)	(kWh)	(kBTU)	(kBTU)	(kWh)	(kWh)	(\$)
Month	Terminal Cooling Coil Load	Terminal Cooling Eqpt Load	Terminal Unit Clg Input	Terminal Heating Coil Load	Terminal Heating Eqpt Load	Terminal Unit Htg Input	Total Electricity	Cost
January	1329	1440	44	111	115	12	56	6
February	2060	2232	69	0	0	0	69	7
March	3579	3879	123	0	0	0	123	13
April	4866	5274	171	0	0	0	171	18
May	6870	7446	264	0	0	0	264	27
June	7816	8472	313	0	0	0	313	32
July	8734	9466	359	0	0	0	359	37
August	7990	8660	323	0	0	0	323	33
September	6893	7471	270	0	0	0	270	28
October	5266	5708	195	0	0	0	195	20
November	3009	3262	106	0	0	0	106	11
December	1173	1271	38	43	44	5	43	4
Total	59586	64582	2275	154	159	17	2292	235



Table C.9. Model results for Okaloosa, FL

<b>GEHP1</b>								
	(kBTU)	(kBTU)	(kWh)	(kBTU)	(kBTU)	(kWh)	(kWh)	(\$)
Month	Terminal Cooling Coil Load	Terminal Cooling Eqpt Load	Terminal Unit Clg Input	Terminal Heating Coil Load	Terminal Heating Eqpt Load	Terminal Unit Htg Input	Total Electricity	Cost
January	1504	1529	64	69	72	8	72	7
February	1727	1757	72	2	4	0	72	7
March	3867	3932	179	0	0	0	179	18
April	4679	4758	219	0	0	0	219	23
May	6993	7111	375	0	0	0	375	39
June	8136	8273	469	0	0	0	469	48
July	9028	9180	529	0	0	0	529	54
August	8787	8936	524	0	0	0	524	54
September	7358	7482	411	0	0	0	411	42
October	4960	5044	236	0	0	0	236	24
November	3066	3118	141	0	0	0	141	14
December	2146	2182	91	0	0	0	91	9
<b>Total</b>	<b>62251</b>	<b>63301</b>	<b>3310</b>	<b>71</b>	<b>76</b>	<b>8</b>	<b>3318</b>	<b>341</b>
<b>GEHP2</b>								
	(kBTU)	(kBTU)	(kWh)	(kBTU)	(kBTU)	(kWh)	(kWh)	(\$)
Month	Terminal Cooling Coil Load	Terminal Cooling Eqpt Load	Terminal Unit Clg Input	Terminal Heating Coil Load	Terminal Heating Eqpt Load	Terminal Unit Htg Input	Total Electricity	Cost
January	965	1110	41	1063	1222	117	158	16
February	1125	1293	47	445	512	52	99	10
March	3748	4309	173	49	55	5	178	18
April	4649	5346	219	0	0	0	219	23
May	7810	8980	414	1	1	0	414	43
June	9298	10691	518	0	0	0	518	53
July	10174	11698	575	0	0	0	575	59
August	10123	11639	582	0	0	0	582	60
September	8222	9454	449	0	0	0	449	46
October	4951	5693	235	8	9	1	236	24
November	2529	2908	115	162	189	18	133	14
December	1669	1918	70	553	660	63	133	14
<b>Total</b>	<b>65262</b>	<b>75040</b>	<b>3438</b>	<b>2282</b>	<b>2648</b>	<b>256</b>	<b>3694</b>	<b>380</b>
<b>GEHP3</b>								
	(kBTU)	(kBTU)	(kWh)	(kBTU)	(kBTU)	(kWh)	(kWh)	(\$)
Month	Terminal Cooling Coil Load	Terminal Cooling Eqpt Load	Terminal Unit Clg Input	Terminal Heating Coil Load	Terminal Heating Eqpt Load	Terminal Unit Htg Input	Total Electricity	Cost
January	3959	4028	137	34	35	3	140	14
February	4068	4124	135	18	20	2	137	14
March	7216	7337	287	0	0	0	287	29
April	8786	8952	356	0	0	0	356	37
May	12290	12522	585	0	0	0	585	60
June	14072	14338	730	0	0	0	730	75
July	15795	16094	833	0	0	0	833	86
August	14607	14883	779	0	0	0	779	80
September	12250	12481	608	0	0	0	608	62
October	8409	8568	347	0	0	0	347	36
November	5797	5907	227	0	0	0	227	23
December	4455	4537	154	23	23	2	156	16
<b>Total</b>	<b>111705</b>	<b>113771</b>	<b>5178</b>	<b>75</b>	<b>79</b>	<b>7</b>	<b>5185</b>	<b>533</b>

Table C.9. Continued

GEHP4								
	(kBTU)	(kBTU)	(kWh)	(kBTU)	(kBTU)	(kWh)	(kWh)	(\$)
Month	Terminal Cooling Coil Load	Terminal Cooling Eqpt Load	Terminal Unit Clg Input	Terminal Heating Coil Load	Terminal Heating Eqpt Load	Terminal Unit Htg Input	Total Electricity	Cost
January	347	376	15	795	813	78	93	10
February	457	496	20	348	355	35	55	6
March	2313	2507	110	21	21	2	112	12
April	3382	3666	159	0	0	0	159	16
May	6205	6725	329	0	0	0	329	34
June	7751	8401	441	0	0	0	441	45
July	8613	9335	499	0	0	0	499	51
August	8003	8673	471	0	0	0	471	48
September	6074	6583	335	0	0	0	335	34
October	2851	3090	137	0	0	0	137	14
November	1264	1370	60	61	65	7	67	7
December	381	413	18	497	519	48	66	7
Total	47641	51635	2595	1721	1773	170	2765	284

Table C.10. Model results for Plant City, FL

<b>GEHP1</b>								
	(kBTU)	(kBTU)	(kWh)	(kBTU)	(kBTU)	(kWh)	(kWh)	(\$)
Month	Terminal Cooling Coil Load	Terminal Cooling Eqpt Load	Terminal Unit Clg Input	Terminal Heating Coil Load	Terminal Heating Eqpt Load	Terminal Unit Htg Input	Total Electricity	Cost
January	3524	3583	155	0	0	0	155	16
February	3934	4000	192	0	0	0	192	20
March	4389	4463	204	0	0	0	204	21
April	6713	6826	345	0	0	0	345	35
May	7916	8049	431	0	0	0	431	44
June	8465	8608	495	0	0	0	495	51
July	9261	9418	546	0	0	0	546	56
August	9097	9251	533	0	0	0	533	55
September	8148	8286	454	0	0	0	454	47
October	7605	7733	410	0	0	0	410	42
November	5038	5123	247	0	0	0	247	25
December	3450	3508	159	0	0	0	159	16
Total	77541	78848	4171	0	0	0	4171	429
<b>GEHP2</b>								
	(kBTU)	(kBTU)	(kWh)	(kBTU)	(kBTU)	(kWh)	(kWh)	(\$)
Month	Terminal Cooling Coil Load	Terminal Cooling Eqpt Load	Terminal Unit Clg Input	Terminal Heating Coil Load	Terminal Heating Eqpt Load	Terminal Unit Htg Input	Total Electricity	Cost
January	3081	3543	138	124	143	13	151	16
February	3897	4481	192	102	122	12	204	21
March	4455	5123	211	19	24	2	213	22
April	7611	8751	388	0	0	0	388	40
May	9016	10367	479	0	0	0	479	49
June	9721	11178	549	0	0	0	549	56
July	10521	12097	599	0	0	0	599	62
August	10432	11995	590	0	0	0	590	61
September	9211	10591	502	0	0	0	502	52
October	8307	9552	445	0	0	0	445	46
November	5134	5903	253	6	6	0	253	26
December	3069	3528	144	193	226	21	165	17
Total	84455	97108	4489	444	521	48	4537	466
<b>GEHP3</b>								
	(kBTU)	(kBTU)	(kWh)	(kBTU)	(kBTU)	(kWh)	(kWh)	(\$)
Month	Terminal Cooling Coil Load	Terminal Cooling Eqpt Load	Terminal Unit Clg Input	Terminal Heating Coil Load	Terminal Heating Eqpt Load	Terminal Unit Htg Input	Total Electricity	Cost
January	6205	6322	232	0	0	0	232	24
February	6713	6840	282	0	0	0	282	29
March	7764	7911	307	0	0	0	307	32
April	11455	11672	520	0	0	0	520	53
May	13971	14235	680	0	0	0	680	70
June	14810	15090	778	0	0	0	778	80
July	16334	16643	867	0	0	0	867	89
August	15550	15844	819	0	0	0	819	84
September	13608	13865	679	0	0	0	679	70
October	11995	12222	572	0	0	0	572	59
November	7680	7825	325	0	0	0	325	33
December	6009	6120	232	0	0	0	232	24
Total	132096	134590	6291	0	0	0	6291	646

Table C.10. Continued

GEHP4								
	(kBTU)	(kBTU)	(kWh)	(kBTU)	(kBTU)	(kWh)	(kWh)	(\$)
Month	Terminal Cooling Coil Load	Terminal Cooling Eqpt Load	Terminal Unit Clg Input	Terminal Heating Coil Load	Terminal Heating Eqpt Load	Terminal Unit Htg Input	Total Electricity	Cost
January	1323	1434	59	48	48	5	64	7
February	1984	2150	99	67	69	6	105	11
March	2591	2809	121	0	0	0	121	12
April	5314	5759	270	0	0	0	270	28
May	7235	7841	389	0	0	0	389	40
June	8258	8950	478	0	0	0	478	49
July	8989	9743	524	0	0	0	524	54
August	8330	9028	481	0	0	0	481	49
September	6827	7400	374	0	0	0	374	38
October	5483	5943	292	0	0	0	292	30
November	2732	2961	134	0	0	0	134	14
December	1261	1367	61	68	72	7	68	7
Total	60327	65384	3281	183	189	18	3299	339

Table C.11. Cost comparison of actual GEHP vs. EHP of different performance ratings for DeBary, FL

	<b>Actual Cost GEHP</b>	<b>EER 9.2 EHP</b>	<b>EER 11.8 EHP</b>	<b>EER 12.8 EHP</b>	<b>EER 15.0 EHP</b>
Month	(\$)	(\$)	(\$)	(\$)	(\$)
Jun-2014	274	359	255	222	155
Jul-2014	321	413	294	255	179
Aug-2014	355	381	272	236	165
Sep-2014	344	337	240	208	146
Oct-2014	276	269	191	166	117
Nov-2014	148	176	126	109	76
Dec-2014	166	92	66	58	41
Jan-2015	155	104	75	66	48
Feb-2015	111	120	86	74	52
Mar-2015	N/A*	180	129	111	78

\* GEHP1 data not recorded

### C.3 Power Query Code for Data Compilation

let

```
Source = Folder.Files("C:\Users\rajeev\Google Drive\USF Work\Heat Pump\Working\GHP data\CERC Data\Merged\main"),
InsertedCustom = Table.AddColumn(Source, "Custom", each fgetmain([Folder Path],[Name])), #"Expand Custom" =
Table.ExpandTableColumn(InsertedCustom, "Custom", {"Date", "Time", "Unkn", "E/G OP SW", "HP SW", "LP SW", "High
pressure", "Low pressure", "HP equiv. temp.", "LP equiv. temp.", "C/P 1 discharge temp.", "C/P 2 discharge temp.", "C/P 3
discharge temp.", "C/P 4 discharge temp.", "C/P intake temp. 1", "C/P intake temp. 2", "Liquid pipe temp.", "Heat ex. liquid
temp.", "Sub heat ex. outlet temp.", "Accumulator outlet temp. 1", "Accumulator outlet temp. 2", "Supercooling heat ex. intake
temp.", "Data spare 1", "Data spare 2", "Data spare 3", "Outside temp.", "E/G oil temp.", "E/G room temp.", "E/G exhaust air
temp.", "Starter voltage", "Igniter voltage", "Fuel gas valve output check input", "Power supply phase", "R-S phase detection", "S-
T phase detection", "T-R phase detection", "E/G side spare input", "Silent mode external input", "Input spare 1", "Input spare 2",
"Compressor 1", "Compressor 2", "Compressor 3", "Compressor 4", "4-way chgov. valve", "Output spare 1", "Fan airflow level",
"Heat ex. fan 1", "Heat ex. fan 2", "Heat ex. fan 3", "E/G coolant pump", "Throttle valve", "Fuel gas valve", "Main heat ex. refrig.
liquid flow valve", "Sub heat ex. refrig. liquid flow valve", "Supercooling valve", "C/P capacity control valve", "Liquid flow control
valve", "Data spare 4", "Compressor heater", "Drain heater", "Oil pan heater", "Fuel gas valve 1", "Fuel gas valve 2", "Starter",
"Starter transformer ", "12 VDC output permission #(0081)iMain#(0081)j", "12 VDC output permission #(0081)iE/G#(0081)j",
"Output data spare 1", "Output data spare 2", "Specified engine RPM", "Actual engine RPM", "Engine igniter spark", "Requested
calculated engine RPM total", "Calculated engine RPM total", "Requested calculated engine RPM", "Calculated engine RPM",
"Succion superheating degree", "Sub heat ex. outlet superheating degree", "Outdoor supercooling degree", "Outdoor heat ex.
supercooling degree", "Data spare 5", "Data spare 6", "Silent mode", "Compressor protect control", "Defrost control", "Cold
district spec. operation", "Periodic inspection", "E/G operation hour", "Requesting power generation amount", "Actual power
generation", "Oil return valve 1", "Oil return valve 2", "Oil return valve 3", "Oil return valve 4", "Hot gas bypass valve", "Output
spare 4", "Output spare 5", "Refrig. gas P supply valve ", "Output spare 9", "Oil return valve", "Refrig. gas valve ", "Output spare
2", "Output spare 3", "Output spare 6", "Output spare 7", "Output spare 8", "Output spare 10"}, {"Date", "Time", "Unkn", "E/G
OP SW", "HP SW", "LP SW", "High pressure", "Low pressure", "HP equiv. temp.", "LP equiv. temp.", "C/P 1 discharge temp.", "C/P
2 discharge temp.", "C/P 3 discharge temp.", "C/P 4 discharge temp.", "C/P intake temp. 1", "C/P intake temp. 2", "Liquid pipe
temp.", "Heat ex. liquid temp.", "Sub heat ex. outlet temp.", "Accumulator outlet temp. 1", "Accumulator outlet temp. 2",
"Supercooling heat ex. intake temp.", "Data spare 1", "Data spare 2", "Data spare 3", "Outside temp.", "E/G oil temp.", "E/G room
temp.", "E/G exhaust air temp.", "Starter voltage", "Igniter voltage", "Fuel gas valve output check input", "Power supply phase",
"R-S phase detection", "S-T phase detection", "T-R phase detection", "E/G side spare input", "Silent mode external input", "Input
spare 1 ", "Input spare 2", "Compressor 1", "Compressor 2", "Compressor 3", "Compressor 4", "4-way chgov. valve", "Output
spare 1", "Fan airflow level", "Heat ex. fan 1", "Heat ex. fan 2", "Heat ex. fan 3", "E/G coolant pump", "Throttle valve", "Fuel gas
valve", "Main heat ex. refrig. liquid flow valve", "Sub heat ex. refrig. liquid flow valve", "Supercooling valve", "C/P capacity control
valve", "Liquid flow control valve", "Data spare 4", "Compressor heater", "Drain heater", "Oil pan heater", "Fuel gas valve 1",
"Fuel gas valve 2", "Starter", "Starter transformer ", "12 VDC output permission #(0081)iMain#(0081)j", "12 VDC output
permission #(0081)iE/G#(0081)j", "Output data spare 1", "Output data spare 2", "Specified engine RPM", "Actual engine RPM",
"Engine igniter spark", "Requested calculated engine RPM total", "Calculated engine RPM total", "Requested calculated engine
RPM", "Calculated engine RPM", "Succion superheating degree", "Sub heat ex. outlet superheating degree", "Outdoor
supercooling degree", "Outdoor heat ex. supercooling degree", "Data spare 5", "Data spare 6", "Silent mode", "Compressor
protect control", "Defrost control", "Cold district spec. operation", "Periodic inspection", "E/G operation hour", "Requesting
power generation amount", "Actual power generation", "Oil return valve 1", "Oil return valve 2", "Oil return valve 3", "Oil return
valve 4", "Hot gas bypass valve", "Output spare 4", "Output spare 5", "Refrig. gas P supply valve ", "Output spare 9", "Oil return
valve", "Refrig. gas valve ", "Output spare 2", "Output spare 3", "Output spare 6", "Output spare 7", "Output spare 8", "Output
spare 10"}))
```

in #"Expand Custom"

### Appendix D Optimization Results - JEPlus

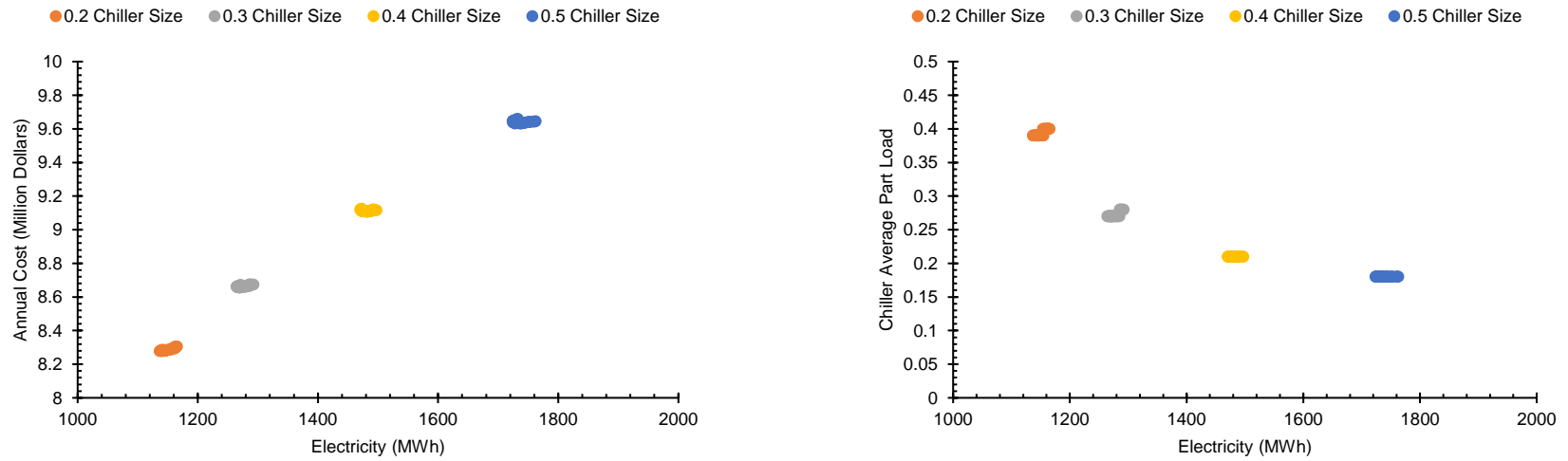


Figure D.1. System optimization results for ice storage model

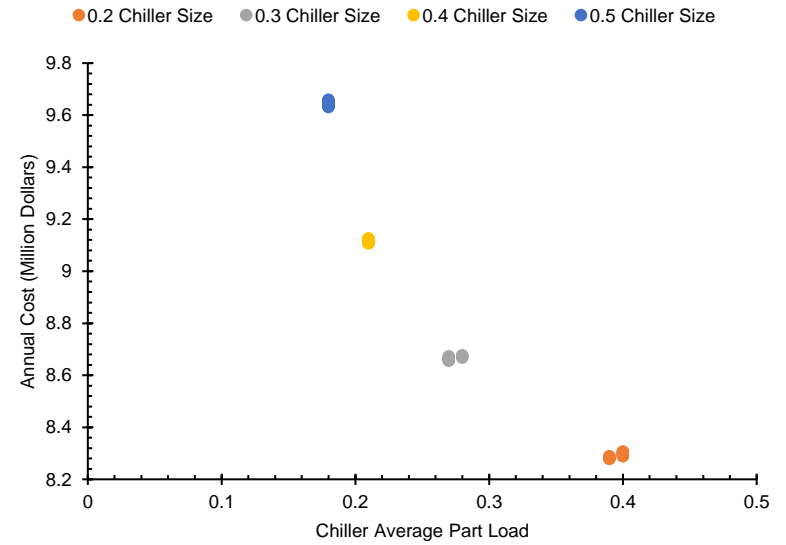
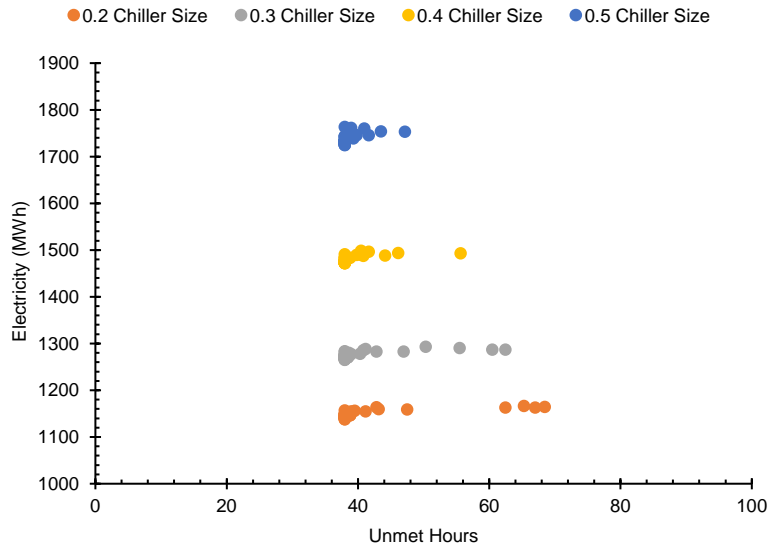
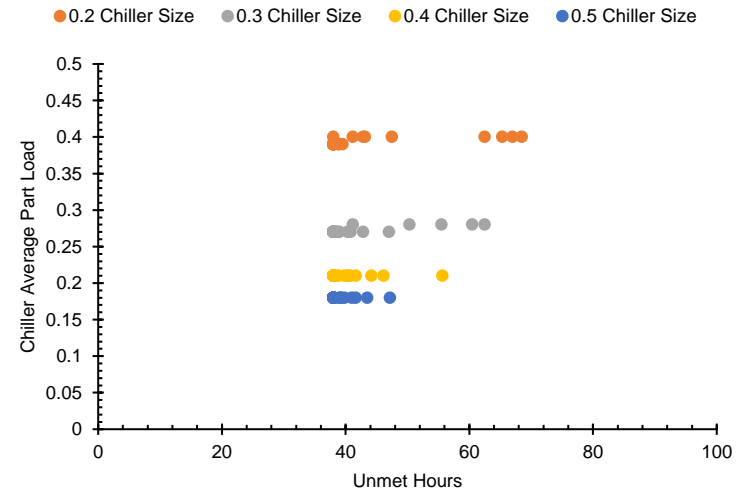
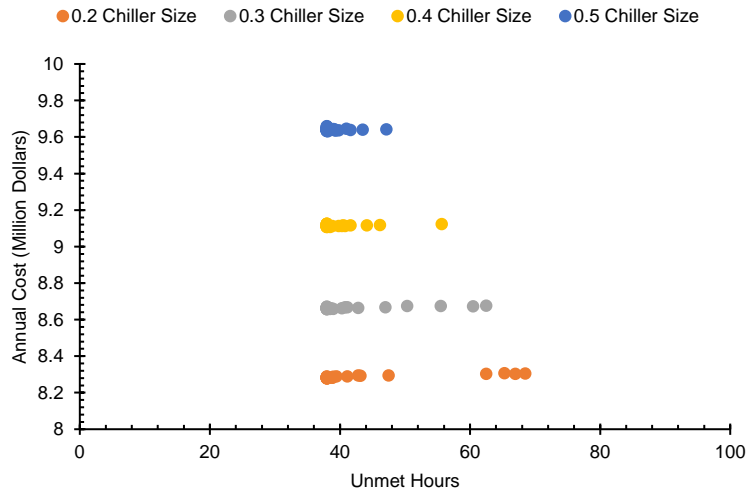


Figure D.1. Continued



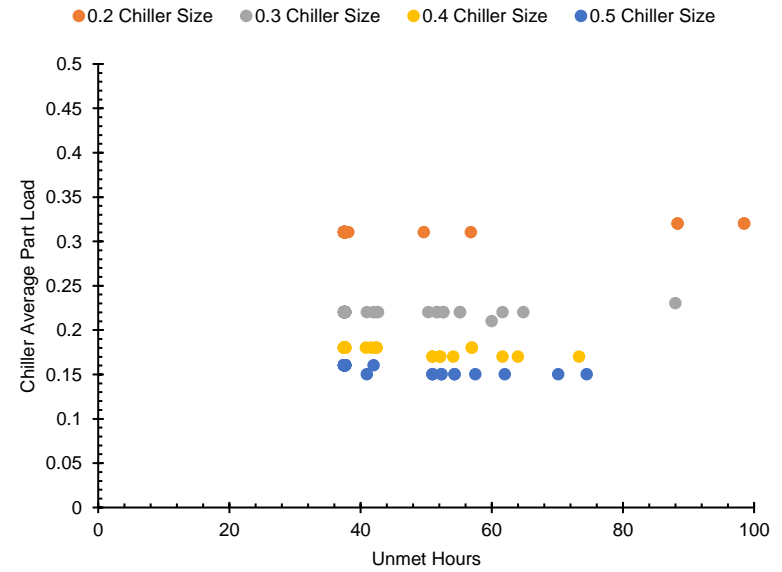
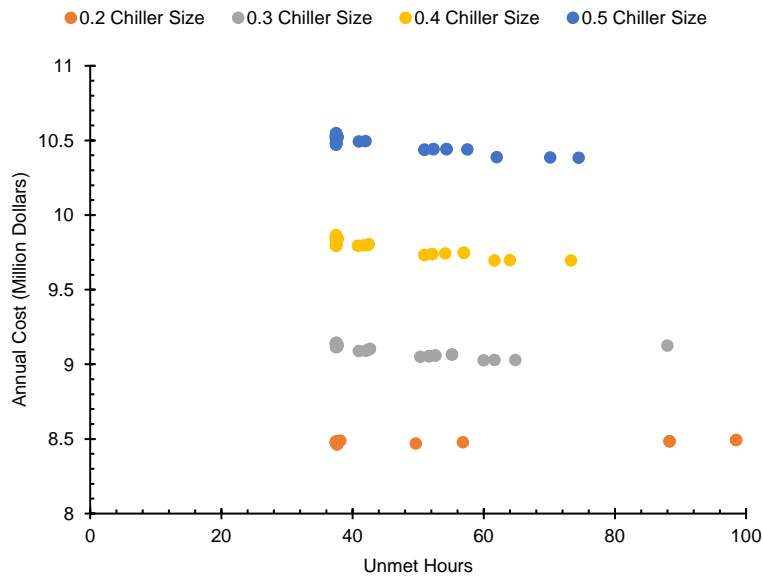
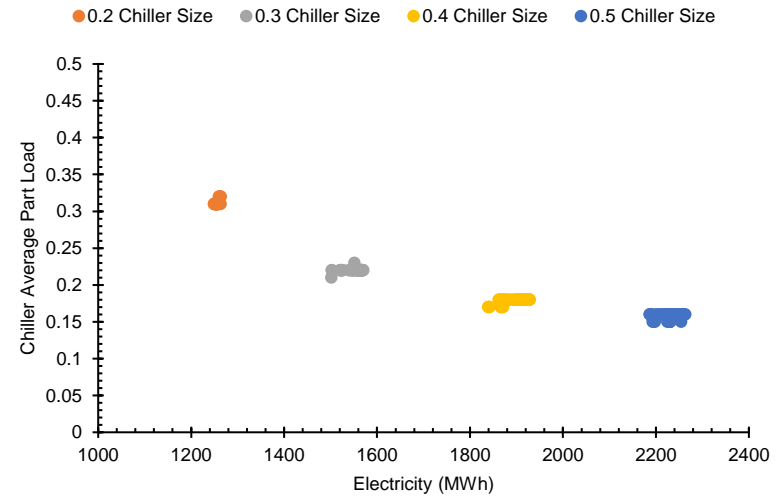
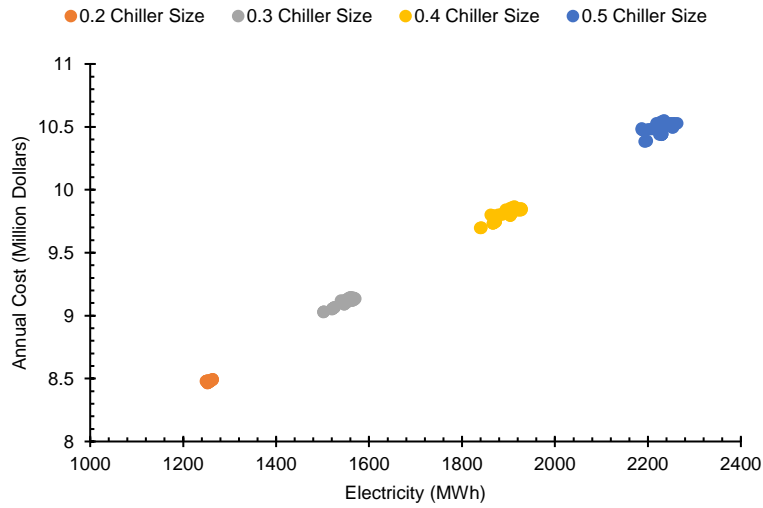


Figure D.2. System optimization results for chilled water mixed tank storage model

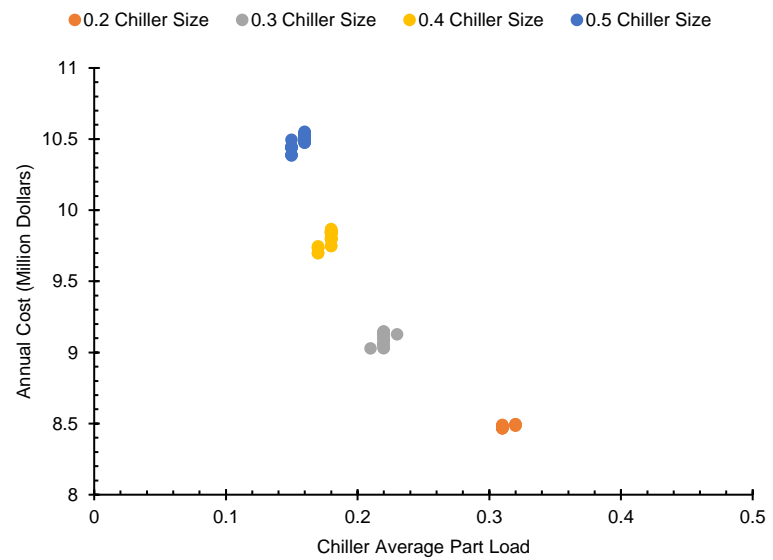
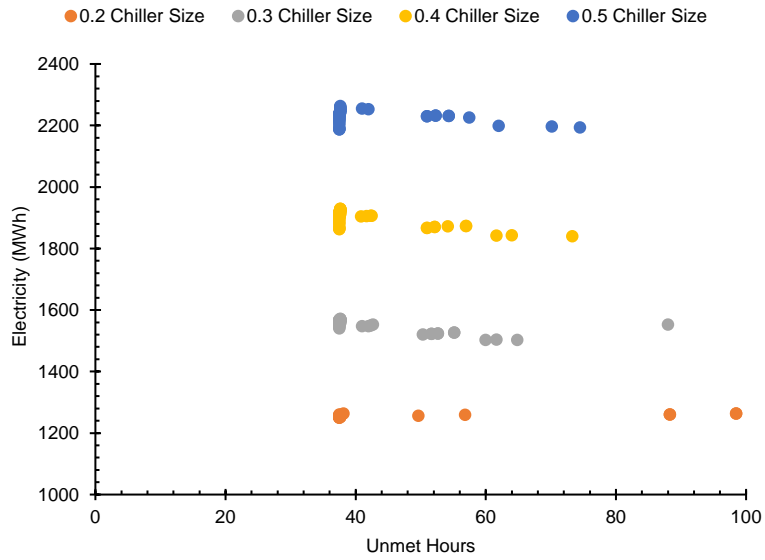


Figure D.2. Continued

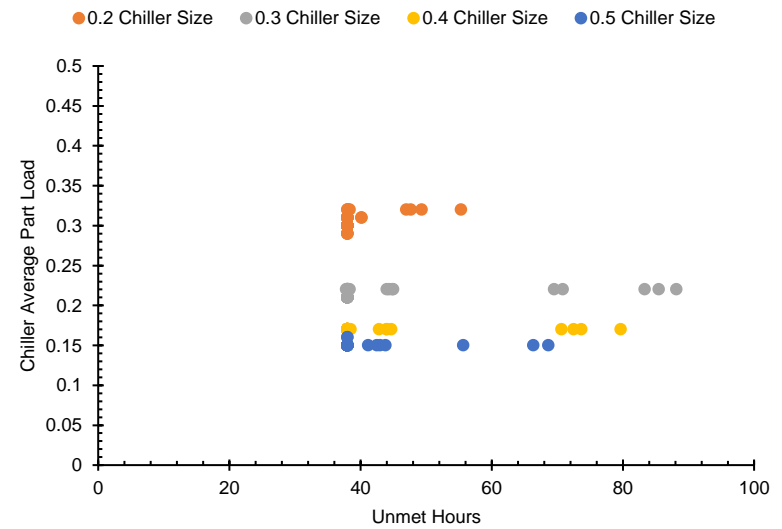
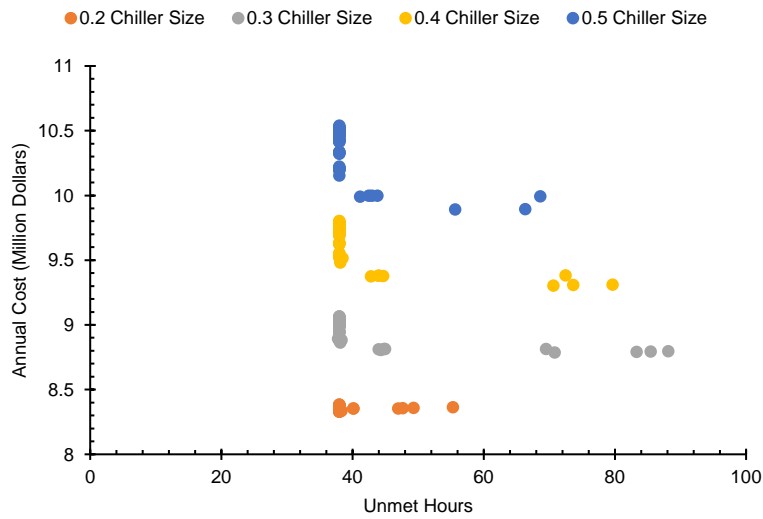
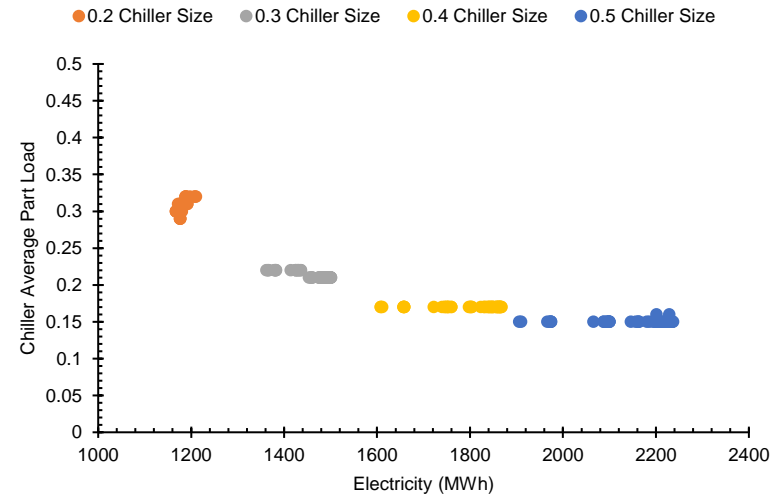
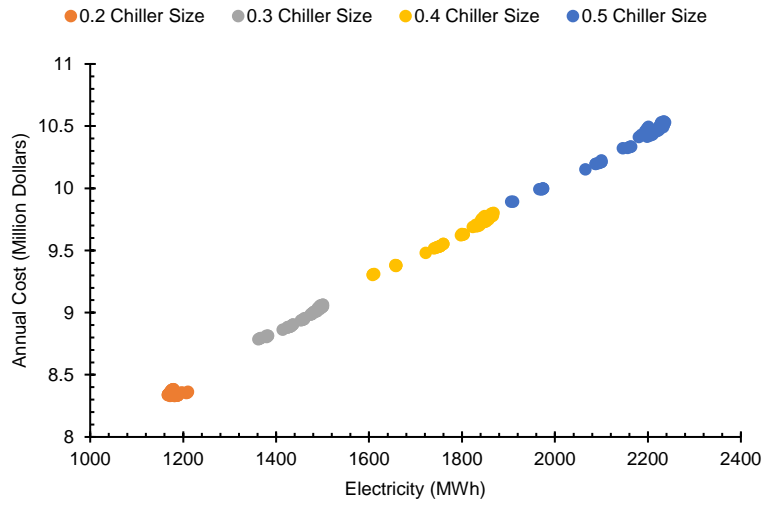


Figure D.3. System optimization results for chilled water stratified tank storage model

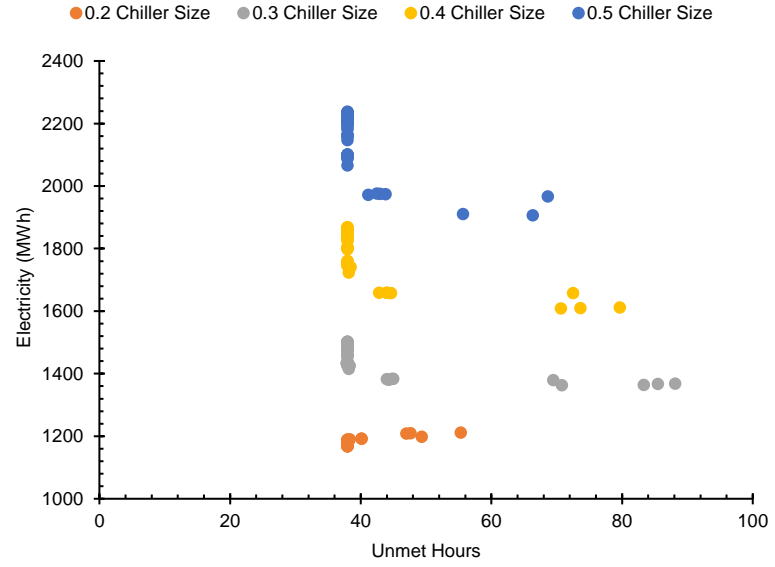
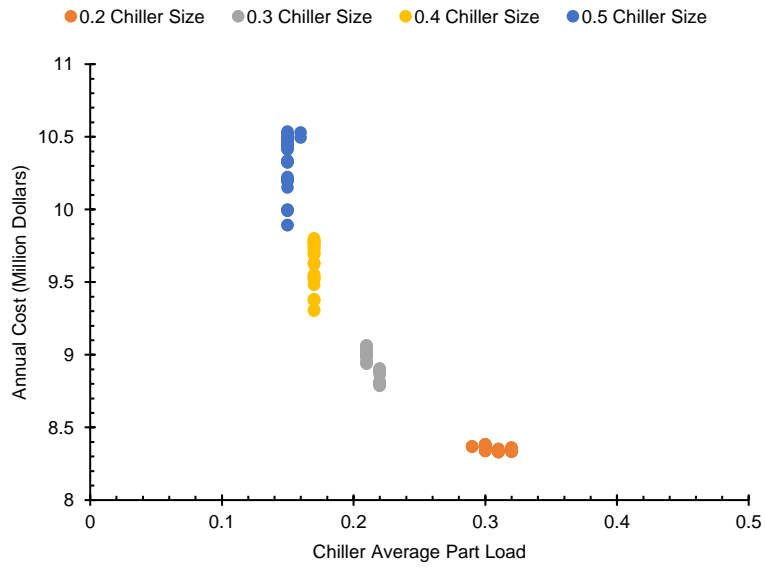


Figure D.3. Continued

## About the Author

Rajeev joined the University of South Florida in fall 2012 as a Ph.D. student in the Department of Chemical and Biomedical Engineering. He is an Indian, born and raised in India. He joined G. B. Pant University of Agriculture and Technology in 1999 to study bachelors in mechanical engineering where he developed an interest in the energy sector and continued his studies in masters in business administration in Power Management from National Power Training Institute (Ministry of Power)-India. A combination of academic skills led Rajeev to join one of the leading private electric utility of Delhi. Rajeev joined a leading energy sector consultancy organization (Feedback Foundation) in New Delhi where he worked as a consultant to various distribution state electricity utilities focusing on distribution business, process improvement, IT implementation in the electricity sector and project management of generation, transmission and distribution project. During this time, Rajeev was inclined towards renewable energy especially solar energy that led him to join an International development organization GIZ to support as a technical expert for commercialization of solar energy applications in residential, commercial and industrial sectors in India. His passion in this field, diverse skills sector experience and an urge to learn advances in technology and research brought him to the University of South Florida for his Ph.D. under the guidance of Dr. Yogi Goswami well known for his contribution to solar energy globally. Rajeev worked on multiple research projects during his stay at the University of South Florida, Tampa where he focused on thermal energy storage, natural gas based air conditioning technology, demand side management and building energy simulations, which is presented in this dissertation.